9-1-1994

THE IMPACT OF ELECTRONIC BALLAST COMPACT FLUORESCENT LIGHTING ON POWER DISTRIBUTION SYSTEMS

Reid Iwao Sasaki
Purdue University School of Electrical Engineering

The Impact of Electronic Ballast Compact Fluorescent Lighting on Power Distribution Systems

Reid Iwao Sasaki

TR-EE 94-28
September 1994

School of Electrical Engineering
Purdue University
West Lafayette, Indiana 47907-1285

THE IMPACT OF ELECTRONIC BALLAST COMPACT FLUORESCENT LIGHTING ON POWER DISTRIBUTION SYSTEMS

Reid Iwao Sasaki

Purdue Electric Power Center

School of Electrical Engineering

Purdue University

1285 Electrical Engineering Building

West Lafayette, IN 47907-1285

TABLE OF CONTENTS

LIST OF TABLES

LIST OF FIGURES

NOMENCLATURE

AC	alternating current
ANSI	American National Standards Institute
AWG	American wire gauge
CF	crest factor
CFL	compact fluorescent lamp
cos	cosine
CRI	color rendering index
DC	direct current
dPF	displacement power factor
DSM	demand side management
emf	electromotive force
EMI	electromagnetic interference
FFT	fast Fourier transform
HF	high frequency
HID	high-intensity discharge
HPS	high-pressure sodium
Hz	hertz
IEC	International Electrotechnical Commission
IEEE	Institute of Electrical and Electronic Engineers
I_L	load current
I_{SC}	short circuit current
I_{Srms}	rms supply current
K	Kelvin
KCL	Kirchhoff's current law

KVL	Kirchhoff's voltage law
kHz	kilohertz
kVA	kilovolt-amperes
LOA	Lights of America
MHz	megahertz
MOSFET	metal-oxide field-effect transistor
NEMA	National Electrical Manufacturers Association
P	active power
PCC	point of common coupling
PF_{sin}	power factor (sinusoidal waveform)
RE	rare earth
RLC	resistor-inductor-capacitor
rms	root-mean-square
S	apparent power
SCR	short circuit ratio
TDD	total demand distortion
THD	total harmonic distortion
tPF	true power factor
UV	ultraviolet
V-I	voltage versus current
VA	volt-ampere
V_{Srms}	rms supply voltage

ABSTRACT

Sasaki, Reid Iwao. MSEE, Purdue University, August 1994. The Impact of Electronic Ballast Compact Fluorescent Lighting on Power Distribution Systems. Major Professor: G.T. Heydt.

Due to the high costs of expanding generation and transmission capacities, utilities have been initiating programs to reduce peak power demand by the customer. A number of these programs, which are commonly referred to as demand side management programs, have turned to the promotion of electronic ballast compact fluorescent lamps (CFLs) as an alternative to traditional incandescent lamps. These larnps provide a higher luminance and increased life as compared to their incandescent counterparts. Unfortunately, electronic ballast CFLs consume large amounts of harmonic current which may prove detrimental to the power distribution system. This thesis presents an introduction to the electronic ballast CFL, including its theory of operation and its potential applications. The experimental results of a number of electronic ballast CFLs investigated are presented. A PSPICE simulation is then presented which models a typical distribution network and the electronic ballast CFL. The results of the simulation are then applied to investigate the derating of a typical distribution transformer, compliance of the system with various harmonic standards, and the derating of the distribution circuit due to triplen neutral currents. The simulation of the lamp is further used to investigate harmonic reduction techniques applied to the electronic ballast CFL.

CHAPTER 1
INTRODUCTION

1.1 Motivation

Over the past few years, the electric power utility industry has been one of America's key industries [1]. With relatively low inflation and interest rates, manufacturing industries, such as the automobile, machinery, and steel industries, are increasing their production. This growth in gross national output causes an increase in consumption of electrical power used to produce those goods. In many cases, however, the annual growth rate of 1.5% has not warranted the expansion of installed generation capacity. Because of the high costs of expanding generation and transmission capacities, utilities have been initiating programs to reduce energy demand by the customer, especially demand during peak periods. These programs, which are commonly referred to as demand side management (DSM) programs, promote such methods as peak-shifting and the use of energy-efficient devices to reduce energy demand. Peak-shifting entails the shifting of loads by the customer during the utility's peak demand hours. By shifting large loads from the utility's peak to off-peak hours, the expansion of peak generation capacity is thus avoided. The cost of peak generation depends on how it is evaluated; however, the range 350-2000 dollars/kilowatt is representative. The promotion of energy-efficient devices is aimed at the reduction of the total peak power demand. Although the use of these devices results in lower revenues for the utility, the savings to utility occurs due to the additional generation and transmission capacity that can be avoided. With the advent of high-power solid-state components, manufacturers have been able to produce devices which are relatively efficient compared to their traditional counterparts. As an

example, energy efficient drives have been promoted to replace conventional electric motors. Typical applications are heating, ventilation, air-conditioning equipment, pumps, and fans. Other energy efficient technologies include microwave drying, superconducting machines, and automatic power factor adjusting devices. Another area which has been targeted for energy efficiency has been lighting. This is the area considered in this thesis.

Compact fluorescent lamps (CFLs) were introduced in the early 1980's, promoting energy efficiency and long lamp life as compared to incandescent lighting. Available for the commercial, industrial, and residential markets, CFLs are available in a variety of shapes and sizes for both new and retrofit applications. Manufacturers offer a number of lamp and ballast combinations which provide an alternative to incandescent and conventional fluorescent lamps. Compact fluorescents offer the energy-efficiency of the conventional fluorescent lamp, while having physical dimensions and luminance characteristics comparable to that of the incandescent lamp.

Because of the relatively high prices of CFLs as compared to their traditional counterparts, their use in the residential sector has been, until recently, limited [2]. To promote the use of these energy saving devices, utility companies have offered rebate programs as a part of their demand side management program Aimed at reducing energy demand by the utility customer, especially in the peak demand period, these rebate programs offer substantial rebates to customers who purchase CFLs. Many utilities are selling CFLs to their customers at prices significantly lower than the manufacturers suggested retail price. In some cases, the utility is actually giving sample CFLs gratis to their customers to promote them [3].

Although many customers are taking advantage of these rebate programs and thus reducing energy demand, utilities may actually encounter unexpected costs in the long run due to the use of these devices which consume and generate harmonic current. When CFLs are a large percentage of the load on a utility's distribution network, losses in the distribution transformers occur due to the increased harmonic current. These losses lead to a decrease of the rated lifetime of the transformer, thus increasing the costs to the utility for the maintenance and replacement.

Large harmonic content in a distribution system should also be a concern for harmonic producing customers and their neighbors. Harmonic presence in voltages and currents cause an increase in heating in the copper windings and iron of motors and other similar electromagnetic machinery [4]. A decrease in life expectancy of these components will lead to increased costs to the utility customer for their maintenance and replacement. Harmonic voltage distortion may also lead to a misoperation of electronic equipment which are dependent of the relative zero-crossings of the supply phase voltages.

1.2 Objectives

The main objectives of this thesis are:

- To study the load characteristics of CFLs with electronic ballasts
- To model electronic ballast CFLs
- To quantify the losses in the distribution system due to CFLs
- To assess the impact and true demand reduction for CFL loads
- To investigate harmonic filtering methods for CFLs.

1.3 Literature summary - fluorescent lighting

The fluorescent lamp may be categorized as a low pressure gas discharge lamp [5]. The discharge which takes place produces two resonance lines of the mercury in the ultraviolet (UV) spectrum, specifically at 185.0 and 253.7 nm. When a potential is applied across the electrodes of the tube, free electrons are emitted from the electrodes and bombard the mercury atoms. The collision between the electrons and the mercury atoms result in heat generation, excitation of the mercury atoms and its molecules, and the ionization of the mercury atoms. Heat generation and the subsequent increase of the gas temperature is the result of elastic collisions that occur between the free electrons and the mercury atoms. The excitation of the mercury atoms and molecules is the result of collisions between the free electrons and the mercury atoms which

cause electrons belonging to the mercury atom to move to a higher energy level. Due to the electrostatic force of the mercury atom, these electrons soon return to their normal energy level. The energy gained by the mercury atom from the electron upon its return path, known as the excitation energy, leaves the mercury atom in the form of electromagnetic energy. This electromagnetic energy, which is in the form of UV radiation, is converted into visible light by means of a fluorescent power which coats the inside of the tube. The ionization of the mercury atoms is the result of collisions between the free electrons and mercury atoms which cause an electron of the mercury atom to be completely removed from its orbit and subsequently become a free electron. The process in which electrical energy is converted into light in a fluorescent lamp is shown pictorially in the diagram below.

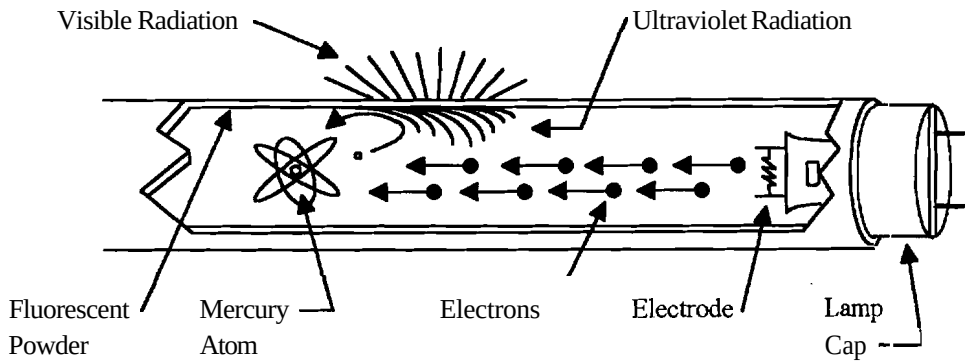

Figure 1.1 Conversion of electrical energy into light in a fluorescent lamp [4]

The main factors which determine the radiation of the two UV resonance lines are the mercury vapor pressure, the auxiliary gas, the current density, and the discharge tube dimensions. These are discussed in detail below.

• Mercury vapor pressure. The fluorescent tube consist of a small amount of mercury necessary for the discharge in the lamp to occur [6]. The saturated mercury vapor pressure is dependent on temperature. In the case of the fluorescent lamp, the pressure of the mercury vapor is determined by the temperature of the coldest spot on

the tube wall, otherwise known as the "cold spot". Because of this dependence, there exists an optimum pressure, and thus temperature, that a specific lamp must operate at for the maximum efficiency of the UV resonance lines produced. If the vapor pressure is too low, the probability that the mercury atom is excited by a free electron decreases and results in a lower luminous output of the lamp. If the vapor pressure is too high, the self-absorption of the UV resonance lines increases and also results in a lower lumiinous output.

• Auxiliary gas. When collisions between the free electrons and mercury atoms occur, the electrons travel a certain distance. The distance covered by these electrons can be summarized as the mean free path length, which is defined as the mean distance covered by the electrons between two collisions. When the mercury vapor pressure is at its optimal level, the mean free path length of the electrons is so great that the probability of the excitation of the mercury atoms and its molecules is low. An auxiliary gas, usually krypton, is added to reduce the mean free path length of the electrons and thus increase the excitation of the mercury atoms and subsequent UV emission [5]. Like the mercury vapor, the auxiliary gas also has an optimal pressure for the maximum luminous efficacy of the mercury discharge. If the ,auxiliary gas pressure is too low, the probability of the excitation of the mercury atoms decreases. If the auxiliary gas pressure is too high, the number of elastic collisions between the free electrons and the auxiliary gas increases and draws energy from the UV producing collisions between the free electrons and the mercury atoms.

• Current density. The energy consumed by the fluorescent tube and the tube wall temperature increase proportionally to an increase in lamp current [5]. If the tube wall temperature exceeds the optimal vapor temperature, there will be a decrease of UV emission. Given constant tube dimensions, an increase in lamp current translates into a higher current density in the tube. A higher current density leacls to both a decrease of the resonance levels due to an increase of excitation of the mercury atoms and also an increase of the absorption of the resonance radiation produced by the

excitation of the mercury vapor. Both of these effects reduce the luminous efficacy of the lamp.

• Discharge tube dimensions. Fluorescent lamp power is a function of both the current through the tube and the lamp voltage, consisting of the voltage across the anode electrode, the cathode electrode, and between the anode and cathode (i.e., the arc voltage) [6]. Given a constant tube diameter, there must be a proportionate increase in arc voltage with an increase in tube length to maintain the optimum tube wall temperature and luminous efficacy. When the tube length is decreased, the tube diameter must be decreased to maintain the optimal luminous efficacy of the lamp. The decrease in tube diameter increases the electric field strength through the tube, thus creating a higher power dissipation per unit of discharge length in the tube.

The literature of the various types of fluorescent lamps may be categorized as conventional lamps, compact units, and electrodeless lamps. These are discussed in detail below.

• Conventional fluorescent lamps. The basic construction of a fluorescent tube consist of the discharge tube, the fluorescent powder, the electrodes, the filling, and the end-caps [5].

The discharge tube is cylindrical in form and serves to contain the filling gas and electrodes. The tube is constructed out of lime glass for straight-tube configurations (e.g. 24", 48", and 96" lengths) and lead glass for bent-tube configurations (e.g. Circline and CFLs). The tube is classified by its diameter and physical configuration. The "T" stands for "Tube" while the number following corresponds to the diameter of the fluorescent tube in eighths of an inch (e.g. the common "T12" stands for the 1 1/2" diameter straight-tube configuration) [2].

The fluorescent powder which coats the inner surface of the discharge tube serves to convert UV produced by the discharge of the lamp into visible light. The visible light produced by the fluorescent powder, otherwise known as luminescence,

can be subdivided into the fluorescence and phosphorescence properties of the powder. Fluorescence can be described as the light produced only when the flucrescent powder is being irradiated by the W radiation produced by the low pressure mercury discharge of the lamp. Phosphorescence can be described as the afterglow produced by the fluorescent powder after it has been irradiated. It is required that the fluorescent powder used have the latter property due to the "dark period" which occurs in fluorescent lamps supplied by an alternating voltage source (e.g., 50 or 60 Hz). When the instantaneous voltage supplying the lamp is below a point where an arc across the electrodes can no longer be produced, current no longer flows through the tube and no W radiation is emitted.

The electrodes of the fluorescent lamp allow the generation of fiee electrons inside of the discharge tube. The electrodes are constructed from tungsted wire and are doubly or triply coated with an emitter material. A metal screen which is electrically isolated from the electrodes often surrounds the electrodes to restrict the sputtering and evaporation of the electrode material, which appears as discharge tube "blackening" near the electrodes.

The filling of the discharge tube consists of a small quantity of mercury and an auxiliary gas. When a voltage is applied across the electrodes.of the lamp, free electrons are produced in the tube. These free electrons excite the mercury atoms and produce a discharge of UV radiation.

The auxiliary gas are necessary for the discharge of the UV radiation and also aid in the starting of the lamp by lowering the effective starting voltage.

The end caps of the fluorescent lamp serve to enclose the tube on both ends and allow connection to the fluorescent fixture. These caps come in many shapes and sizes and are fitted with either one or two contacts apiece. End caps fitted with one contact are used in fixtures which only allow cold starting of the lamp while caps fitted with two contacts must be used in fixtures which preheat the electrodes prior to starting (e.g., rapid start lamps).

• Compact fluorescent lamps. As its name suggests, the CFL is a compact version of the traditional fluorescent lighting fixture described above. CFL's are most commonly found in lengths no greater than approximately 25". Their design powers generally range from 7 to 40 watts and produce an illuminance comparable to incandescent and traditional fluorescent fixtures of higher power [7].

The physical construction of the CFL is similar to that of the conventional fluorescent lamp, consisting of the discharge tube, the fluorescent powder, the electrodes, the filling, and the end-caps. To reduce the overall size of the CFL, the length of the discharge tube is reduced significantly as compared to conventional fluorescent lamps. In order to keep the luminous flux of the lamp constant (given the decrease in tube length), the diameter of the tube is also reduced in order to increase the strength of the electric field through the tube. In order to further reduce the size of the lamp, the discharge tube is literally folded in half The folding of the tube also allows both end-caps to be enclosed in a single housing. It also allows the incorporation of the starter, base, and (in some cases) ballast in the same housing.

CFLs are found in many types of physical configurations. One type is the single-ended twin-tube which is a U-shaped tube with filaments on both ends. Another type is the single-ended quad-tube which is similar to the twin-tube except that it consist of twice of the number of tubes. The twin- and quad-tube configurations are commonly found in 1/2" and 5/8" diameters (designated as "T4" and "T5" sizes, respectively) and have two-pin bases for connection to the ballast. Other types of CFL:; include square-shaped, globe-shaped, reflector, and Circline configurations. Finally, the integral CFL includes the lamp and the ballast housed in an Edison screw-in lamp base. The attributes for the various types of CFLs currently available are shown below in Table (1.1).

Table 1.1 Attributes of various types of CFLs [8]

Lamp Type	Ballast Type	Lamp Power	Efficacy[1]	Lamp Life[2]	Overall Length
Incandescent	none	25-150	8-20	750-2,000	< 7"
T-4 Twin-Tube	magnetic	5-13	25-50	10,000	4-7.5"
T-4 Quad-Tube	magnetic	9-26	35-55	10,000	4.5-8"
T-5 Twin-Tube	magnetic	18-40	50-60	<20,000	9-22.5"
	electronic	18-40	70-85	15,000	9-22.5"
Integral Ballast Lamp	magnetic	15[3]	45-50	9,000	6-9"
	electronic	17-27[3]	55-65	9,000-10,000	5-8"
Circline	magnetic	20-40	35-60	12,000	6.5-16"
	electronic	22-30	80-85	9,000	diameter

Note:;: (1) Efficacy is defined as lumens output / system watts input

(2) Lamp life in hours, based on 3 hours per start

(3) Includes ballast power

Due to the vast number of possible of combinations of lamp shapes, powers, and base types, the National Electrical Manufacturers Association (NEMA) has developed a generic designation system for non-integral CFLs [9]. The NEMA lamp product code for CFLs consists of the following elements:

CF [Lamp Shape] [Lamp Power] / [Base Designation]

where

[Lamp Shape] = "T" (twin-tube), "Q" (quad-tube), "S" (square shape), or "M" (miscellaneous shape not covered by the other designators),

[Lamp Power] = power consumed by lamp, and

[Base Designation] = manufacturer base designation code.

For example, the NEMA generic designation code for a typical 13-watt T-4 twin-tube CFL would be CFT13W/GX23.

One of the reasons for the high efficacy of CFLs is the rase earth (RE) phosphors used in the fluorescent powder used to coat the tube [10]. These RE phosphors are able to produce high lumen output from CFLs which have a high power density in the small diameter tube used. The use of conventional halophosphors in CFLs would lead to a rapid and severe depreciation in luminance of the lamp. The RE phosphors used in CFLs also have excellent color rendering properties and various color temperatures which are obtainable by combining these phosphors. CFLs are available in several color temperatures for incandescent retrofit applications and special effect lighting applications. These color temperatures (expressed in Kelvins) range from 2700 K for a warm "incandescent" color rendering to 4100 K for a cooler "bluish" color rendering. CFLs with a color temperature of 3500 K produce a neutral-white light, similar to that of traditional fluorescent lamps. The quality of the light produced by a CFL is measured by its Color Rendering Index (CRI) which is on a scale of 100. The CRI determines how "true" or "natural" colors appear under the light. As a reference, a standard incandescent bulb have a color temperature of 2800 K artd a CRI of 93 [11]. Typical color temperatures used for standard CFLs and their corresponding CRIs and lumen equivalents are shown below in Table (1.2). The environmental impact of RE phosphors may be a concern if discarded CFLs are sent to conventional landfills. These phosphors are toxic and some attention has been given to alternative formulas for CFL phosphors.

Table 1.2 Color temperature options of standard CFLs [5]

Color Temperature	Nominal CRI	Matches
2700 K	82	Warm white, incandescent, white high-pressure sodium (HPS)
3000 K	85	Warm white, incandescent, halogen, other 3000 K fluorescent and high-intensity discharge (HID) lamps
3500 K	85	Halogen, other 3500 K fluorescent lamps
1100 K	85	Cool white, metal halide, other 4100 K fluorescent and HID lamps
5000 K*	85	C/D50 and all other high color temperature fluorescent and HID sources

Note: *not as many product available as other color temperatures

Because of their relatively small physical size, high efficacy, and long life, the use of CFLs is being promoted in both the residential and commercial sectors. Suggested applications for CFLs are shown below in Tables (1.3) and (1.4) for the residential and commercial sectors, respectively. Typical commercial applications for specific types of CFLs are also shown below in Table (1.5).

Table 1.3 Suggested residential applications for CFLs [8]

Kitchens	Living Rooms	Bedrooms	Bathrooms	Utility Areas	Exterior
:Recessed downlights	Task lights	Task lights	Mirror lights	Stairways	Lanterns
Under cabinet lights	Swing arm lamps	Closet lights	Recessed downlights	Laundry rooms	Garage lights
	Under cabinet lights		Shower & tub lights	Attics	Path lights
	Recessed downlights			Closets	Security lights
	Wall washers			Crawl spaces	

Table 1.4 Suggested commercial applications for CFLs [8]

General Lighting	Accent & Specialty Lighting	Decorative & Portable Lighting	Utility Lighting	Exterior Lighting
Recessed downlights	Recessed & track-mounted wall washers	Wall sconces	Security lighting	Landscape floodlights
Suspended luminaires	Under cabinet lights	Chandeliers	Step lights	Pedestrian post top and bollard lights
Indirect lighting systems	Cove lights	Table & floor lamps	Exit signs	Step lights
	Case display lights	Makeup & dressing lights	Task lighting	Under rail lights
	Modular strip outlining			Vandal resistant security lights
	Sign and display lights			

Table 1.5 Commercial applications for specific types of CFLs [9]

	Downlights	Surface Lights	Pendant Fixtures	2' x 2' Fixtures	Sconces	Exit/Step Fixtures	Floodlights
Incandescent	+	+	+	-	+	+	+
T-4 Twin-Tube	+	+	-	-	+	+	+
T-4 Quad-Tube	+	+	+	-	+	-	-
T-5 Twin-Tube	-	+	-	++	+	-	+
Integral Ballast	+	-	++	-	-	-	-
Circline	-	+	+	-	+	-	-
Reflector Unit	++	-	+	-	-	-	+

++ Uniquely superior lamp choice

\+ Suitable lamp choice

\- Unsuitable lamp choice

• Electrodeless fluorescent lamps. One of the main causes of failure of fluorescent lamps is the degradation of lamp electrodes. Also, the glass-metal bonds required to introduce connections to lamp electrodes are costly and sometimes difficult to manufacture. For these reasons, an electrodeless design was developed for fluorescent lighting [12]. Referred to as the H-discharge method, the electrodeless design incorporates a lamp tube surrounded by an air-core coil. This coil is supplied by a high-frequency (e.g., 1-100 MHz) power source which produces an electromagnetic field inside the lamp tube. This field causes the mercury vapor in the tube to ionize and subsequently phosphors produce luminous output.

Similar to the electronic ballast CFL, the electrodeless fluorescent lamp is a compact electronic ballast mercury discharge light source. The electrodeless fluorescent consumes approximately the same power as a typical CFL (approximately 25 .watts), while producing a comparable luminous output (approximately 1,000 lumens). The advantage of the electrodeless design is the relative long-life due its lack of electrodes. The power source for the electrodeless lamp comprises a rectifier/inverter circuit, similar to that of the CFL, to generate the high-frequency RF current required by the lamp. In 1994, electrodeless designs are expected to be introduced commercially.

Two types of ballasts, electromagnetic and electronic, are available for use with fluorescent lamps. The ballast serves to provide the starting voltage to the lamp, limit the current consumed by the lamp, and help stabilize supply voltage variations [5]. Ballasts are available in internal and external configurations, referred to as integral and adapter ballasts, respectively. Both the electromagnetic and electronic ballasts will be described in detail below.

• Electromagnetic ballasts. Electromagnetic ballasts consists of a wirewound coil connected in series with the lamp is available for use with conventional and compact fluorescent lamps [13]. These types of ballasts limit current to the fluorescent lamp by serving as a high impedance load in series with the lamp at line frequency.

Due: to their inductive nature, electromagnetic ballasts consume approximately 15 to 25 percent of the rated lamp power which is dissapated as heat. In addition, many of these types of ballasts suffer from a low displacement power factor (approximately 0.5 lagging power factor.)

Electromagnetic ballasts are also responsible for both the generation and limitation of harmonic current. Harmonic current is generated by the ballast due to its nonlinear magnetic characteristics but is also limited by the ballast due to its inductive nature. A typical supply voltage and current for a fluorescent lamp with an electromagnetic ballast is shown below.

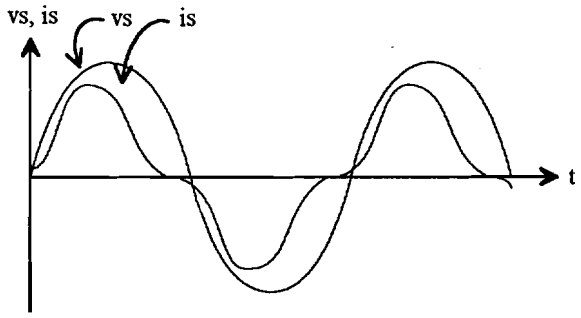

Figure 1.2 Supply voltage and current for a fluorescent lamp with an eledromagnetic ballast

- Electronic ballasts. Electronic ballasts consist of solid state devices used to create a high frequency ac voltage supplied to the lamp [14]. The line voltage supplied to the ballast is converted into a dc voltage using a full-wave bridge rectifier and a filter capacitor. Unlike the electromagnetic ballast which supplies the lamp with a line frequency current of 50160 Hz, the electronic ballast provides the lamp with 25 to 50 kHz frequency current using an inverter.

There are a number of advantages of using an electronic ballast as opposed to an electromagnetic ballast [9]. When an electromagnetic ballast is used to energize a fluorescent lamp, the mercury discharge loses most of its electrons and ions when the current reverses through the tube. This is due to a de-ionization of the gas in the tube

which is supplied with a 50160 Hz ac voltage source. Thus, the discharge needs to be re-ignited periodically, which requires additional power from the electromagnetic ballast. Alternatively, for fluorescent lamp energized with an electronic ballast (with a switching frequency greater than 10 kHz), the discharge occurring in the tube does not require periodic re-ignition. Because of the relatively high switching frequency of the electronic ballast, the gas in the discharge tube does not suffer from an appreciable de-ionization and a sufficient number of electron carriers required for discharge remain after current reversal. Thus, there is no power required to re-ignite the discharge, which results in a 10% increase in luminous flux produced by the discharge tube. Other advantages of using a electronic ballast instead of an electromagnetic ballast include decreased size and weight, increased efficacy (lumens/watt), decreased 50160 Hz hum, and increased lamp life.

There are also disadvantages of using an electronic ballast as opposed to an electromagnetic ballast. Because the electronic ballast incorporates a bridge rectifier/filter capacitor combination to convert the supply ac voltage into a dc voltage, a large amount of current distortion is injected into the voltage supply. The relatively small conduction time of rectifier/filter capacitor combination creates a current waveform which is rich in odd harmonics and also has a relatively high crest factor. A typical supply voltage and current for a fluorescent lamp with an electronic ballast is shown below. Another disadvantage of the electronic ballast is the radio frequency interference which is induced by the high switching frequency of the ballast's inverter.

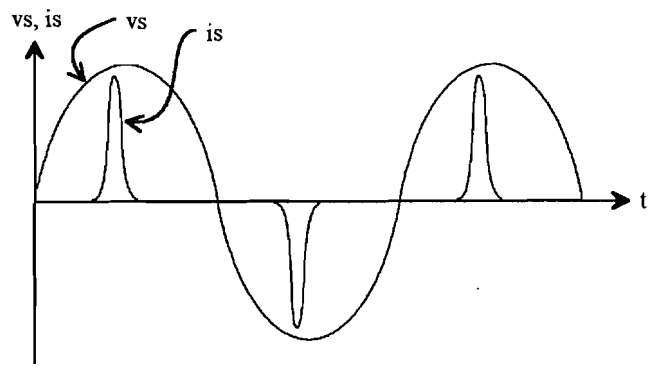

Figure 1.3 Supply voltage and current for a fluorescent lamp with an electronic ballast

1.4 Literature summary - power quality

The literature of electric power quality is voluminous. For purposes of assessing the impact of CFLs, it is convenient to examine power factor and the various IEEE standards relating to power quality. These are discussed briefly below.

- Power factor. The power factor in the case of sinusoidal voltage and current waveforms can be defined as the ratio of the active power to the apparent power consumed by the load [15]. This can be expressed for the sinusoidal case as,

$$PF_{(sinusoidal)} = dPF = tPF = \frac{\text{Active Power}}{\text{Apparent Power}} = \frac{P}{S} \qquad (1.4.1)$$

where

$$P = V_{Srms} I, \quad \cos 8$$
$$S = V_{,} \quad I,$$

The values of V_{Srms} and I, are the rms values of the terminal voltage and current, respectively. The angle 8, referred to as the power factor angle, is the phase difference between the voltage and current waveforms. When the current lags the voltage, a lagging power factor is obtained and the load is referred to be inductive with a positive power factor angle ($0 > 0$). When the current leads the voltage, a leading power factor is obtained and the load is referred to be capacitive with a negative power factor angle ($0 < 0$). Note that inductive loads ($0 < 0 < 90$) causing a lagging power factor may be compensated to a unity power factor by adding a capacitor in parallel across the load terminals. For the sinusoidal voltage and current case, the power factor is the cosine of the angle between the current and voltage. This angle is also the angle between the fundamental v(t) and i(t). Therefore the displacement power factor and displacement factor also apply. In the sinusoidal case, the true power factor (tPF) and the displacement power factor (dPF) are the same and are simply termed "power factor".

Switched electronic loads usually cause distortion in load current [16]. This distortion is due to the non-continuous conduction of current through the load. This switching causes the load current to become nonsinusoidal and subsequently affects the power factor. The term "power factor" for the nonsinusoidal case needs further explanation.

True power factor, tPF, is defined as

$$\text{tPF} = \frac{P_{\text{total}}}{S} \tag{1.4.2}$$

where

$$P_{\text{total}} = \sum_{i=1}^{\infty} |V_i||I_i|\cos\theta_i$$

$$S = |V_{rms}||I_{rms}|.$$

Displacement power factor, dPF, is defined as

$$\text{dPF} = \frac{P_1}{S} \tag{1.4.3}$$

where

$$P_1 = |V_1||I_1|\cos\theta_1,$$

$$S = |V_{rms}||I_{rms}|.$$

In the nonsinusoidal case, tPF can not always be corrected to unity through simple power factor correction (i.e., capacitors). For example, for the nonsinusoidal case

$$v(t) = \cos(t) + 0.01\cos(3t)$$
$$i(t) = \cos(t) + \cos(3t),$$

it can be easily shown that

$$\text{dPF} = 1.0000$$
$$\text{tPF} \approx 0.7141$$

In this case, power factor correction using capacitors is ineffective since the fundamental voltage and current are already in phase.

- IEEE Standard 519-1992 [4] - Practices and requirements for harmonic control. IEEE Standard 519-1992 provides recommended practices for electric power systems that are subjected to non-linear loads. The standard includes information on harmonic generation, system response characteristics, the effects of harmonics, harmonic control, and recommended practices for individual customers and utilities.

The generation of harmonics in a power system can be attributed to the use of rectifiers, arc furnaces, static var compensators, inverters, electronic phase controllers, cycloconverters, switched mode power converters, and pulse width modulated drives, as defined in IEEE Standard 519-1992. All of these devices may cause harmonics in the voltage and/or current waveshape provided by the utility. In the case of devices containing solid state components to achieve switching, voltage harmonics can be attributed to voltage notching due to commutation periods while current harmonics can be attributed to discontinuous conduction due to the switching of the solid state components.

The system response characteristics to harmonic loads on a distribution system determines the effect of these loads. The flow of harmonic currents in a distribution network is dependent on the system short-circuit capacity, the placement and size of capacitor banks, the characteristics of the loads on the system, and finally, the balanced/unbalanced conditions of the system.

Normally in a distribution network, harmonic currents tend to flow between the harmonic load and the lowest system impedance. In most cases, this will be the utility source or point of generation. When capacitor banks and load characteristics are taken into effect, parallel and/or series resonant conditions may appear in the distribution system, causing oscillations and further producing an increase in voltage distortion. Because of this fact, a thorough investigation of the characteristics of the installed capacitor banks and loads must be done to avoid resonances.

Specifically, IEEE Standard 519-1992 provides recommended practices for harmonic control for both the utility and individual customer. Because of the wide range of harmonic- producing loads described above, three harmonic indices have been

recommended for the individual customer to provide a meaningful insight of harmonic effects [4]. These indices include:

(1) Depth of notches, total notch area, and distortion (RSS) of bus voltage distorted by commutation notches (low-voltage systems),

(2) Individual and total voltage distortion, and

(3) Individual and total current distortion.

The development of Indices (2) and (3) will be discussed in detail below. Index (1) will not be discussed because it does not apply to a distribution lighting Feeder loaded with CFLs. The CFLs studied are single-phase line-to-neutral devices which do not cause voltage commutation notches.

The harmonic voltage distortion on a distribution is a function of the total injected harmonic current and the system impedance at each of the harmonic frequencies [4]. Because of this relation, current distortion limits have been developed to curtail voltage distortion produced by individual customers. The objectives of developing current distortion limits are to:

(1) Limit the harmonic injection from individual customers so that they will not cause unacceptable voltage distortion levels for normal system characteristics, and

(2) Limit the overall harmonic distortion of the system voltage supplied by the utility.

Note that the total injected harmonic current is dependent on the number of individual customers injecting harmonic current and the size of each customer. Thus, the harmonic current limits developed are dependent upon customer size. The size of the customer is determined by its short-circuit ratio (SCR) at the point of common coupling (PCC) with the customer-utility interface. The SCR for a customer may be defined as

$$\text{SCR} = \frac{I_{sc}}{I_L} \tag{1.4.4}$$

where

I_{sc} = utility system short-circuit current capacity at the PCC

I_L = customers maximum demand load current (fundamental frequency component) at the PCC

Note that the SCR is an indication of the "stiffness" of the bus at the PCC. Thus, customers which represent a relatively large portion of the utility's total system load will have a more stringent current distortion limit than smaller customers.

The basis for current distortion limits are to limit the maximum individual frequency voltage harmonic to tolerable levels. These voltage harmonic limits and corresponding SCRs are shown below in Table (1.6).

Table 1.6 Basis for IEEE 519-1992 harmonic current limits [4]

SCR at PCC	Maximum Individual Frequency Voltage Harmonic (%)	Related Assumption
10	2.5-3.0	Dedicated system
20	2.0-2.5	1-2 large customers
50	1.0-1.5	A few relatively large customers
100	0.5-1.0	5-20 medium size customers
1,000	0.05-0.10	Many small customers

Table (1.7) shows the current distortion limits for general distribution system (120 V through 69,000 V) for corresponding SCRs at the PCC. The index used to determine the maximum allowable harmonic current distortion allowable for a specific SCR is the total demand distortion (TDD). The TDD is defined as the harmonic current distortion in percent of maximum demand load current.

Table 1.7 IEEE 519-1992 current distortion limits for general distribution systems (120 V through 69,000 V) [4]

Maximum Harmonic Current Distortion in Percent of I_L

Individual Harmonic Order (Odd Harmonics)

I_{sc}/I_L	< 11	$11 \le h < 17$	$17 \le h < 23$	$23 \le h < 35$	$35 \le h$	TDD
<20*	4.0	2.0	1.5	0.6	0.3	5.0
20<50	7.0	3.5	2.5	1.0	0.5	8.0
50<100	10.0	4.5	4.0	1.5	0.7	12.0
100<1000	12.0	5.5	5.0	2.0	1.0	15.0
>1000	15.0	7.0	6.0	2.5	1.4	20.0

Notes: (1) Total Demand Distortion (TDD) = harmonic current distortion in % of maximum demand load current (15 or 30 minute demand)

(2) Even harmonics are limited to 25% of the odd harmonic limits above

(3) Current distortions that result in a dc offset, e.g., half-wave converters, are not allowed

(4) *All power generation equipment is limited to these values of current distortion, regardless of actual I_{sc}/I_L

• IEC Standard 555-2 [17] - Disturbances in supply systems caused by household appliances and similar electrical equipment. The IEC Standard 555-2, which is practiced in European countries, is a standard focused on harmonic current content at the equipment level. Unlike IEEE Standard 519-1992 which focuses on harmonic content at the utility system level, IEC 555-2 is an equipment specification stating the allowable amount of harmonic current produced by electronic devices. The equipment covered by IEC 555-2 is subdivided into "Classes" and is summarized in Table (1.8). Equipment considered in "Class D" are defined as having a current waveshape which falls below the envelope shown in Figure (1.4) for more than 95% of the positive half cycle.

Table 1.8 IEC *555-2* defined equipment classes [17]

Class	Description	Examples
A	Balanced 3-phase equipment and equipment not falling into another category	Small (< 15 HP) 3-phase ASDs
B	Portable and similar tools	Small (< 5 HP) 1-phase ASDs and appliances with ASDs
C	Lighting equipment, including dimmer controls	Fluorescent lighting (other than compact) and lighting dimmers
D	Equipment having an input current which falls below the Class D defining envelope*for more than 95% of the positive half cycle	Computers, compact fluorescent lighting, controllers, consumer electronic:;

Note: * See Figure (1.4) for IEC 555-2 Class D defining envelope

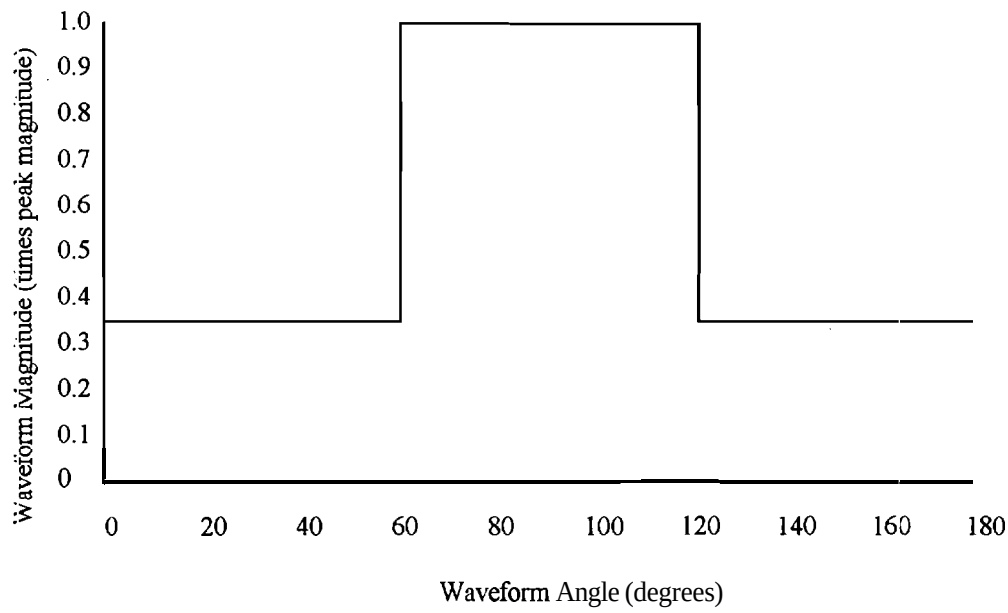

Figure 1.4 IEC *555-2* Class D defining envelope [17]

The maximum harmonic current allowed is specified for the individual harmonic orders. These limits are shown in Tables (1.9), (1.10), arid (1.11) for Classes A, C, and D, respectively. Note that these harmonic limits are for equipment supplied by 230 volts line to neutral or 400 V line to line. If the equipment is supplied

with a different voltage (i.e., 120 volts line to neutral or 208 volts line to line), the limits stated in Tables (1.9) through (1.11) must be multiplied by a factor equal to the actual supply voltage divided by 230 volts or 400 volts, respectively.

Table 1.9 IEC 555-2 Class A harmonic limits [17]

Harmonic Order (n)	Maximum Current (Amperes)
Odd Harmonics Only	
3	2.3
5	1.14
7	0.77
9	0.4
11	0.33
15 < n < 39	0.15 x (15/h)
Even Harmonics	
2	1.08
4	0.43
6	0.3
8 < n < 40	0.23 x (8/h)

Note: **Harmonic current limits for Class A equipment and certain Class C equipment using phase-controlled lamp dimmers**

Table 1.10 IEC *555-2* Class C harmonic limits [17]

Harmonic Order (n)	Maximum Percent of rms current
2	2
3	30
5	10
7	7
9	5
11 < n < 39	3

Note: Harmonic current limits for Class C equipment greater than 25 watts

Table 1.11 IEC *555-2* Class D harmonic limits [17]

Harmonic Order (n)	Maximum Harmonic Current	
	Relative (mA/W)	Absolute (Amperes)
Odd Harmonics Only		
3	3.6	1.08
5	2	0.6
7	1.5	0.45
9	1	0.3
11 < n < 39	0.6 x (11/n)	0.18 x (11/h)
Even Harmonics		
2	1	0.3
4	0.5	0.15

Notes: (1) Harmonic current limits for Class D equipment and Class C equipment with input power less than 25 watts.

(2) Relative limits apply to equipment with power consumption up to 300 watts.

(3) Equipment with power consumption lower than 10 watts shall be treated as 10 watts.

- Green Seal Standards for CFLs [6]. Due to potential effects of CFLs on the environment, Green Seal, an independent non-profit organization, has provided a set of standards for CFLs. These standards are summarized in Table (1.12). Green Seal, which encourages consumers to purchase "environmentally preferable" products, tests various CFLs for their compliance with the standards. The Green Seal Standards for CFLs have been adopted by 19 utilities in the Northwest Residential Efficient Appliance and Lighting Group (NWREAL), Pacific Gas & Electric Co., and the Sacramento Municipal Utility District.

Table 1.12 Green Seal Standards for CFLs [6]

Standard	Description
Color Rendering Index	80 or greater
Color Temperature	2,600 to 3,100K unless otherwise specified on the package
Mercury	20 milligrams maximum (drops to 10 milligrams in 1996)
Package Information	Information on packaging indicating characteristics of enclosed CFL
Power Quality	No requirements for basic certification. Class A designation is given to products with these characteristics: • Power factor greater than 0.9 • Harmonic distortion less than 33 percent
Product Life	8,000 hours at 3 hours per start
Radioisotopes	Zero by August 1, 1996
Starting	4 seconds at minimum rated operating temperature
System Efficacy	Built-in ballast: less than 10 watts 40 lumens/watt 10 to 15 watts 45 lumens/watt more than 15 watts 55 lumens/watt Lamps alone: less than 7 watts 40 lumens/watt 7 to 9 watts 50 lumendwatt 9 to 13 watts 55 lumens/watt 13 to 18 watts 60 lumens/watt more than 18 watts 62 lumens/watt
Toxins in Packaging	(Addedtogether, the total concentration of lead, cadmium, mercury, and hexavalent chromium must not exceed 250 parts per million (drops to 100 parts per million on January 1, 1994)

• IEEE Standard C57.110-1986 [18] - Transformer derating for harmonic loads. This recommended practice set forth by the American National Standards Institute (ANSI) and the Institute of Electrical and Electronics Engineers (IEEE) establishes two methods for the current derating of power transformers when connected to loads which consume nonsinusoidal currents. The standard applies to nonsinusoidal load currents which have a harmonic load factor (which is defined as the ratio of the effective value of all the harmonics to the effective value of the fundamental harmonic) greater than 0.05 per unit.

Transformer losses can be divided into no-load loss and load loss. The ANSI/IEEE C57.110-1986 establishes a current derating factor . for- power transformers by accounting for the increased load loss due to nonsinusoidal load currents. Thus, no-load loss is not accounted for in the derating procedures.

Two methods are given in ANSI/IEEE C57.110-1986 for the derating of power transformers subject to nonsinusoidal load currents. Both methods determine the current handling capability of power transformers without the loss of normal rated life expectancy. The first method, primarily for use by transformer design engineers, requires access to detailed information on loss density distribution within the transformer windings. The less-accurate second method, primarily for use by the transformer user, requires access to certified test report data only. It is assumed in both methods that the harmonic characteristics of the load current are known. The latter method for derating a transformer will be described below.

With access to certified test report data, the following equation for the derating of a transformer may be used,

$$I_{\max}(\text{pu}) = \left[\frac{P_{\text{LL-R}}(\text{pu})}{1+\left[\left(\sum_{h=1}^{h_{\max}} f_h^2 h^2 / \sum_{h=1}^{h_{\max}} f_h^2\right) P_{\text{EC-R}}(\text{pu})\right]} \right]^{1/2} \qquad (1.4.4)$$

where

$I_{\max}$ (pu) Maximum permissible rms nonsinusoidal load current (per unit of rated rms load current)

$P_{\text{LL-R}}$ (pu) Load loss density under rated conditions

(per unit of rated load I^2R loss density)

$P_{EC\text{-}R}$ (pu) Winding eddy-current loss under rated conditions (per unit of rated load I^2R loss)

f_h Harmonic current distribution factor for harmonic "h" (equal to the harmonic "h" component of current divided by the fundamental 60 Hz component of current for any given loading level)

h Harmonic order.

Using the above equation, it' is assumed that the nonsinusoidal load current applied to the transformer has an rms magnitude of 1.00 per unit. It is also assumed that the per unit rms current for harmonic order "h" is terms of the rated rms load current, I_h (pu), is known. In other words, the harmonic distribution of the load current applied to the transformer is assumed to be known.

The harmonic current distribution factor, f_h, can be determined for a specific harmonic order, h, by dividing I_h by the rms current at the fundamental frequency of 60 Hz (h=1), I_1.

The per unit eddy-current loss in the region of highest loss density defined for 60 Hz operation at rated current, $P_{ec\text{-}r}$ (pu), can be obtained from certified test report data for the individual transformer which is usually provided by the manufacturer. The maximum per unit local loss density under rated conditions, $P_{ll\text{-}r}$ (pu), can then be defined as $1 + P_{ec\text{-}r}$ (pu).

The maximum permissible per unit rms nonsinusoidal load current in terms of the rated rms load current, I_h (pu), is then obtained using the equation shown above. The maximum permissible rms nonsinusoidal load current can be obtained by multiplying I_h (pu) by the rms sine wave current under rated frequency and load conclitions, I_1.

It should be noted that this procedure for the derating of a transformer when supplying nonsinusoidal load currents produces a conservative derating factor. This is due to the fact that procedure produces a derated current factor for a load current applied to the transformer which is 100% nonlinear. In most practical cases, the load

applied to the distribution transformer will consist of a percentage of linear load which will not contribute to excessive losses in the transformer.

1.5 Electronic ballast CFLs and the electric utility

The major concern of the electronic ballast CFL on the utility distribution system is their low true power factor due to the large current harmonic distortion associated with them [19]. Most electronic ballast CFLs are notorious for the relatively large current harmonic distortion (> 100%) and large crest factors which they produce [20]. Unlike an incandescent lamp which has a power factor of 1.00, an electronic ballast CFL produces a relatively low true power factor of approximately (0.50). Due to their low true power factor, electronic ballast CFLs consume nearly twice the amount of apparent power than real power (assuming a power factor of approximately 50%.) This increase in apparent power consumption will lead to an increased in cost to both the utility and large utility customers.

Manufacturers of CFLs are stating that the use of a lower power CFL with an luminous output equivalent to that of an incandescent lamp will lead to large energy savings to its user. This statement is only true for the residential utility customer who is billed for their active power consumption only. In this case, the utility is actually at a disadvantage because it has support the increased consumption of reactive power by these devices by the use of power factor correction devices, such as capacitors and synchronous condensers. The utility is thus faced with the entire economic burden of the purchase and maintenance of these devices. In addition, it should be noted that the previously mentioned power factor correction methods will only be effective for CFL loads with electromagnetic ballast. In many electronic ballast CFLs, the fundamental components of the voltage and current are nearly in phase, leading to a dPF close to unity. The low true power factor obtained is caused by the large harmonic distortion in the current waveform and the application of capacitors may actually be detrimental to the power factor instead of improving it [21].

In the case of large utility customers who are often billed for their apparent power consumption (instead of active power), the energy savings stated by the manufacturer due to the use of CFL's must be derated to obtain the actual savings seen by the customer. To obtain the equivalence rating of a CFL to that of an incandescent lamp (e.g. 20 watts CFL equivalent to 75 watts incandescent), manufacturers often use an index of relative luminous efficacy which has dimensions of lux per vvatt. In other words, it is a measure of the luminous output of the lamp per one watt input to the lamp. Since CFL's consume relatively large amounts of apparent power as compared to incandescent lamps (where apparent power equals active power), the relative luminous efficacy of a CFL must be in terms of lux per VA to account for the reactive power consumed by the CFL [2]. By derating the equivalence rating stated by the manufacturer, it will be found by the customer that the economic benefits of using CFLs will not be as great as anticipated.

Additional references on the impact of CFLs on distribution systems include:

- Residential load-shape data for incandescent lamps and CFLs [25],
- Harmonics from residential customers [26],
- Voltage distortion forecasts for distribution feeders with nonlinear loads [27],
- Economic evaluation of harmonic effects on distribution feeders with nonlinear loads [28], and
- Identification of the true energy savings realized from high efficiency electronic loads [29].

CHAPTER 2

MODELING OF COMPACT FLUORESCENT LAMPS AND THE DISTRIBUTION SUPPLY

2.1 Introduction

The investigation of the impact of electronic ballast CFLs on the distribution network was approached by simulating the model of a typical CFL and distribution network using PSPICE. This chapter discusses the various components of the model, which include:

- the electronic ballast CFL
  (consisting of the EMI filter, bridge rectifier, HF oscillator,,and fluorescent tube)
- the distribution network
  (consisting of the distribution transformer, transmission line, and voltage source).

The explanation of the components listed above will be described in detail in the sections to follow.

2.2 Modeling of the electronic ballast CFL

The electronic ballast CFL consists of four sections: the electromagnetic interference (EMI) filter, the bridge rectifier, the high-frequency oscillator, and the fluorescent tube. These sections are shown pictorially for a typical electronic ballast CFL in Figure (2.1). In addition, each section will also be described in detail below.

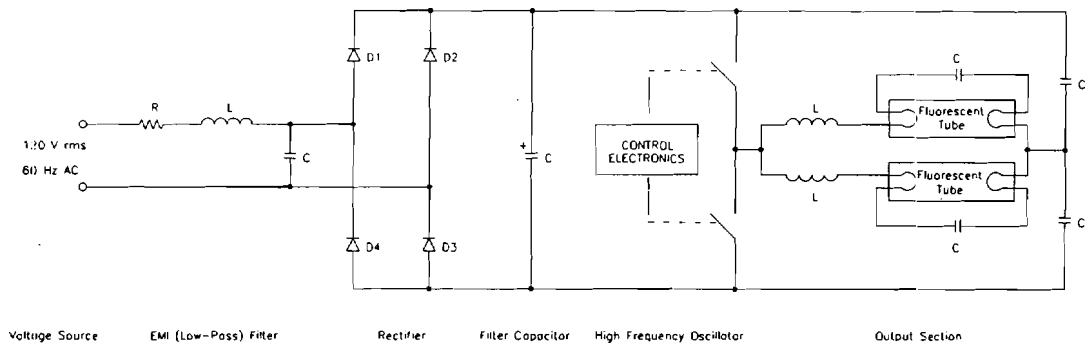

Figure 2.1 Schematic diagram of a typical electronic ballast CFL

• Electromagnetic interference (EMI) filter. The purpose of the EMI filter is to filter the current supplied by the source (connected to the input of the filter) from unwanted harmonic currents consumed by the load (connected to the output of the filter). In essence, the EMI filter is a two-port network, serving as a low-resistance path to the neutral leg for unwanted harmonic currents consumed by the source. Shown below is the schematic diagram for a typical EMI filter used in electronic ballast CFLs.

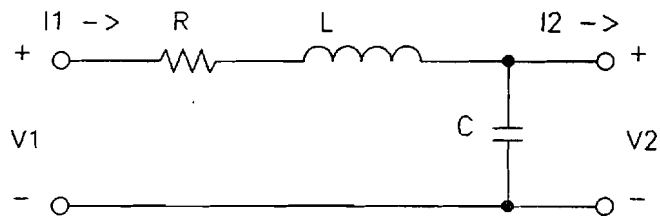

Figure 2.2 Typical EMI filter used in electronic ballast CFLs

The series impedance, Z, which is on the phase leg, consists of a resistor, R, and an inductor, L, connected between the input and output of the filter. The shunt admittance, Y, which is on the output-side of the filter, consists of a capacitor, C, connected between the phase and neutral legs.

The filter may be analyzed as a simple two-port network using the equation (written in matrix form):

$$I_{\text{bus}} = Y_{\text{bus}} V_{\text{bus}} \tag{2.2.1}$$

where

$$I_{\text{bus}} = \begin{bmatrix} I_1 \\ -I_2 \end{bmatrix}, \; Y_{\text{bus}} = \begin{bmatrix} y_{11} & y_{12} \\ y_{21} & y_{22} \end{bmatrix}, V_{\text{bus}} = \begin{bmatrix} V_1 \\ V_2 \end{bmatrix}.$$

Note the negative sign preceding I_2, due to the convention used in Figure (2.2). Also note that Y_{bus} is the admittance matrix, where y_{11} and y_{22} are the sum of all admittances connected to nodes 1 and 2, respectively, and y_{12} and y_{21} are the negative of the admittances connecting nodes 1 and 2. Substituting the admittance parameters for the EMI filter into Y,

$$Y_{\text{bus}} = \begin{bmatrix} \frac{1}{z} & -\frac{1}{z} \\ -\frac{1}{z} & (\frac{1}{z} + y) \end{bmatrix} \tag{2.2.2}$$

where

$$z = \mathrm{R} + j\omega L \text{ and } y = j\omega C.$$

Substituting Equation (2.2.2) into Equation (2.2.1),

$$\begin{bmatrix} I_1 \\ -I_2 \end{bmatrix} = \begin{bmatrix} \frac{1}{z} & -\frac{1}{z} \\ -\frac{1}{z} & (\frac{1}{z} + y) \end{bmatrix} \begin{bmatrix} V_1 \\ V_2 \end{bmatrix}. \tag{2.2.3}$$

Rewriting Equation (2.2.3) in standard form,

$$I_1 = \tfrac{1}{z} V_1 - \tfrac{1}{z} V_2, \tag{2.2.4}$$

$$-I_2 = -\tfrac{1}{z} V_1 + \left(\tfrac{1}{z} + Y\right) V_2. \tag{2.2.5}$$

Solving Equation (2.2.5) for V_1,

$$V_1 = (yz + 1) V_2 + z I_2. \tag{2.2.6}$$

Substituting Equation **(2.2.6)** into Equation **(2.2.4)** and solving for **I,,**

$$I_1 = yV_2 + I_2 . \tag{2.2.7}$$

Rewriting Equation **(2.2.6)** and Equation **(2.2.7)** in matrix form,

$$\begin{bmatrix} V_1 \\ I_1 \end{bmatrix} = \begin{bmatrix} (yz+1) & z \\ y & 1 \end{bmatrix} \begin{bmatrix} V_2 \\ I_2 \end{bmatrix}. \tag{2.2.8}$$

Thus, the frequency response of V_1 and **I,** at the input of the filter can be determined given the values of R, L, C, V_2, and **I,.**

- Bridge rectifier. The purpose of the single-phase full-wave bridge rectifier is to convert the ac supply voltage into a dc voltage which is supplied to the high-,frequency oscillator. The construction of the full-wave bridge rectifier is based on the half-wave rectifier with a freewheeling diode [15]. **A** typical half-wave rectifier with a freewheeling diode is shown below in Figure **(2.3).**

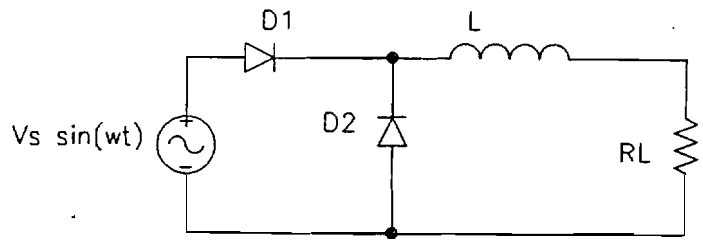

Figure **2.3** Half-wave rectifier with a freewheeling diode

Note that the freewheeling diode D_2 allows the continuous conduction of current through the load R_L during the period when D_1 is not conducting. The full-wave bridge rectifier consists of two half-wave rectifiers with freewheeling diodes connected as shown below in Figure **(2.4).** The advantages of the full-wave configuration are that the ac source contains no dc component and for the same ac voltage source, the ripple on the dc voltage and the average output voltage are equal

to twice that of the half-wave configuration. The disadvantage of the full-wave configuration is that the ac source and the dc load cannot share the same ground since they have no common terminal.

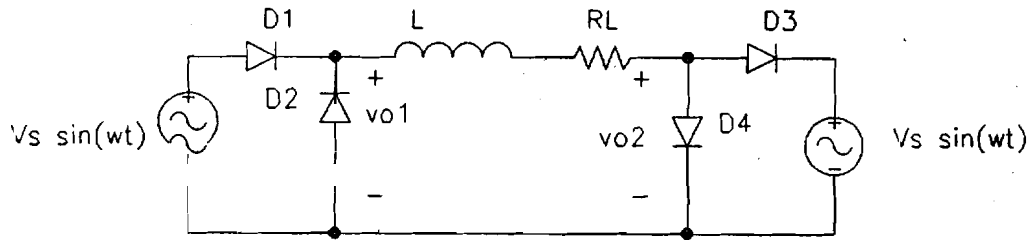

Figure 2.4 Full-wave bridge rectifier constructed from two half-wave bridge rectifiers

Since the two ac voltage sources used to construct the full-wave rectifier in Figure (2.4) are identical, the anode of D, and cathode of D_2 may be connected. Thus, only a single ac source is required, as shown in Figure (2.5).

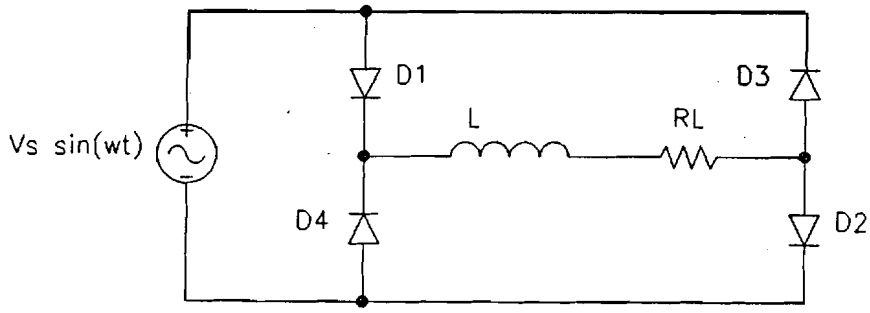

Figure 2.5 Equivalent circuit of a full-wave rectifier with a single supply

The average output dc voltage of a single half-wave rectifier shown in Figure (2.3) is

$$\langle v_{o1} \rangle = \frac{1}{2\pi} \int_0^{2\pi} V_s \sin(\omega t) d(\omega t) = \frac{V_s}{\pi} \qquad (2.2.9)$$

The average output dc voltage of the full-wave bridge rectifier may be derived from Equation (2.2.9) and Figure (2.4),

$$\langle v_o \rangle = \langle v_{o1} \rangle - (\gamma) \quad = \frac{V_s}{\pi} - (-g) = \frac{2V_s}{\pi} \tag{2.2.10}$$

Although the full-wave bridge rectifier produces a dc ripple voltage with a fundamental frequency equal to twice that of the half-wave rectifier, the amount of ripple voltage is still significant. To reduce the ripple voltage content, a low-pass filter is placed between the output of the rectifier and the load. The low-pass filter may either be an inductor placed in series between the output of the rectifier and the load or a capacitor placed in parallel across the output of the rectifier and the load. In most cases, an electrolytic capacitor is used due to the relatively large size and high cost of inductors.

When a low-pass capacitive output filter is added to the output of the bridge rectifier, the operating characteristics of the rectifier changes and the output voltage differs from that shown in Equation (2.2.10). Since the derivation of a bridge rectifier with a capacitive output filter is quite involved, the equations for a simple half-wave rectifier with a capacitive output filter and resistive load (shown below in :Figure (2.6)) will be presented.

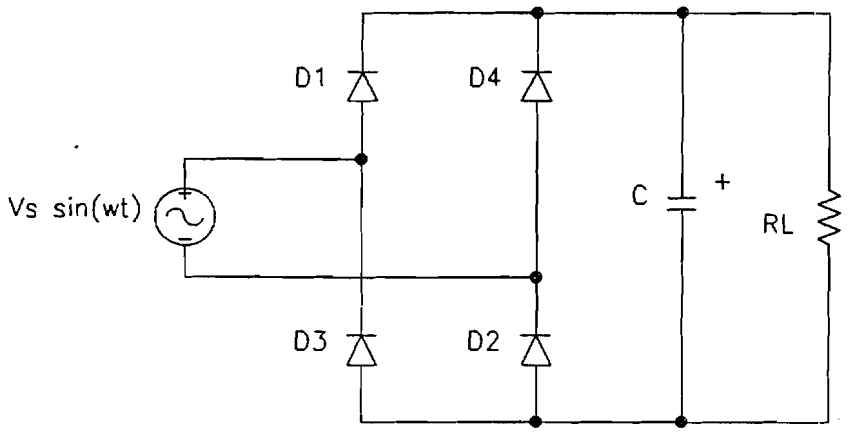

Figure 2.6 Full-wave bridge rectifier with a capacitive output filter

Note that the purpose of the phase angle a is to shift the time axis t=O to the point where the diode is just beginning to conduct. The angle at which the diodes ceases to

conduct is designated as β. The output voltage and source current during the conduction period of the diode, t=O to t=β/ω, can then be found to be [22]

$$v_o(t) = V_s \omega RC e^{-\frac{1}{RC}} \cos\alpha + V_s[\sin(\omega t + \alpha) - \omega RC \cos(\omega t + \alpha)] \qquad (2.2.11)$$

$$i_s(t) = \frac{V_s}{R_s} \omega RC \left[\cos(\omega t + \alpha) - e^{-\frac{1}{RC}} \cos\alpha \right] \qquad (2.2.12)$$

where

$$R_s << R_L,$$
$$\frac{R_s R_L}{R_s + R_L} = R \cong R_s,$$
$$1 + (\omega RC) \cong 1, \text{ and}$$
$$\frac{R_L}{R_s + R_L} \cong 1.$$

The conduction period of the diode can be qualitatively viewed from a. plot of the output voltage and the supply voltage and current. As shown below in Figure (2.7), the diode begins to conduct at time α/ω where the output voltage v_o across the capacitor is less than the supply voltage v_s. The charging of the capacitor, as defined in Equation (2.2.12) for a resistive load, ceases at time β/ω. It should be noted that the large harmonic current distortion which is produced by CFLs is due to the short conduction time (β–α)/ω produced by this rectifier/capacitive output filter combination.

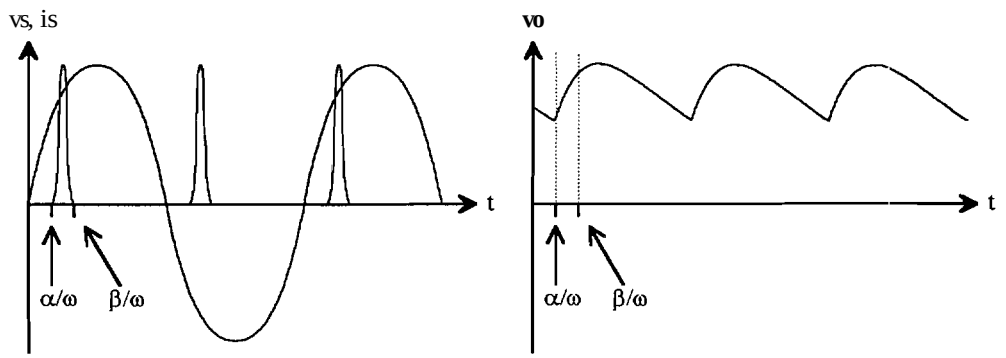

:Figure 2.7 Supply voltage and current and output voltage characteristics of a full-wave bridge rectifier

• High-frequency oscillator. The purpose of the high-frequency oscillator of the electronic ballast is to supply a high-frequency AC voltage to the output circuitry and fluorescent tube. This is accomplished by placing two controlled solid-state switches in series across the output of the bridge rectifier. The output section for a single-tube configuration is connected between the positive and common terminals of the oscillator. In the case of a twin-tube configuration, the additional output section is connected between the negative and common terminals of the oscillator. Typical single- and twin-tube configurations are shown below in Figure (2.8).

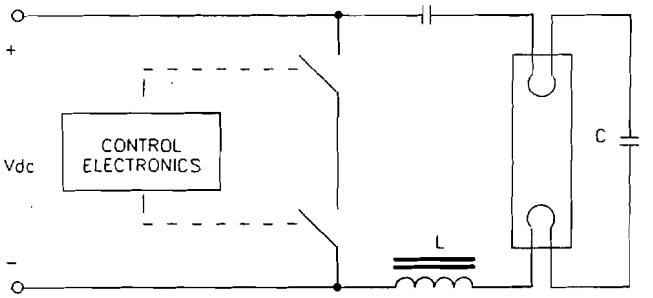

(a) Single–tube configuration

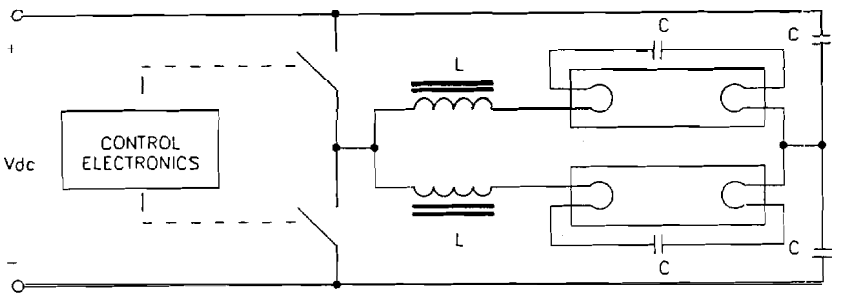

(b) Twin–tube configuration

Figure 2.8 Typical high frequency oscillator configurations used in electronic ballast CFLs

As shown in Figure (2.8), the oscillator consists of two controllable solid-state switches to convert the rectified DC voltage into the desired high-fi-equency AC voltage supplied the output section of the CFL. Typically, power MOSFETs are used to implement the switching of the oscillator. Shown below in Figure (2.9), the power MOSFET is a controllable solid-state switch, capable of withstanding relatively large "off" state voltages and "on" state currents.

Figure 2.9 Schematic symbols for an n-channel MOSFET and HEXFET

The MOSFET is a three-terminal solid-state device consisting of a gate, drain, and source terminal. It is essentially a "full-on/full-off" switch, controlled by the voltage applied across its gate and source terminals, v_{GS}. When the applied v_{GS} is below the threshold voltage of the MOSFET, the device supports the open-circuit drain-to-source voltage. When the applied v_{GS} exceeds the threshold voltage, the device conducts and current is allowed to flow from the drain to the source terminal. In other words, the MOSFET supports a positive voltage across its drain and source terminals when off and allows a positive current to flow from its drain to source terminal when on.

In applications where bi-directional current flow between the drain and source is required, a rectifier diode (sometimes referred to as a "freewheeling" diode) is placed across the drain and source terminals of the MOSFET. With the anode of the freewheeling diode connected to the source terminal and the cathode connected to the drain, current is also allowed to flow from the source to the drain terminal of a n-channel MOSFET. Some manufacturers incorporate both the MOSFET and

freewheeling diode in a single package (e.g., International Rectifier's IRF624 HEXFET). The schematic symbol for a n-channel HEXFET is shown in Figure (2.9).

The output section for a typical electronic ballast CFL consists of two capacitors, C_1 and C_2, an inductor, L, and the fluorescent tube, such as that shown previously in Figure (2.8). If the fluorescent tube is modeled as a fixed resistor in the steady-state, an equivalent output section (with a resistance R_{tube} substituted for the fluorescent tube) may drawn for the LOA 30 watt Circline CFL as shown below in Figure (2.10).

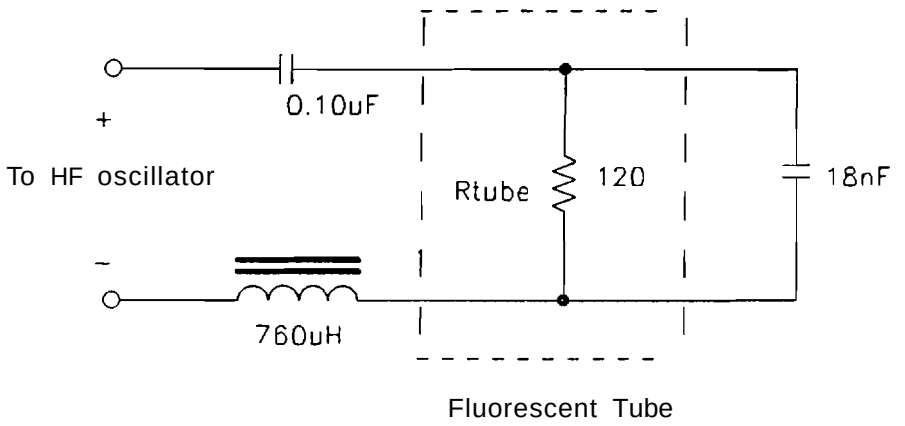

Figure 2.10 Equivalent output section of the LOA 30 watt Circline electronic ballast CFL

The state equations for the output section shown in Figure (2.10) may be derived by defining

$$\overline{Q} = \begin{bmatrix} q_1 \\ q_2 \\ q_3 \end{bmatrix} = \begin{bmatrix} v_{C_1} \\ v_{C_2} \\ i_L \end{bmatrix}$$

as the state variables of the circuit. Applying KVL to the circuit yields,

$$v_{osc} = q_1 + q_2 + Lq_3'. \qquad (2.2.13)$$

Applying KCL at node 2 yields,

$$-C_1 q_1' + \tfrac{1}{R} q_2 + C_2 q_2' = 0. \tag{2.2.14}$$

Finally, applying KCL at node 2 yields,

$$-C_1 q_1' = q3. \tag{2.2.15}$$

Rewriting Equations (2.2.13) through (2.2.15) in matrix form yields,

$$\begin{bmatrix} -C_1 & 0 & 0 \\ -C_1 & C_2 & 0 \\ 0 & 0 & L \end{bmatrix} \overline{Q'} = \begin{bmatrix} 0 & 0 & 1 \\ 0 & -\frac{1}{R} & 0 \\ -1 & -1 & 0 \end{bmatrix} \overline{Q} + \begin{bmatrix} 0 \\ 0 \\ 1 \end{bmatrix} v_{osc} \tag{2.2.16}$$

Solving Equation (2.2.16) for $\overline{Q'}$ yields,

$$\overline{Q'} = \overline{A} \cdot \overline{Q} + \overline{B} \cdot v_{osc} \tag{2.2.17}$$

where

$$\overline{A} = \begin{bmatrix} 0 & 0 & -\frac{1}{C_1} \\ 0 & -\frac{1}{RC_2} & -\frac{1}{C_2} \\ -\frac{1}{L} & -\frac{1}{L} & 0 \end{bmatrix} \text{ and } \overline{B} = \begin{bmatrix} 0 \\ 0 \\ \frac{1}{L} \end{bmatrix}.$$

- Fluorescent tube. The fluorescent tube consists of an inert gas and a small amount of mercury housed by a glass tube and end-caps. When a voltage is applied across the electrodes of the tube, mercury-discharge occurs and a number of the electrons in the tube emit UV radiation. This UV radiation reacts with the fluorescent coating on the inside of the tube and produces visible light. Further detailed information on the process in which electric energy is converted into light in a fluorescent lamp is given in Section (1.3).

2.3 Modeling of the distribution network

The distribution network modeled consists of three sections: the distribution transformer, the transmission line, and the voltage source. These sections are shown pictorially in the schematic diagram below. In addition, each section will also be described in detail below.

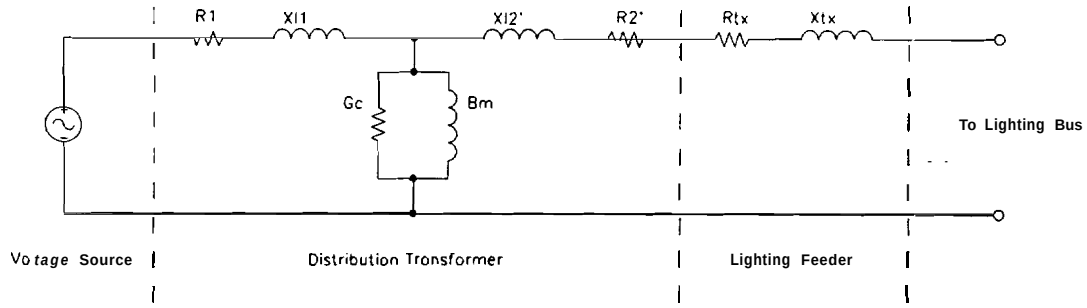

Figure 2.11 Schematic diagram of a typical distribution network

• Distribution transformer. The transformer is magnetically coupled circuit, consisting of a primary winding and a secondary winding magnetically coupled by an higli-permeability iron core [23]. When an alternating current is applied to the primary winding, an alternating mutual flux is produced in the iron core which induces an alternating current to flow in the secondary winding. Depending on the ratio of primary to secondary windings, the transformer may step-up or step-down the voltage applied across the primary winding, which appears across the secondary winding. A simplified diagram of a transformer is shown below in Figure (2.12).

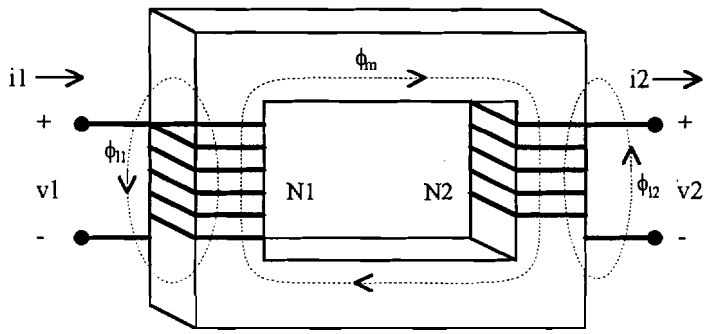

Figure 2.12 Simplified diagram of a transformer

Due to the conductive nature of the iron-core of the transformer, the mutual flux induced in the core also produces eddy currents to flow in the core. Because the iron-core has a resistance associated with it, these eddy currents produce losses appearing as heat dissipated from the core, otherwise known as I^2R losses. To reduce eddy current losses, transformer cores are usually constructed from thin laminated sheets of iron. Two typical transformer core constructions are shown below in Figure (2.13). The core-type construction consists two "legs", with the primary and secondary windings wound on both legs, while the shell-type construction consists of three legs, with the primary and secondary windings wound on the center leg.

As shown in Figure (2.12), both the primary and secondary windings have a leakage flux associated with them. Unlike the mutual flux which is confined to the core of the transformer and links both windings, the leakage flux travels largely in air and links only the winding it is associated with. To reduce the amount of leakage flux produced by the windings, the primary and secondary windings are subdivided into sections and are placed as close together as possible. In the core-type construction, the primary and secondary windings are subdivided between the two core legs and are wound concentrically on the legs. In the shell-type construction, the primary and secondary windings are subdivided into a number of "pancakes" and are alternately wound on the center leg. These winding methods are also shown in Figure (2.13) below.

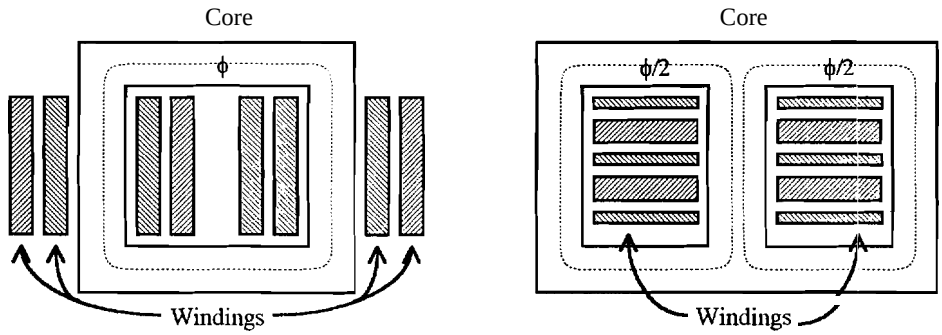

(a) Core-type **(b)** Shell-type

Figure **2.13** Typical transformer core constructions and winding methods

Before deriving the equivalent circuit used to model the transformer, the following equations need defining,

$$F = NI \tag{2.3.1}$$

$$\lambda = N\varphi \tag{2.3.2}$$

$$e = \frac{d\lambda}{dt} = N\frac{d\varphi}{dt} \tag{2.3.3}$$

where

F = magnetomotive force (mmf) associated with winding,

N = number of turns in winding

I = current flowing through winding,

λ = flux linkage associated with winding,

φ = flux associated with winding, and

e = electromotive force (emf) associated with winding.

When a time-varying voltage V_1 is applied across the primary winding, a leakage flux φ_{l1} is produced such that V_1 equals the sum of the voltage drop due to the primary resistance, $R_1 I_1$, the voltage drop due to the leakage reactance, $X_{l1} I_1$, and the counter emf, E, . This can also be stated as,

$$V_1 = R_1 I_1 + X_{l1} I_1 + E_1 \tag{2.3.3}$$

where

V_1 = primary terminal voltage,

I_1 = primary winding current,

R_1 = primary winding resistance,

X_{l1} = primary winding leakage reactance ($= \omega L_{l1}$), and

E_1 = primary counter emf.

Equation (2.3.3) may be expressed pictorially as shown in Figure (2.14) below. Note that all voltages, currents, fluxes, and emf's shown are phasors.

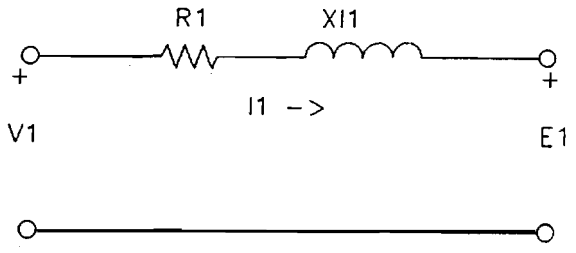

Figure 2.14 Equivalent circuit for Equation (2.3.3)

The mutual flux, 0 , which is confined to the iron-core and thus links both the primary and secondary windings, is created by the combined mmfs produced by the current flowing through the primary and secondary windings. The primary current I_1 must counteract the demagnetizing effect of the current flowing in the secondary winding and also must produce the mmf to obtain the resultant mutual flux **O.** Thus I_1 may be rewritten as

$$I_1 = I_2' + I_\varphi \tag{2.3.4}$$

where

I_1 = primary current,

I_2' = load current, and

I_φ = exciting current.

The load current I_2' is the component of the primary curreni: required to counteract the mmf of the secondary current I_2. It is equal to the secondary current referred to the primary as in an ideal transformer. The exciting current is the component of the primary current required to produce the mmf to obtain the mutual flux Φ. Due to the nonlinear magnetic properties of the iron-core, the waveform of the exciting current is nonsinusoidal. Since the exciting current is often small in comparison to the load current, it may be approximated as an equivalent sine wave which has the same rms value and frequency and produces the same average power as the actual exciting current waveform. When this is done, the exciting current may be further resolved into a core-loss component and a magnetizing component. Thus, exciting current I_Φ may be rewritten as

$$I_\Phi = I_c + I_m \tag{2.3.5}$$

where

I_Φ = exciting current,

I_c = core-loss current, and

I_m = magnetizing current.

The core-loss current I_c flows through a resistance whose conductance is G_C. The power dissapated in the core-loss conductance, $E_1 G_C$, is responsible for eddy current losses in the core due to the mutual flux. The magnetizing current I_m flows through an inductor whose susceptance is B_2. The magnetizing susceptance B_2 varies with the saturation of the iron-core. The division of the exciting current into the core-loss and magnetizing branches is shown pictorially in Figure (2.15).

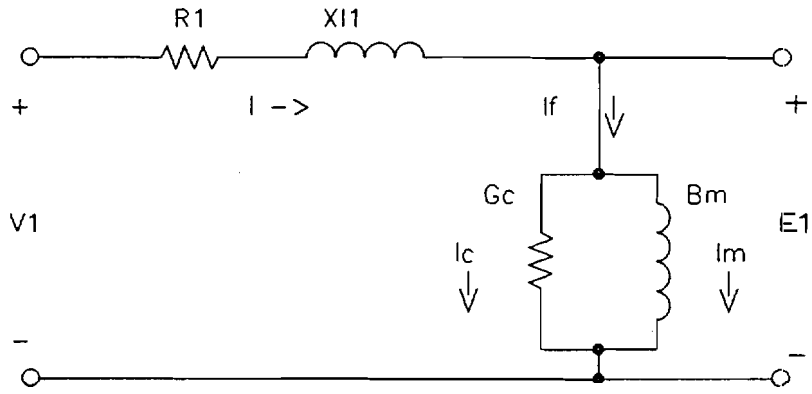

Figure **2.15** Equivalent circuit for Equation **(2.3.5)**

The resultant mutual flux Φ induces an emf E_2 which links both the primary and secondary windings. The emfs E, and E_2 may be represented pictorially as an ideal transformer, as shown below in Figure **(2.16).**

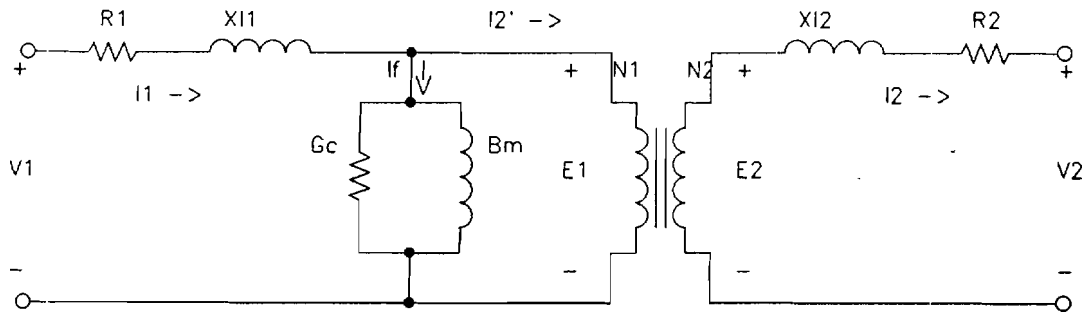

Figure **2.16** Equivalent transformer circuit including ideal transformer

Similar to the primary winding, the secondary winding also has a winding resistance R_2 and leakage reactance X_{l2}. The terminal voltage V_2 appearing across the secondary winding may be written as,

$$V_2 = -R_2 I_2 - X_{l2} I_2 + E_2 \qquad (2.3.6)$$

where

V_2 = secondary terminal voltage,

I_2 = secondary winding current,

R_2 = secondary winding resistance,

X_{l2} = secondary winding leakage reactance (= ωL_{l2}), and

E_2 = secondary counter emf.

The transformer circuit shown in Figure (2.16) may be further simplified by referring the secondary variables V_2, I,, R_2, and X_{l2} to the primary. The equivalent T-circuit for the transformer with all secondary variables referred to the primary winding is shown below in Figure (2.17).

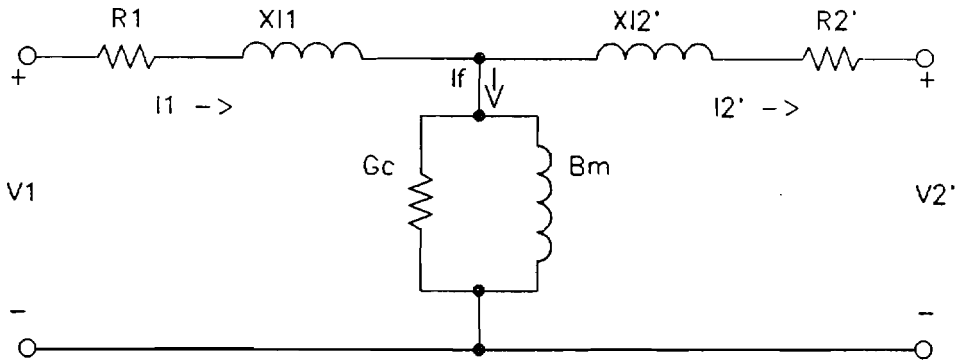

Figure 2.17 Equivalent T-circuit representation of transformer

The values for the primary and secondary winding resistances and leakage reactances may be obtained experimentally by performing a short-circuit test on the transformer. This is done by short-circuiting the secondary winding of the transformer (usually taken as the low-voltage side) and applying a relatively small .voltage (2 to 12% of rated) across the primary winding of the transformer (usually taken as the high-voltage side). The applied short-circuit voltage, V_{sc}, and resulting short-circuit current and power, I_{sc} and P_{sc}, may be measured. The values for the equivalent winding impedance and its equivalent winding resistance and leakage reactance components may be obtained from the following equations,

$$Z_{eq} = Z_{sc} = \frac{V_{sc}}{I_{sc}} \qquad (2.3.7)$$

$$R_{eq} = R_{sc} = \frac{P_{sc}}{I_{sc}^2} \tag{2.3.8}$$

$$X_{eq} = X_{sc} = \sqrt{|Z_{sc}|^2 - R_{sc}^2} \tag{2.3.9}$$

where

Z, = equivalent primary and secondary winding impedance,

R_{eq} = equivalent primary and secondary winding resistance, and

X_{eq} = equivalent primary and secondary winding leakage reactance:.

Note that Z_{eq}, R, and X_{eq} are the equivalent impedance, resistance, and leakage reactance of the primary and secondary windings combined The values of the independent primary and secondary winding resistances and leakage reactances may be obtained by assuming that R, = R_2 = 0.5 R, and $X_{l1} = X_{l2} = 0.5\, X_{eq}$ when all impedances are referred to the same side.

The values for the core-loss conductance and the magnetizing susceptance may be obtained experimentally by performing a open-circuit test on the transformer. This is done by open-circuiting the secondary winding of the transformer (usually taken as the high-voltage side) and applying the rated voltage across the primary winding of the transformer (usually taken as the low-voltage side). The applied open-circuit voltage, V_1, and resulting exciting current and power dissapated in the primary winding, I_φ and P,, may be measured, respectively. The values (referred to the primary winding) for the exciting admittance and its core-loss conductance and magnetizing susceptance components may be obtained from the following equations,

$$Y_\varphi = Y_{oc} = \frac{I_\varphi}{V_1} \tag{2.3.10}$$

$$G_c = G_{oc} = \frac{P_1}{V_1^2} \tag{2.3.11}$$

$$B_m = B_{oc} = \sqrt{|Y_{oc}|^2 - G_{oc}^2}\ . \tag{2.3.12}$$

- Transmission line. The equivalent circuit used to model the distribution lighting feeder was the short transmission line model [30]. Shown below in Figure (2.18), the single-phase short transmission line model consists of a series impedance, Z_{tx}, which includes the resistance, R_{tx}, and reactance, X_{tx}, associated with the line.

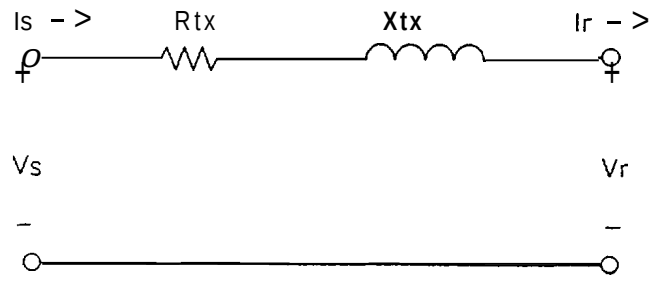

Figure 2.18 Single-phase short transmission line model

The sending end voltage, V_S, and sending end current, I,, are located at the connection between the distribution transformer secondary and the lighting feeder. The receiving end voltage, V_R, and receiving end current, I,, are located at the connection between the lighting feeder and the lighting bus. It should be noted that the sending and receiving end currents are equal, i.e.,

$$I_S = I_R . \tag{2.3.13}$$

The voltage at the sending end may be expressed as

$$V_S = V_R + I_R Z. \tag{2.3.14}$$

- Voltage source. For purposes of simulation, an ideal voltage source was used to model the voltage bus supplying the distribution lighting feeder. For the single-phase case, a pure 60 Hz sinusoidal ac voltage source with a rms value of 120 volts and zero phase shift was used to model the single-phase line-to-neutral voltage bus, i.e.,

$$V_s = 120\sqrt{2}\ \sin(2\pi 60t). \tag{2.3.15}$$

For the three-phase case, three identical ac voltage sources phase shifted by 120 degrees from each other was used to model the three-phase wye-connected voltage bus, i.e.,

$$V_A = 120\sqrt{2}\ \sin(2\pi 60t) \tag{2.3.16}$$

$$V_B = 120\sqrt{2}\ \sin(2\pi 60t - 120^\circ) \tag{2.3.17}$$

$$V_C = 120\sqrt{2}\ \sin(2\pi 60t - 240^\circ). \tag{2.3.18}$$

CHAPTER 3

EXPERIMENTAL RESULTS AND SIMULATION DEVELOPMENT

3.1 Introduction

The main objectives of this thesis are to identify the harmonic current distortion produced by commercially available electronic ballast CFLs and their effects on the power distribution system. Experimental data of a number of electronic ballast CFLs is first presented to identify the current distortion produced by these lamps. A simulation of the electronic ballast CFL is then developed for purposes of application in a distribution network model.

The tests shown in Chapters 3 and 4 are organized as shown in Table (3.1). The test numbers generally begin with a lamp designation shown in Table (3.2). The designations "E" and "S" refer to "experimental" (i.e., laboratory measurements) and "simulation", respectively. Thus, Test 5E refers to the experimental results from Lamp 5, the Phillips Earthlight SL18/27; Test 8S refers to the simulation results from Lights of America 2030; etc. The designators "O", "OP", and "VI" refer to the tube current characteristics, tube power consumption, and tube voltage versus current characteristics, respectively. Tests 1E through 8VIS are described in Chapter 3. The designator "B" refers to boost converter modifications to the electronic ballast described in Chapter 4. The designator "T" refers to three phase tests which are also described in Chapter 4.

Table 3.1 Summary of experimental and simulation plots

Test No.	Figure No.	Lamp No.	Measured	Simulated	Phases	Measured/Calculated Quantities
1E	3.2	1	X		1	V, I, FFT_I
2E	3.3	2	X		1	V, I, FFT_I
3E	3.4	3	X		1	V, I, FFT_I
4E	3.5	4	X		1	V, I, FFT_I
5E	3.6	5	X		1	V, I, FFT_I
6E	3.7	6	X		1	V, I, FFT_I
7E	3.8	7	X		1	V, I, FFT_I
8E	3.9	8	X		1	V, I, FFT_I
8OE	3.11	8	X		1	$I_{\mathrm{fil}}^{\mathrm{in}}$, $I_{\mathrm{fil}}^{\mathrm{out}}$, I_{tube}
8OPE	3.12	8	X		1	V_{tube}, I_{tube}, $\mathrm{P}_{\mathrm{tube}}$
8VIE	3.13	8	X		1	V_{tube}, I_{tube}
8S	3.19	8		X	1	V, I, FFT_I
8OS	3.2	8		X	1	$I_{\mathrm{fil}}^{\mathrm{in}}$, $I_{\mathrm{fil}}^{\mathrm{out}}$, I_{tube}
8OPS	3.21	8		X	1	V_{tube}, I_{tube}, $\mathrm{P}_{\mathrm{tube}}$
8VIS	3.22	8		X	1	V_{tube}, I_{tube}
8VES	3.26	8	X	X	1	V_{tube}
8IES	3.27	8	X	X	1	I_{tube}
8OPES	3.28	8	X	X	1	$\mathrm{P}_{\mathrm{tube}}$
8ES	3.29	8	X	X	1	V, I
8BS	4.4	8		X	1	V, I, FFT_I
8TS	4.6	8		X	3	V_A, I_N, $\mathrm{FFT}_{\mathrm{In}}$
8TE	4.7	8	X		3	V_A, I_N, $\mathrm{FFT}_{\mathrm{In}}$

Table 3.2 Incandescent lamps and CFLs evaluated

Lamp No.	Manufacturer	Model #	Power (watts)	Average Lumen Output	P (hours)
1	General Electric	Soft White	15	110	2,500
2	Sylvania	Soft White	60	810	700
3	Sylvania	Energy Saver	67	1,080	700
4	Osram	DULUX EL15W	15	900	10,000
5	Phillips	Earthlight SL18/27	18	Not available	Not available
6	General Electric	BIAX FLE20DBX/SPX27	20	1,200	8,000
7	General Electric	BIAX FLC26	26	1,500	10,000
8	Lights of America	2030	30	2,250	10,000

3.2 Experimental results

A large majority of the electronic ballast CFLs currently available produce significant amounts of harmonic current distortion. To identify the characteristics of the current distortion produced by these lamps, the voltage and current characteristics of a number of electronic ballast CFLs produced by various manufacturers were obtained experimentally. As a reference, three incandescent lamps were also evaluated. The manufacturer-provided data for each lamp is summarized in Table (3.2) shown previously.

The circuit used to evaluate the lamps is shown below in Figure (3.1). A transformer was used to couple the voltage source and the lamp under test to isolate the oscilloscope input from the line voltage. A single phase 240V/120V 1.5 kVA distribution transformer with a 3.5% impedance was used to minimize the effect of harmonic filtering due to the transformer.

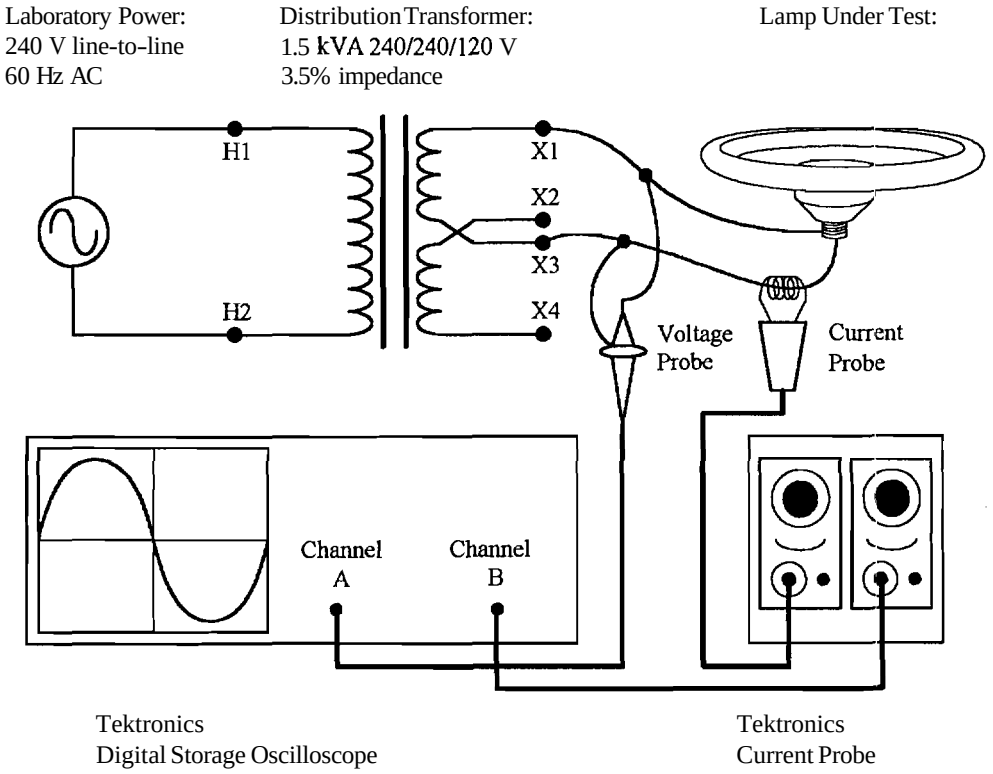

Figure 3.1 Circuit used for experimental evaluation of lamps

The voltage and current waveforms obtained for each lamp from the Tektronics data acquisition unit was then fed into MATLAB and the results were plotted, as shown in Figures (3.2) through (3.9) on the following pages. For each lamp, the supply current waveform (solid) is shown on the top graph along with the scaled supply voltage waveform (dashed) shown as a reference. The fast Fourier transform (FFT) of the supply current was computed by MATLAB and is shown on the bottom graph. In addition, MATLAB was also used to compute the rms values of the supply voltage and current (V_{rms} and I_{rms}), the fundamental supply voltage and current (V_{1rms} and I_{1rms}), the active and apparent power consumed by the lamp (P and S), the displacement and true power factor (dPF and tPF), the total harmonic distortion of the voltage and current (THD_v and THD_i), and finally, the crest factor (CF) of the current. The data obtained for each lamp is summarized in Table (3.3).

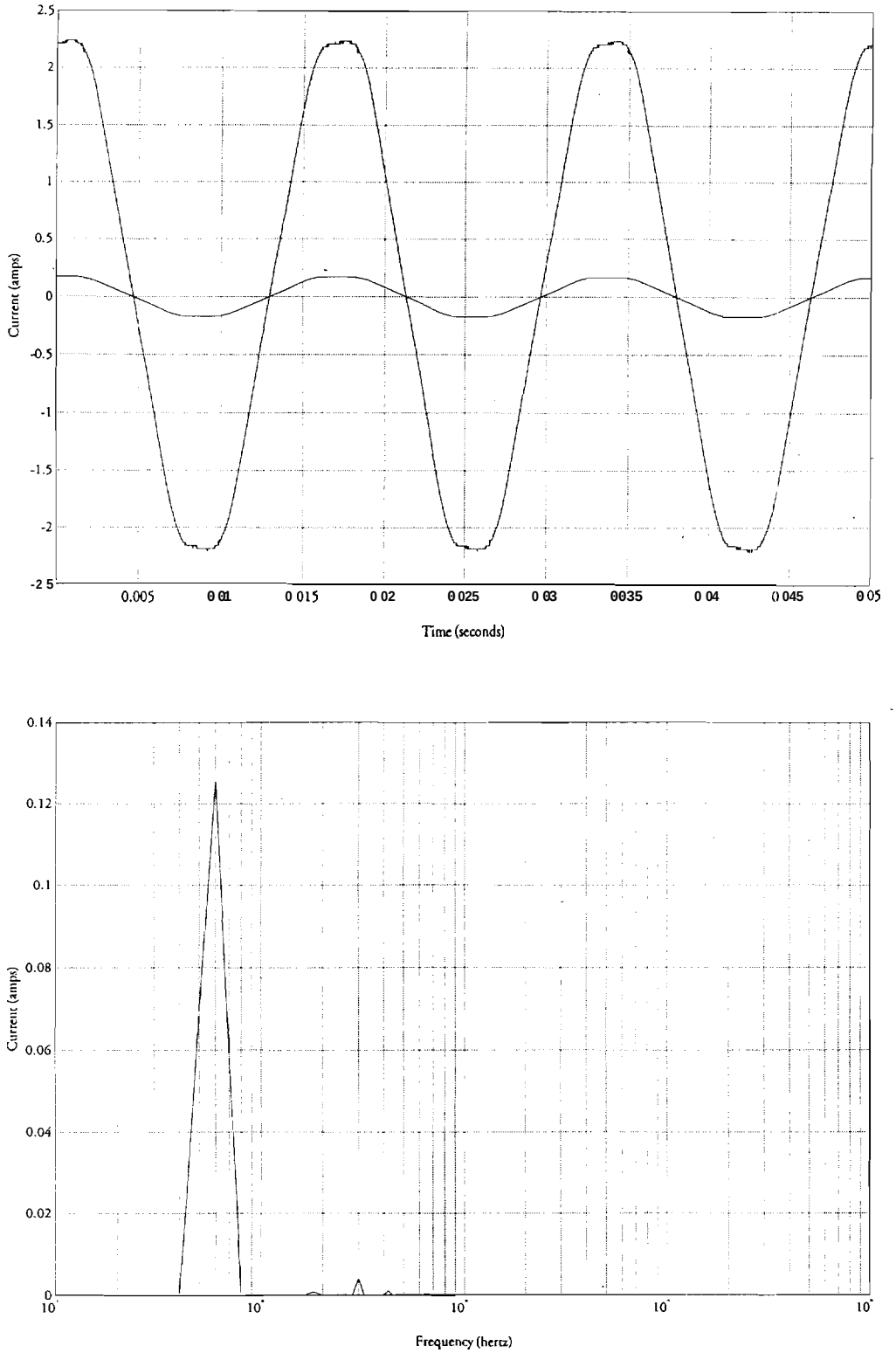

Figure 3.2 Test 1E: Plots of experimental supply voltage and current obtained from General Electric 15 W incandescent lamp

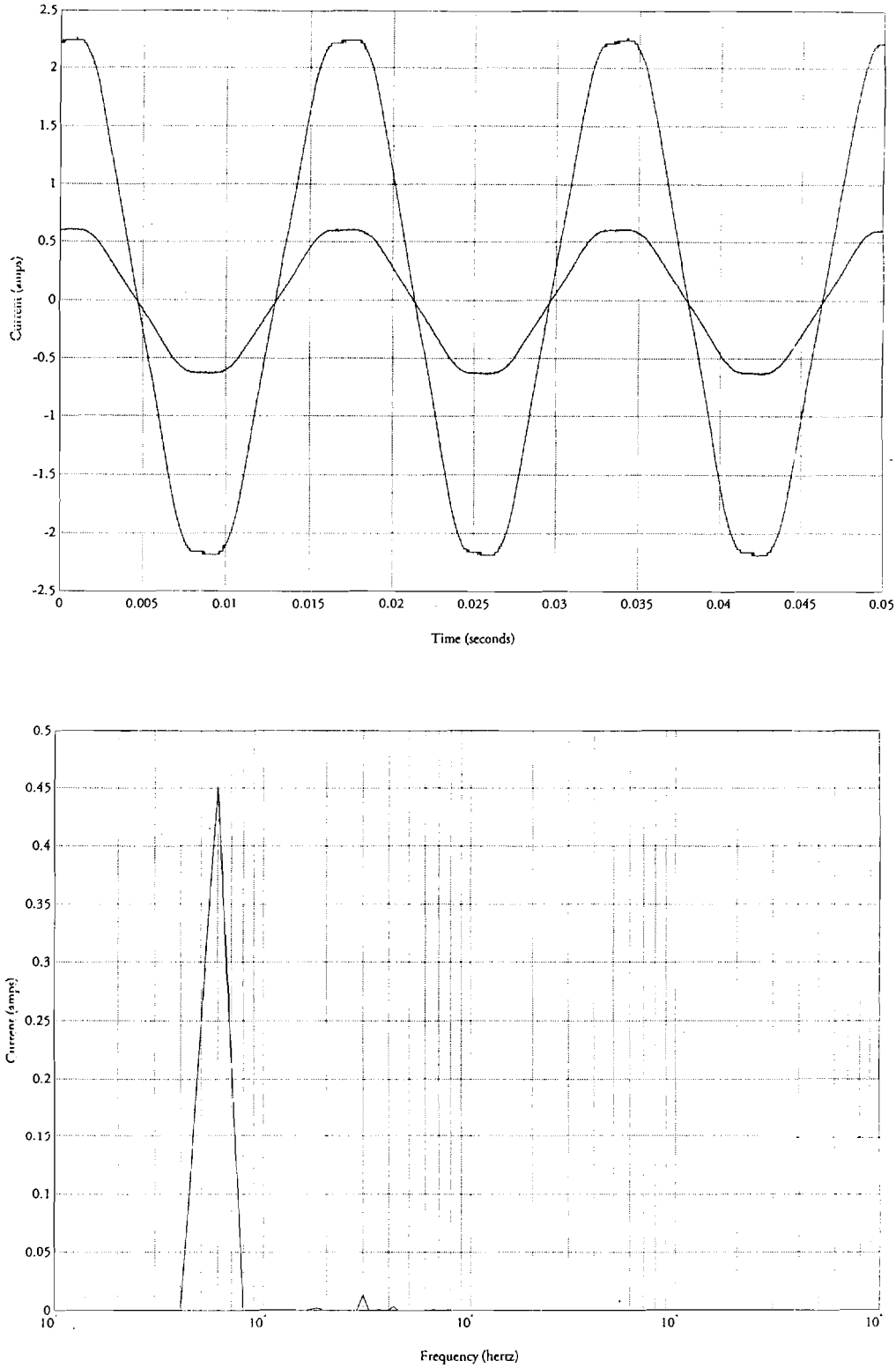

Figure 3.3 Test 2E: Plots of experimental supply voltage and current obtained from Sylvania 60 W incandescent lamp

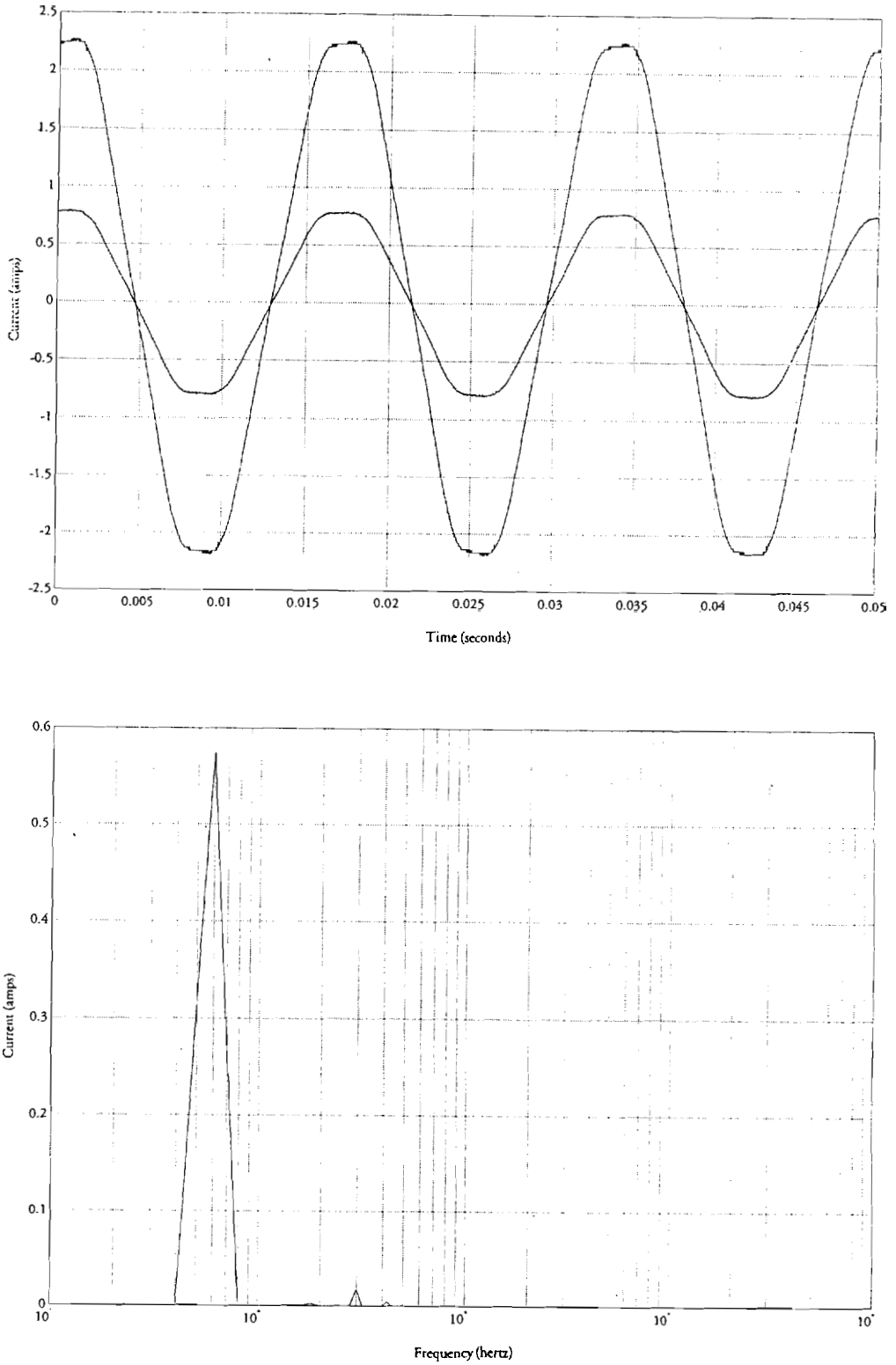

Figure 3.4 Test 3E: Plots of experimental supply voltage and current obtained from Sylvania 67 W Energy Saver incandescent lamp

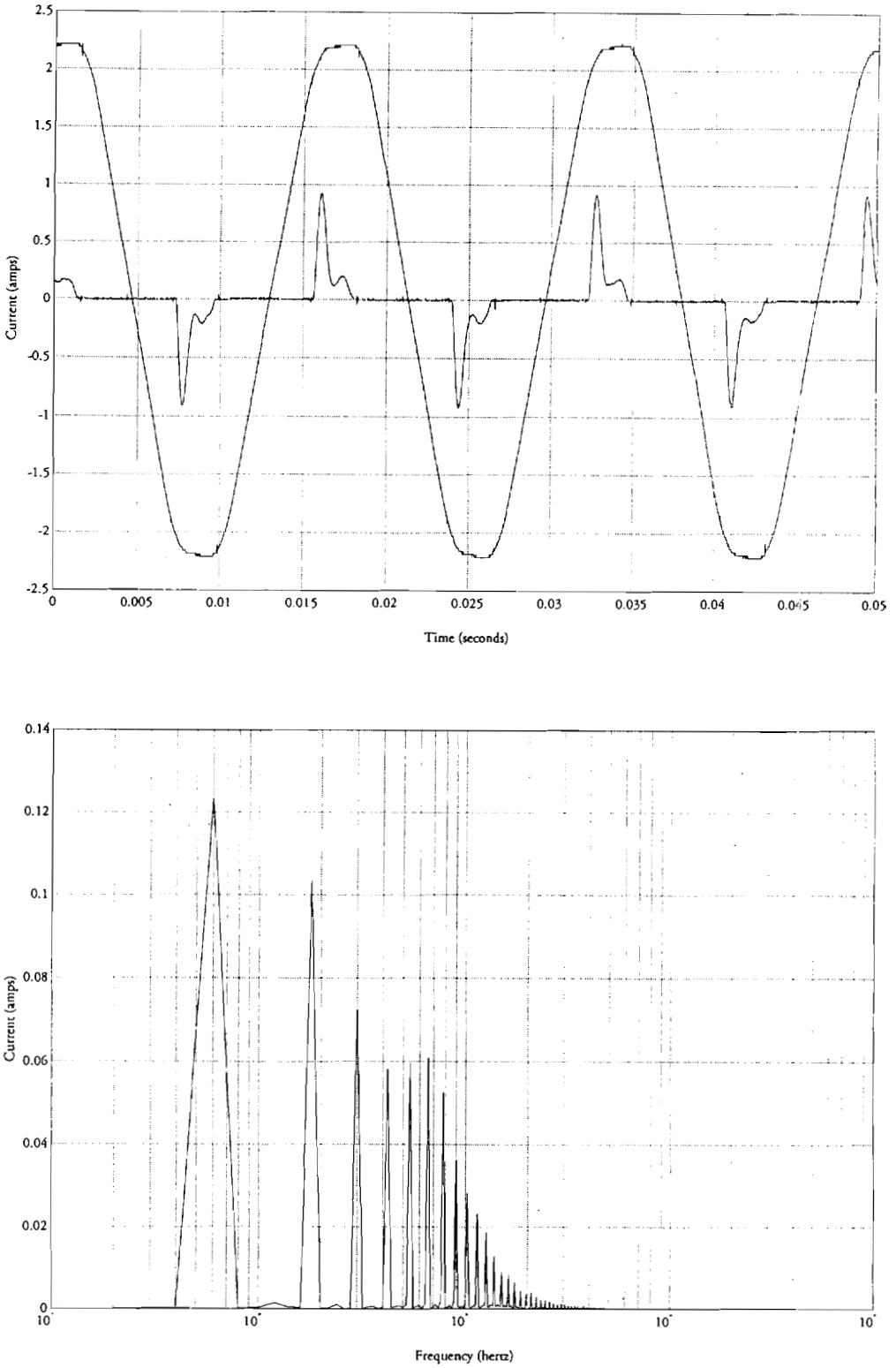

Figure 3.5 Test 4E: Plots of experimental supply voltage and current obtained from Osram DULUX EL15W 15 W electronic ballast CFL

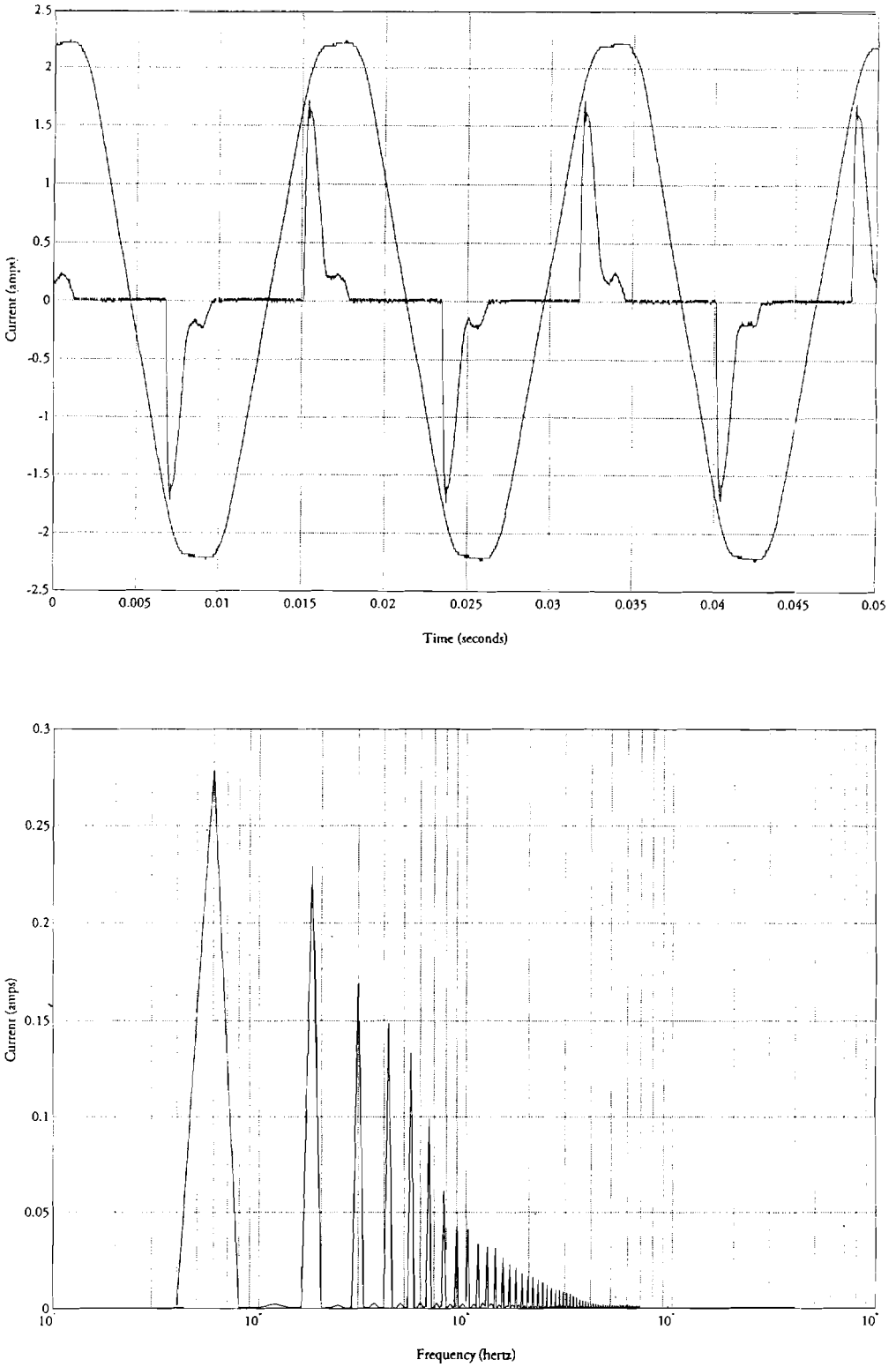

Figure 3.6 Test 5E: Plots of experimental supply voltage and current obtained from Phillips Earthlight SL18/27 18 W electronic ballast CFL

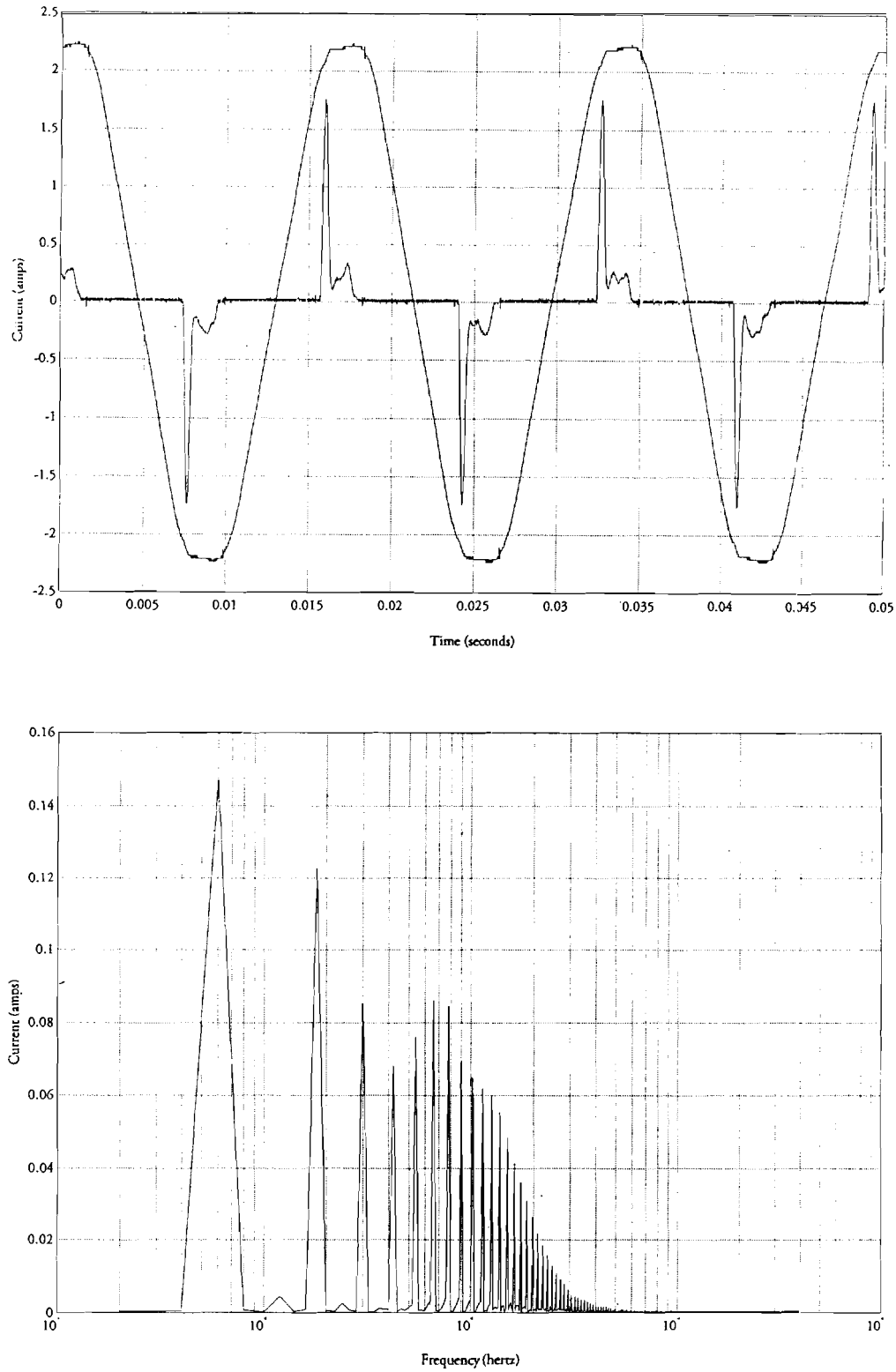

Figure 3.7 Test 6E: Plots of experimental supply voltage and current obtained from General Electric BIAX FLE20DBX/SPX27 20 W electronic ballast CFL

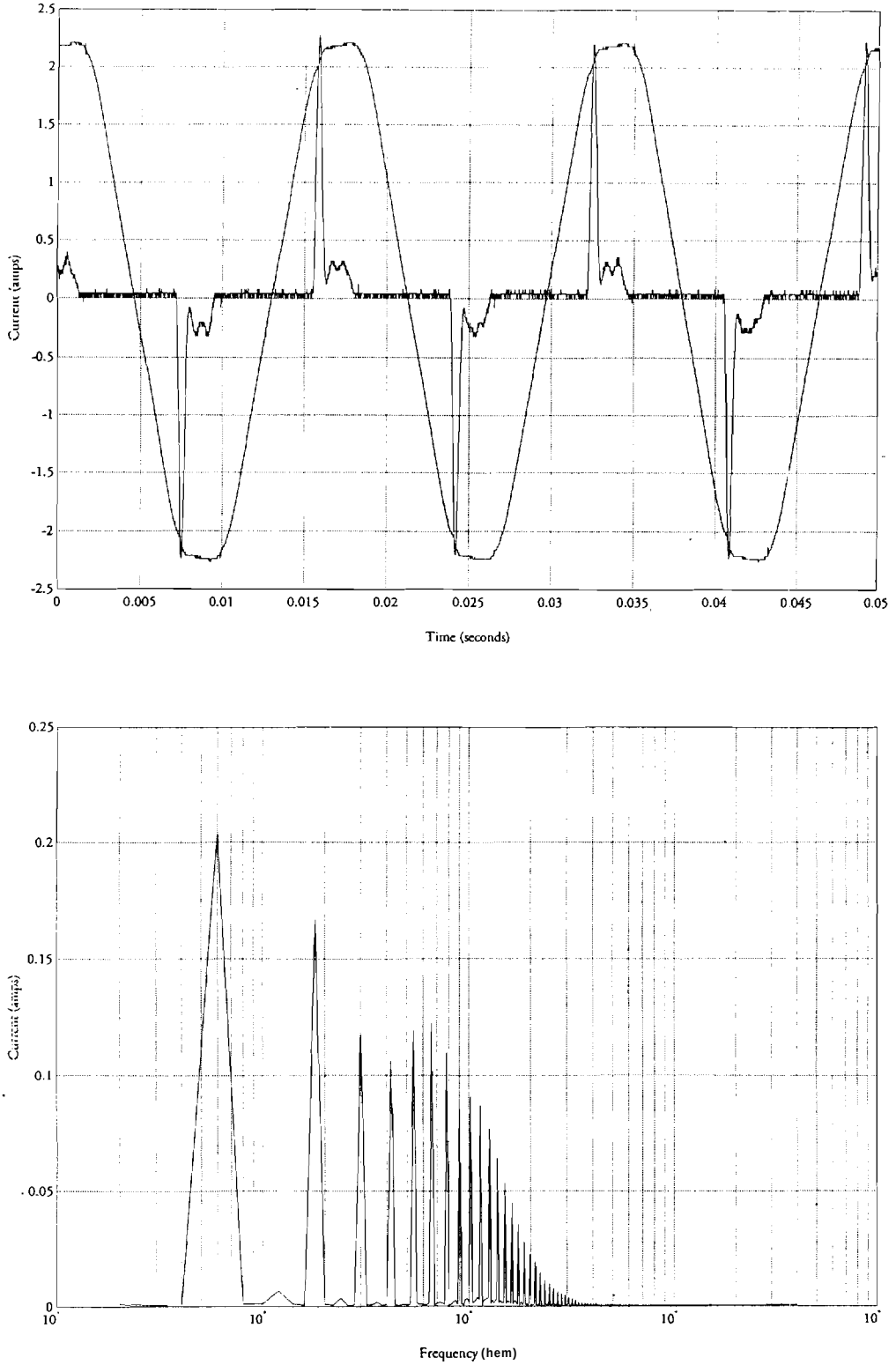

Figure 3.8 Test 7E: Plots of experimental supply voltage and current obtained from General Electric BIAX FLC26 26 W electronic ballast CFL

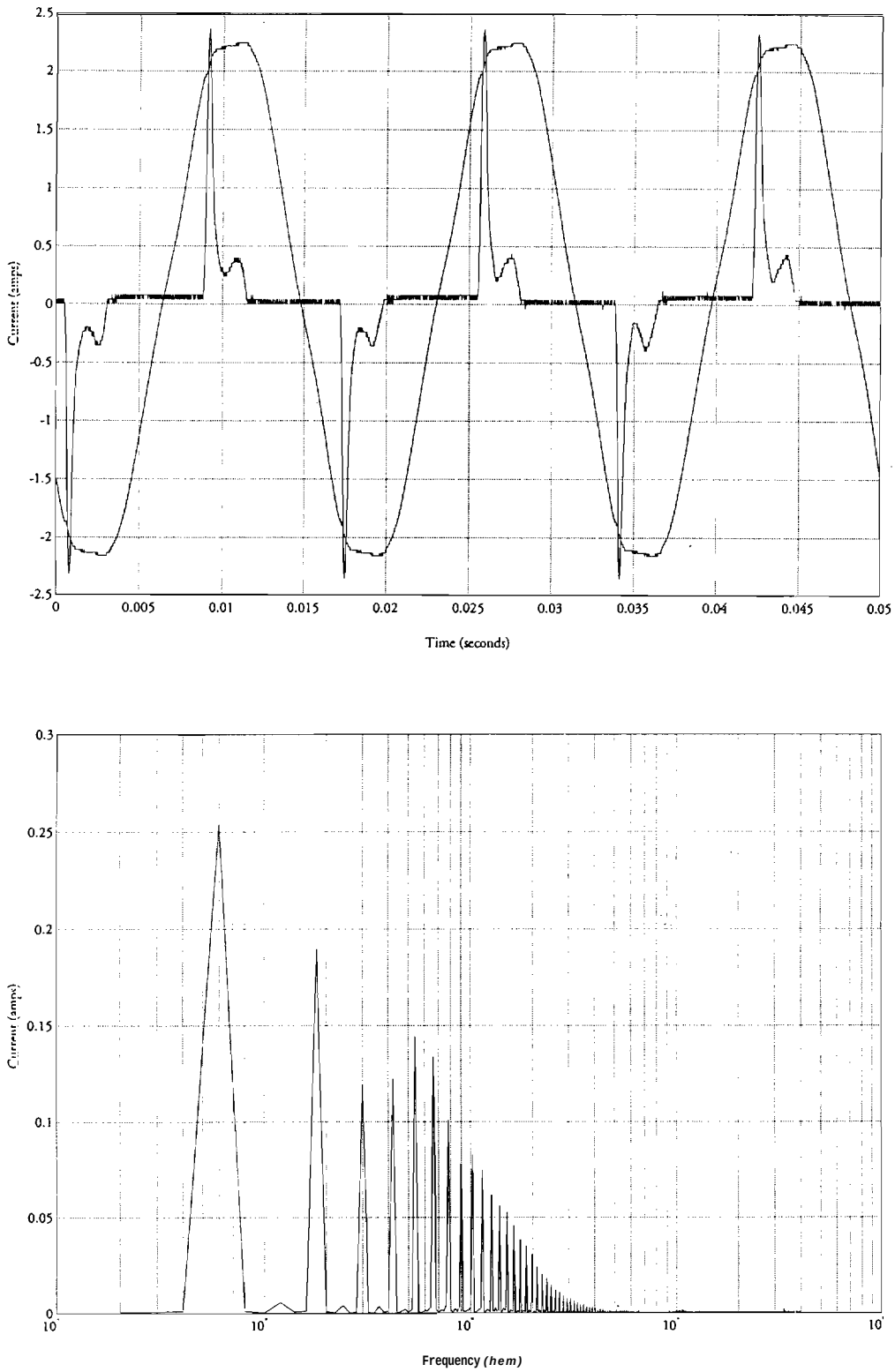

Figure 3.9 Test 8E: Plots of experimental supply voltage and current obtained from Lights of America 2030 30 W Circline electronic ballast CFL

Table 3.3 Data obtained from experimental evaluation of lamps

Lamp No.	Figure No.	V_{1rms} (volts)	I_{1rms} (amps)	V_{rms} (volts)	I_{rms} (amps)	P (watts)	S (VA)	tPF	dPF	THD_v (%)	THD_i (%)	CF
1	3.2	121.66	0.13	121.72	0.13	15.35	15.35	1	1	3.2	3.33	1.36
2	3.3	121.76	0.45	121.82	0.45	55.14	55.15	1	1	3.17	3.19	1.35
3	3.4	121.53	0.58	121.59	0.58	70.05	70.05	1	1	3.15	3.22	1.37
4	3.5	121.67	0.12	121.73	0.22	14.44	26.85	0.54	0.96	3.14	147.1	4.22
5	3.6	122	0.28	122.06	0.47	30.9	57.83	0.53	0.89	3.25	137.15	3.63
6	3.7	122.1	0.15	122.17	0.31	17.19	38.32	0.45	0.95	3.24	187.27	5.61
7	3.8	122.32	0.2	122.39	0.42	23.58	51.94	0.45	0.93	3.26	182.09	5.37
8	3.9	120.85	0.25	120.95	0.47	28.29	56.36	0.5	0.91	4.09	153.04	5.07

Note: **The MATLAB code used to calculate the data show in the table above may be found in Appendix A.**

3.3 Simulation development

In order to investigate the effects of the electronic ballast CFL on the distribution system, a simulation of a general electronic ballast CFL was developed, as described in Section 2.2. The simulation of the electronic ballast CFL was based on the Lights of America (LOA) Model 2030 30 watt Circline electronic ballast CFL. The experimental supply and tube voltage and current characteristics of the LOA CFL served as a comparison to those obtained from the simulation. PSPICE was selected to simulate the LOA CFL because of the relatively large number of components contained in the electronic ballast circuit.

Due to the unknown voltage versus current (V-I) characteristics of the fluorescent tube, the model used to simulate the tube was derived experimentally. The output section of a Lights of America (LOA) 30 watt Circline electronic ballast CFL is shown below in Figure (3.10). The output section consists two capacitor:;, C, and C_2, an inductor, L, and the fluorescent tube. Capacitor C_2 connects the terminal of one of the electrodes to the terminal of the other electrode. The remaining electrode of one the filaments is connected in series with C, to one of the output terminals of the

high-frequency oscillator. The remaining electrode of the other filament is connected in series with L to the other output terminal of the oscillator.

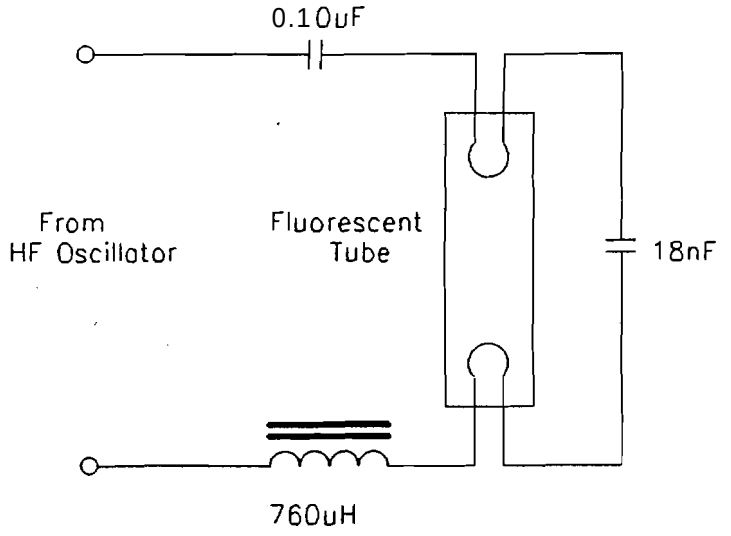

Figure 3.10 Output section of LOA 30 W Circline electronic ballast CFL

The V-I characteristic of the fluorescent tube was determined by obtaining the steady-state voltage across two filaments on opposite ends of the tube and the steady-state current through the tube. The tube voltage, V_{tube}, was obtained by measuring the voltage across the terminals of the tube connected to the electronic ballast. The tube current, I_{tube}, was obtained by measuring the current entering one of the terminals of a filament, I_{fil}^{in}, and the current leaving the other terminal of the filament, I_{fil}^{out}, and taking the difference of the two (i.e., $I_{tube} = I_{fil}^{in} - I_{fil}^{out}$). The currents I_{fil}^{in}, I_{fil}^{out}, and I_{tube} are shown in Figure (3.11). In addition, V_{tube}, I_{tube}, and the tube power, P_{tube}, are shown in Figure (3.12). Finally, the V-I characteristic of the tube is shown in Figure (3.13).

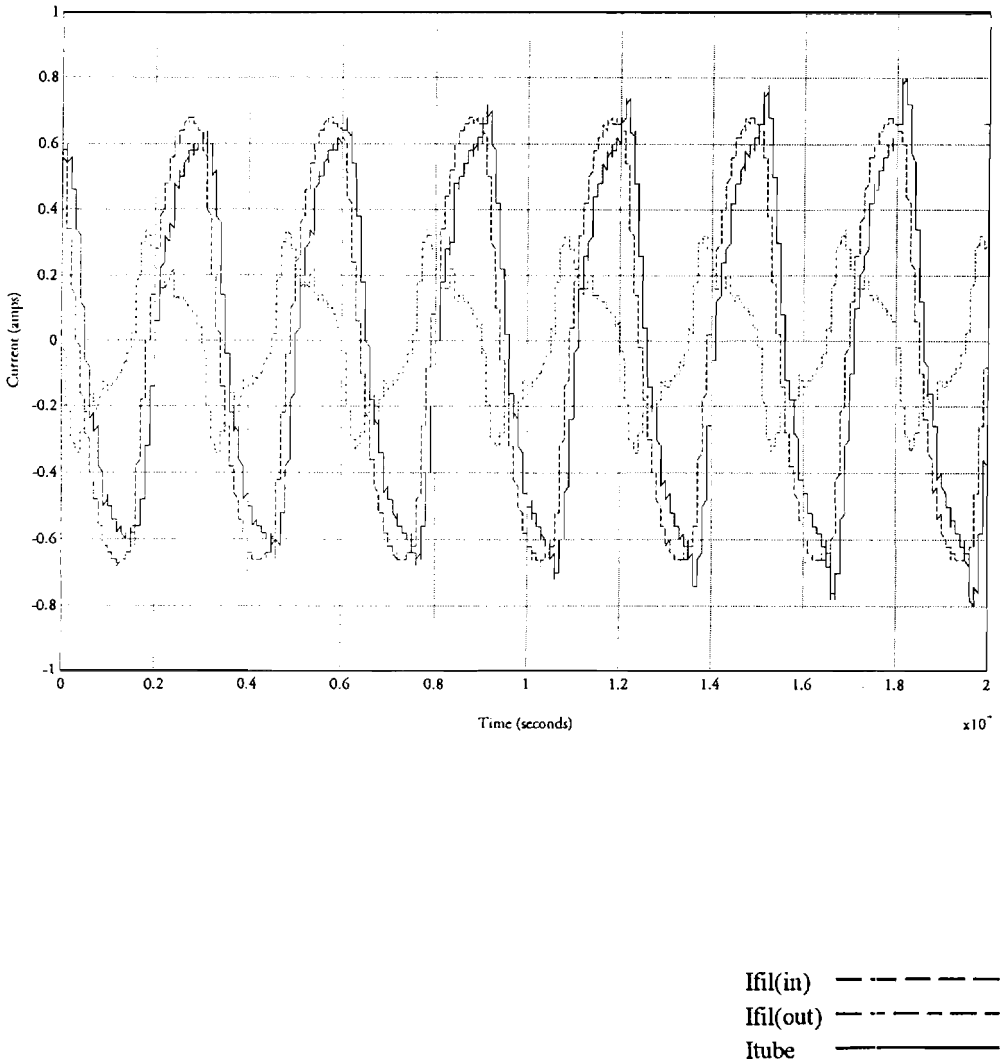

Figure 3.11 Plot of experimental filament and tube currents obtained from LOA 30 W Circline electronic ballast CFL

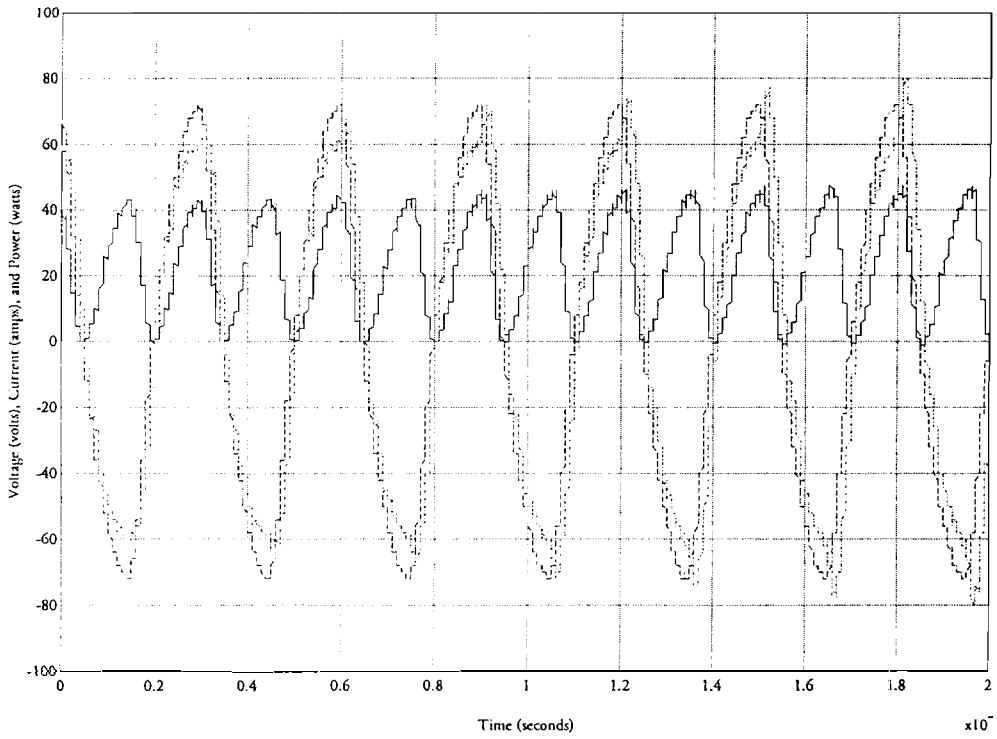

Figure 3.12 Plot of experimental tube voltage, current, and power obtained from LOA 30 W Circline electronic ballast CFL

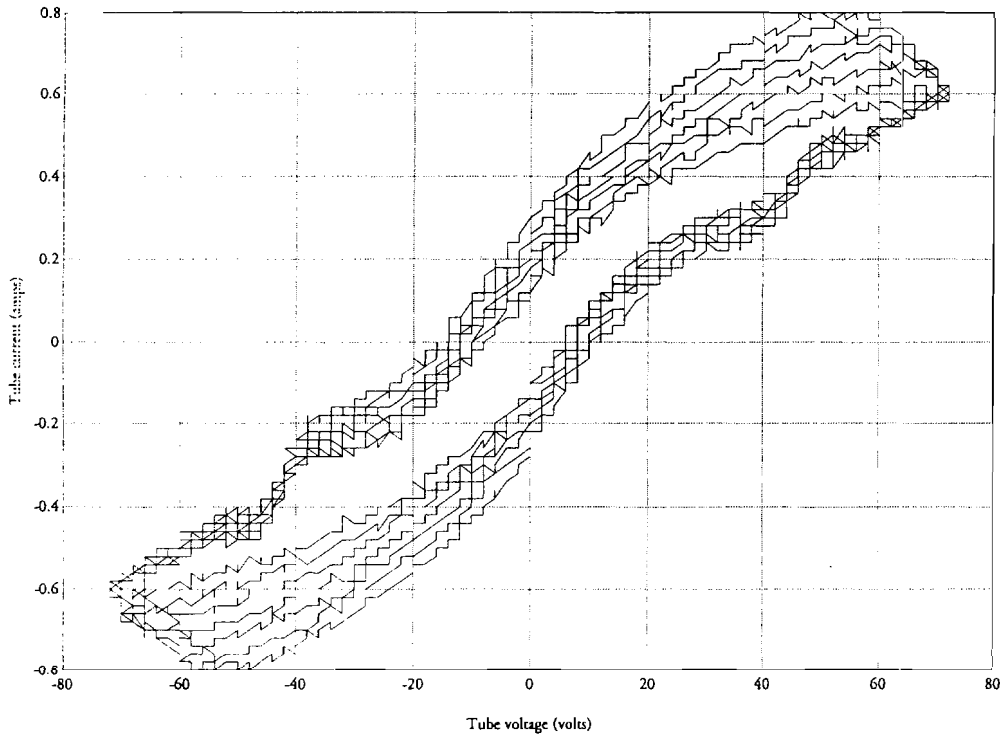

Figure 3.13 Plot of experimental tube V-I characteristic obtained from LOA 30 W Circline electronic ballast CFL

The V-I characteristic obtained by taking the measurements of the tube voltage and current in the steady-state (i.e., after the lamp had been on for at least 15 minutes) was nearly linear. Thus, the fluorescent tube was modeled as a resistor in the steady-state. The value of the resistor was determined by interpolating a line representing the resistance value on the V-I characteristic of the fluorescent tube. For the 'V-I characteristic of the LOA 30 watt Circline CFL shown in Figure (3.13), the equivalent steady-state fluorescent tube resistance was estimated to be 120 ohms.

To determine the relationship between the switching of the high-frequency oscillator and the component values of the output section, the equivalent output section of the LOA 30 watt Circline CFL was analyzed. Note that for negligible values of C_2, the output section may be approximated as a series RLC circuit as shown below in Figure (3.14). A unit-step voltage was then applied to the series RLC circuit and the current response shown below in Figure (3.15) was obtained from PSI'ICE.

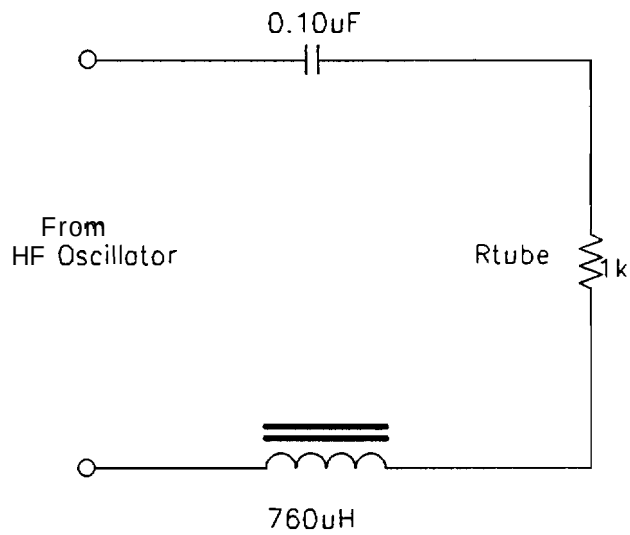

Figure 3.14 Output section of LOA 30 W Circline electronic ballast CFL approximated as a series RLC circuit (C_2 negligible)

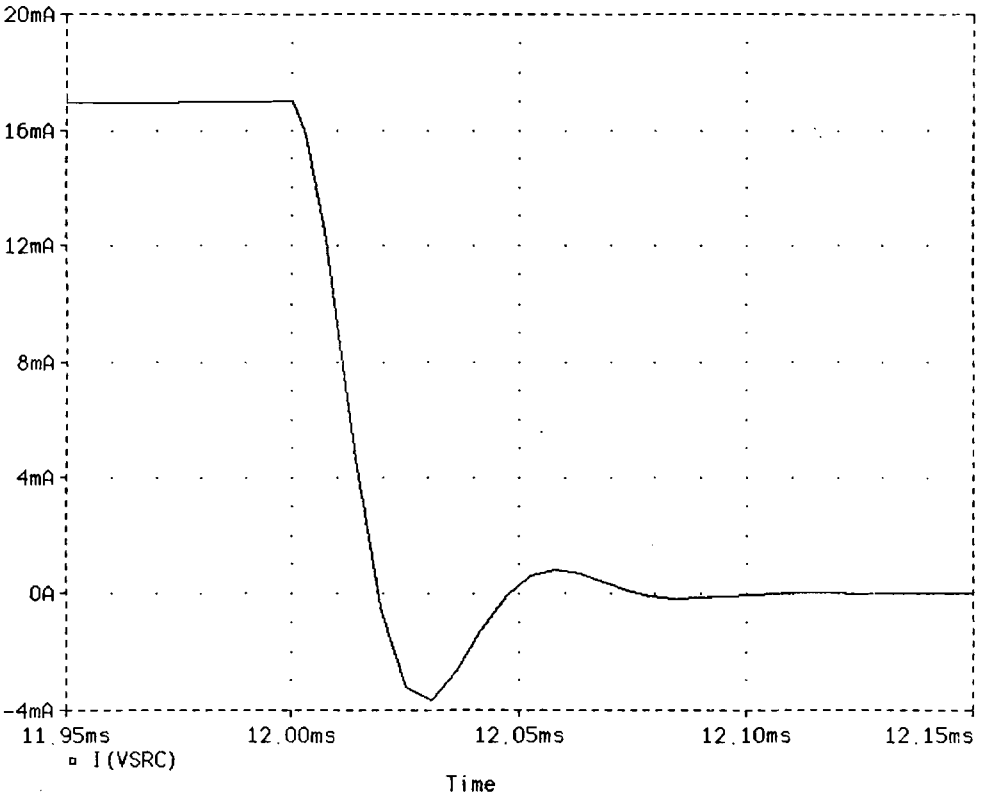

Figure 3.15 Unit-step response to RLC circuit obtained from PSPICE

From Figure (3.15), it is apparent that the unit-step current response of the approximated RLC circuit is underdamped. The underdamped response may be expressed as

$$i(t) = e^{-\alpha t}(B_1 \cos \omega_d t + B_2 \sin \omega_d t) \qquad (3.3.1)$$

where

B,, B_2 = arbitrary constants selected to satisfy initial conditions,
$\alpha = \frac{R}{2L}$ (exponential damping coefficient),
$\omega_o = \frac{1}{\sqrt{LC}}$ (resonant frequency), and
$\omega_d = \sqrt{\omega_o^2 - \alpha^2}$ (natural resonant frequency).

When the specific component values used in the LOA CFL are substituted,

$$\omega_o = \frac{1}{\sqrt{LC}} = \frac{1}{\sqrt{(760\mu H)(0.10\mu F)}} = 114,707.8 \text{ rad/sec}$$

$$f_o = \frac{\omega_o}{2\pi} = \frac{114,707.8}{2\pi} = 18.256 \text{ kHz}$$

$$T_o = \frac{1}{f_o} = 54.78\mu \text{sec}.$$

The switching frequency of the LOA CFL was measured to be

$$f = \frac{1}{T} = \frac{1}{26\mu \text{sec}} = 38.461 \text{ kHz}.$$

Note that the switching frequency is approximately twice that of the resonant frequency of the approximated series RLC output circuit of the LOA CFL. The high-frequency oscillator of the electronic ballast allows the charging and discharging of the output circuitry. When M_2 is on (and M_1 is off), the oscillator charges the series RLC circuit. When M_1 is on (and M_2 is off), the series RLC circuit discharges and the current through the circuit exhibits an underdamped response.

The schematic diagrams of a typical electronic ballast CFL and the LOA CFL are shown in Figures (3.16) and (3.17), respectively. The individual sections of the

electronic ballast CFLs are denoted in each figure. The EMI filter and bridge rectifier sections were modeled in PSPICE exactly as shown in Figure **(3.17).** The output section of the CFL was also modeled as shown except for the fluorescent tube, which was modeled as a resistor (as described in Section **2.2).** For purposes of simulation, a pair voltage controlled switches and four diodes were used in place of the HEXFETs shown below in Figure **(3.1**8).

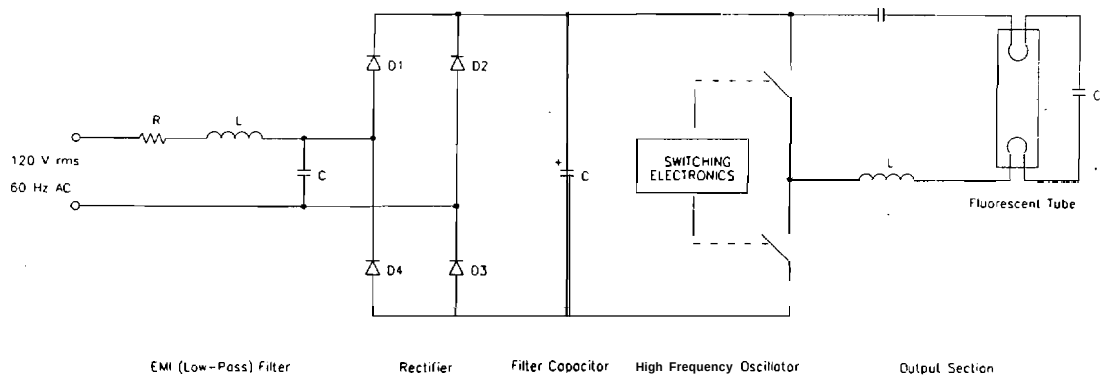

Figure **3.16** General schematic for a typical electronic ballast CFL

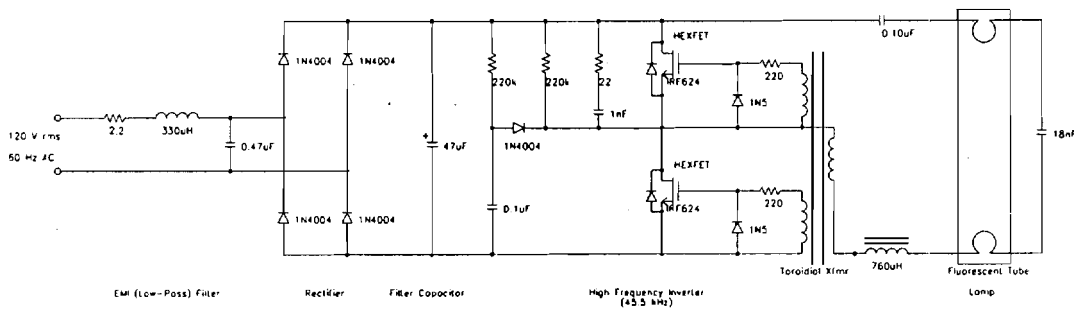

Figure **3.17** Schematic for LOA 30 W Circline electronic ballast CFL

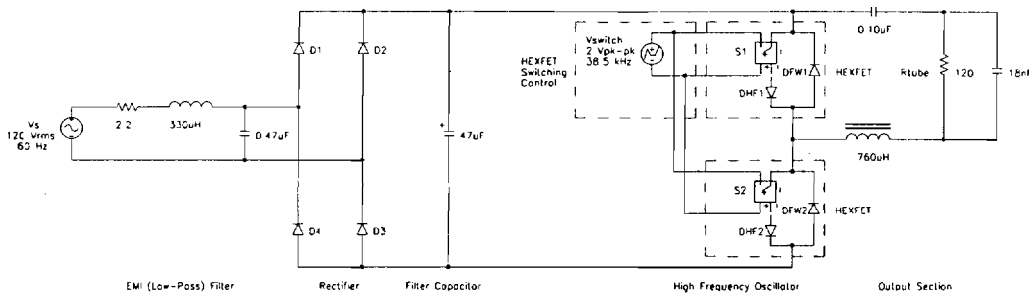

Figure 3.18 PSPICE simulation schematic for LOA 30 W Circline electronic ballast CFL

The listing used for the PSPICE simulation of the LOA electronic ballast CFL is shown below. The PSPICE source listing begins with the title of the file. All lines beginning with an asterisk ("*") are comment lines and are ignored by PSPICE. The listing then continues with the nodal definition of the schematic diagram to be evaluated by PSPICE. The definition of a schematic component includes the component name, the nodal connections of the component, and the value or description of the component. Note that the component names for resistors, inductors, capacitors, diodes, and voltage sources must begin with the letter R, L, C, D, and V, respectively.

```
CFL1D.CIR

* SINGLE-PHASE PSPICE SIMULATION
* LOA 2030 CIRCLINE CFL

*** BEGIN SCHEMATIC DIAGRAM DEFINITION ***

* Voltage source, VS=169.7sin(wt)
VS    0   1   SIN(0 169.7 60 0 0 0)

* AC-side EMI filter
R12   1   2   2.2
L23   2   3   330uH
C30   3   0   0.47uF
```

```
* Rectifier diodes
D1    3    4    DDEFAULT
D2    0    4    DDEFAULT
D3    5    0    DDEFAULT
D4    5    3    DDEFAULT

* DC-side filter capacitance, C45
C45   4    5    47uF

* RC timing network
*R420  4    20   220K
*R47   4    7    220K
*R421  4    21   22
*C217  21   7    1nF
*D207  20   7    DDEFAULT
*C200  20   5    0.1uF

* HEXFET switching model
DHF1  4    6    DDEFAULT
SHF1  6    7    11   0    SMOD1
DFW1  7    4    DDEFAULT
DHF2  7    8    DDEFAULT
SHF2  8    5    11   0    SMOD2
DFW2  5    7    DDEFAULT
VHF   11   0    PULSE(-1.01 1.01 0 lu lu 15.0e-6 30.0e-6)

* Fluorescent tube model
C49   4    9    0.10uF
L710  7    10   760uH
C910  9    10   18nF
RTUBE 9    10   120

*** END SCHEMATIC DIAGRAM DEFINITION ***

* Define part models
.model DDEFAULT D
.model SMOD1 VSWITCH [RON 0.01 VON 1.O]
.model SMOD2 VSWITCH [RON 0.01 VON -1.O]

* Transient analysis
.tran   12.5u   0.0666667

* Define transient analysis options
.options GMIN = 1.0u ; *ipsp*
```

```
.options ITL4 = 10000
.options ITL5 = 0
.options RELTOL = 0.01

* Enable graphic processor
.probe I(VS)

* Print output table
.print tran V(1,0) I(VS)

.END
```

The plot of the supply voltage and current obtained from the simulation is shown in Figure (3.19). Plots of the tube voltage, current, and power obtained from the simulation are shown in Figures (3.20) through (3.22). Note that Figures (3.20) through (3.22), obtained from the PSPICE simulation, correspond to Figures (3.11) through (3.13), which were obtained experimentally.

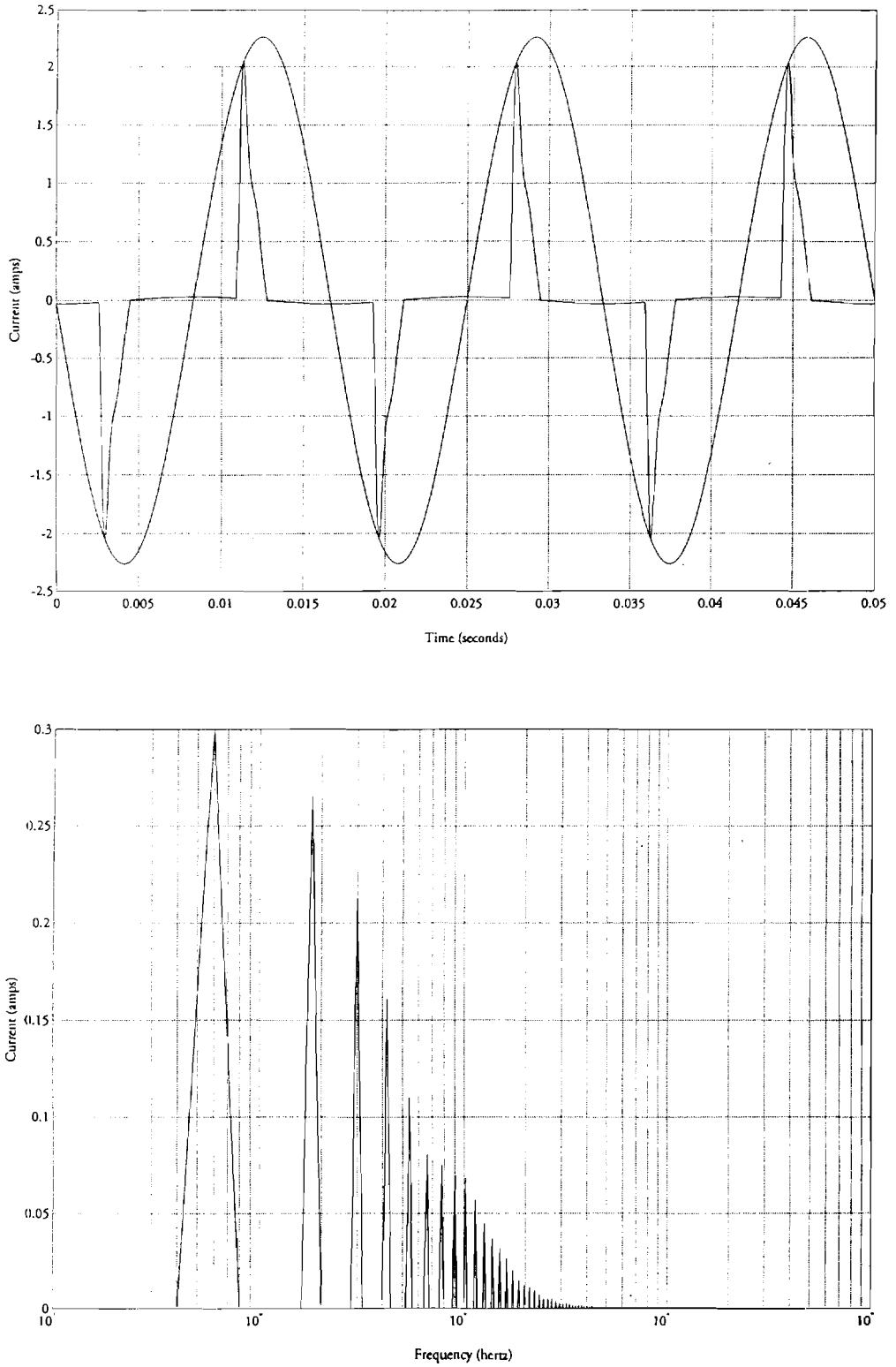

Figure 3.19 Test 8S: Supply voltage and current plots obtained from PSPICE simulation of LOA **2030 30 W** Circline electronic ballast CFL

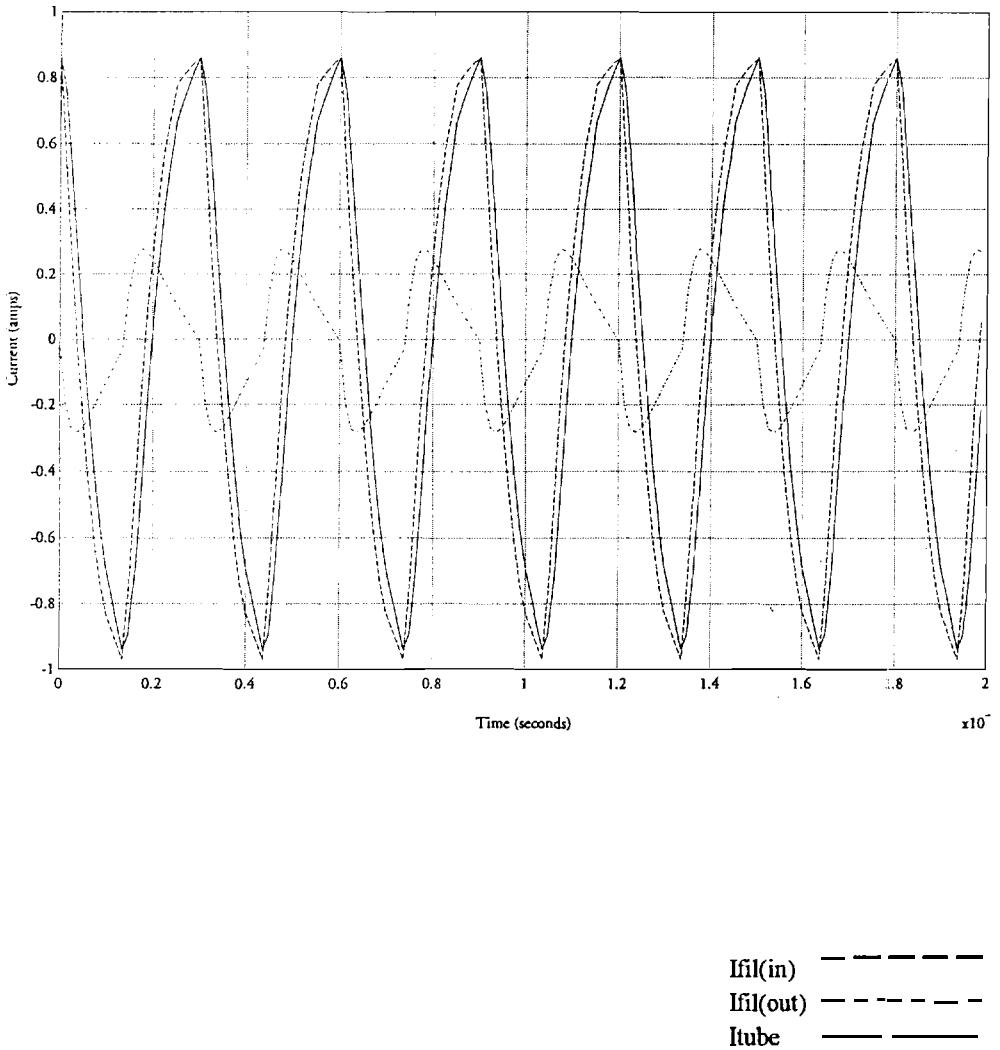

Figure 3.20 Plot of filament and tube currents obtained from PSPICE simulation of LOA 30 W Circline electronic ballast CFL

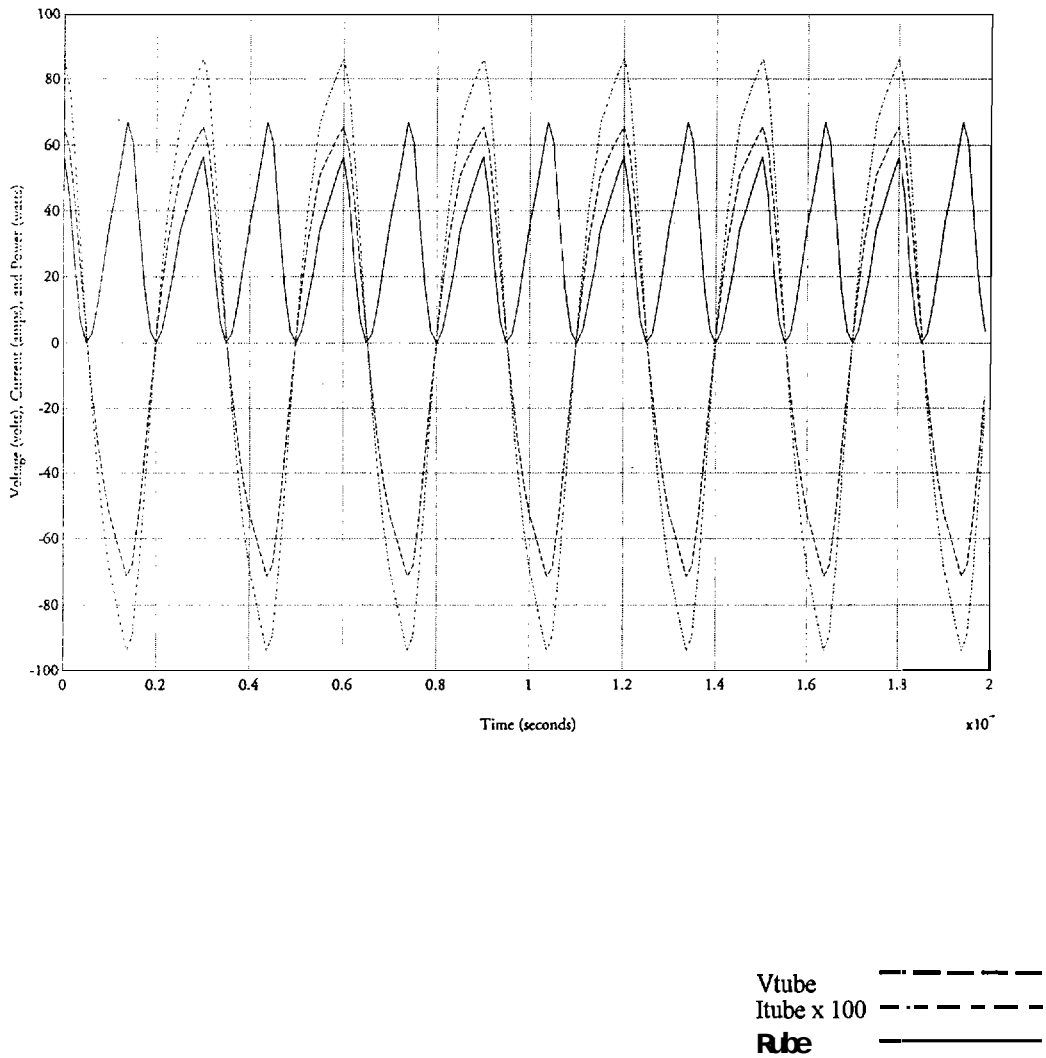

Figure 3.21 Plot of tube voltage, current, and power obtained from PSPICE simulation of LOA **30** W Circline electronic ballast CFL

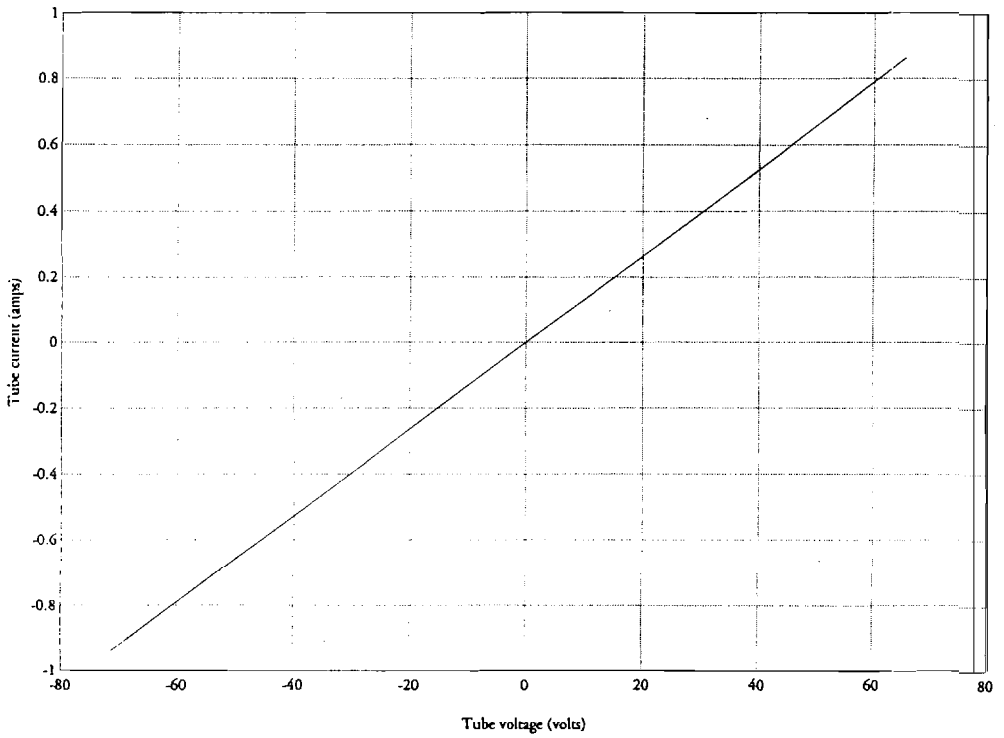

Figure **3.22** Plot of tube V-I characteristic obtained form PSPICE simulation of LOA **30** W Circline electronic ballast CFL

3.4 Main observations from Tests 1E-8E

In this section, general observations are summarized for the CFLs tested in the laboratory. The main points of this summary relate to:

- General remarks on the range of harmonic distortion, power factor, and crest factor
- Compliance with IEEE Standard 519-1992
- Compliance with IEC Standard 555-2
- Compliance with Green Seal Standard for CFLs (power quality)

Figure (3.23) shows a comparison of supply current THD for the various lamps tested. Figure (3.24) shows a comparison of the supply current crest factors between the various lamps tested. Figure (3.25) shows a comparison of the true and displacement power factors. Note that the true power factor of the CFLs are approximately 40% lower than the displacement power factor. Also note that the displacement power factors shown for the CFLs refer to the supply current leading the supply voltage.

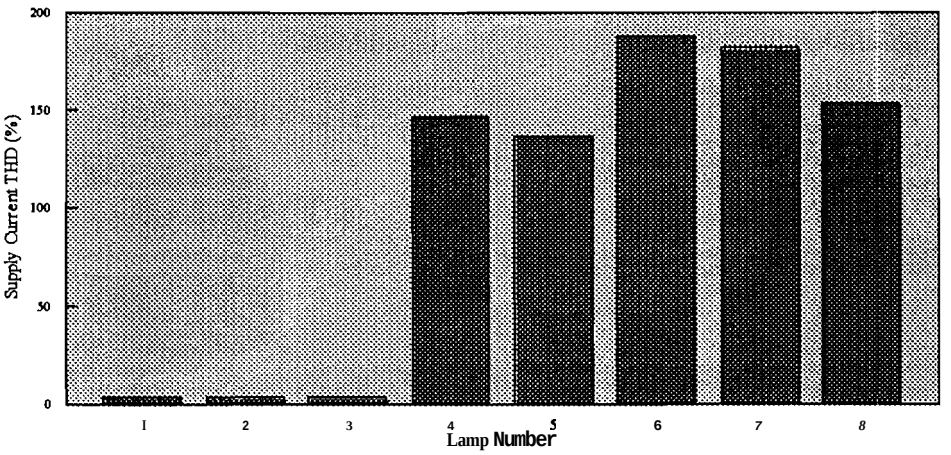

Figure 3.23 Comparison of supply current THD obtained experimentally

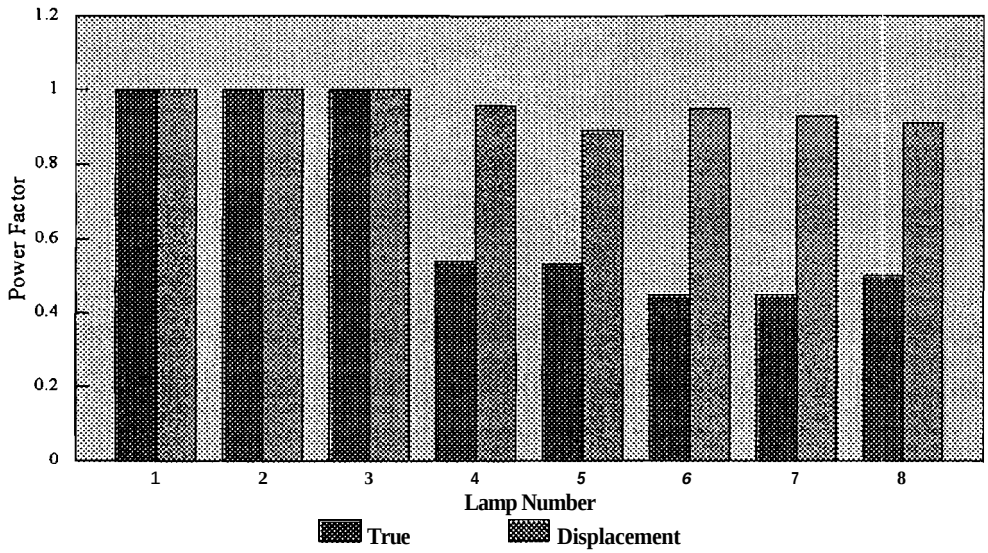

Figure 3.24 Comparison of true and dispacement power factors obtained experimentally

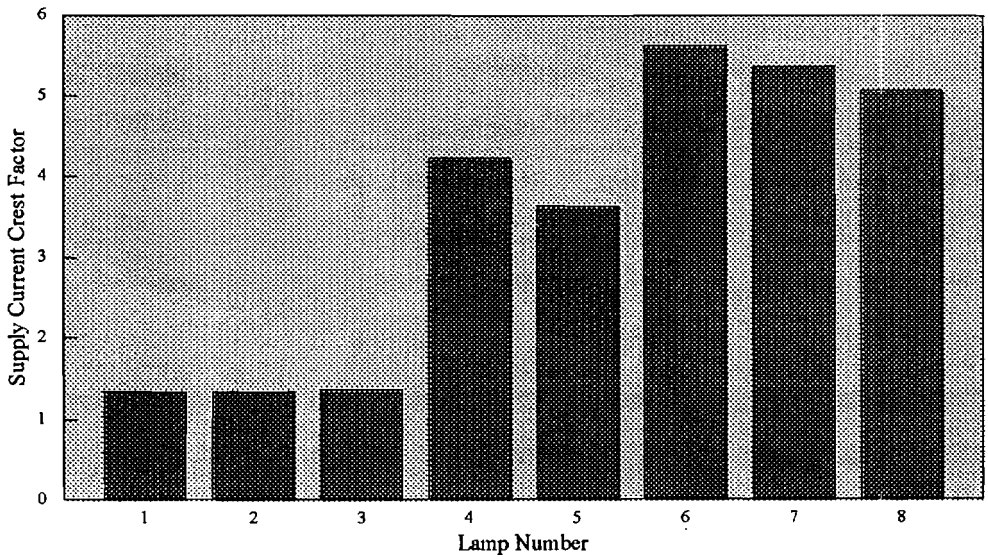

Figure 3.25 **Comparison of supply current crest factors obtained experimentally**

Table (3.4) shows the compliance of each lamp tested with the: cited IEEE, IEC, and Green Seal standards. These standards are described in detail in Section (1.4). Note that all the CFLs tested violate the IEEE 519-1992, IEC 555-2, and Green Seal standards; however, note that it is assumed that the entire electrical load is a CFL load. Also, a short circuit ratio of < 20 is assumed.

Table 3.4 Lamp compliance with IEEE 519-1992, IEC 555-2, and Green Seal standards (100% CFL load)

Lamp No.	IEEE 519-1992		IEC 555-2		Green Seal Standards	
	Maximum individual harmonic amplitude	Current total demand distortion (TDD)	Maximum harmonic current (Class D)		Power Quality (Class A compliance)	
			Odd	Even	tPF	THD_i
1*	Complies	Complies	Complies	Complies	N/A	N/A
2*	Complies	Complies	Complies	Complies	NIA	N/A
3*	Complies	Complies	Complies	Complies	N/A	N/A
4	Violated	Violated	Violated	Violated	Violated	Violated
5	Violated	Violated	Violated	Violated	Violated	Violated
6	Violated	Violated	Violated	Violated	Violated	Violated
7	Violated	violated	Violated	Violated	Violated	Violated
8	Violated	Violated	Violated	Violated	Violated	Violated

.Note: * Incandescentlamps

Green Seal Standards only applicable for CFLs

Table (3.5) shows the harmonic standard compliance of each lamp tested with a combination of nonlinear and linear load. Unlike Table (3.4) which assumes a electrical load of 100% CFLs, Table (3.5) assumes a 50% diversity load factor. A 50% diversity corresponds to a 1 to 1 ratio of CFL to linear (i.e., resistive) load. The definition of diversity load factor used in this case is the ratio of nonlinear rms load current to linear rms load current. For example, a circuit with a 50% diversity load

factor would correspond to 1 amp of rms of CFL load and 1 amp rms of linear load. A short circuit ratio of < 20 is also assumed.

Table 3.5 Lamp compliance with IEEE 519-1992, IEC 555-2, and Green Seal standards (50% CFL load and 50% linear load)

Lamp No.	IEEE 519-1992		IEC 555-2		Green Seal Standards	
	Maximum individual harmonic amplitude	Current total demand distortion (TDD)	Maximum harmonic current (Class D)		Power Quality (Class A compliance)	
			Odd	Even	tPF	THD_i
1*	Complies	Complies	Complies	Complies	N/A	N/A
2*	Complies	Complies	Complies	Complies	N/A	N/A
3*	Complies	Complies	Complies	Complies	N/A	N/A
4	Violated	Violated	Violated	Violated	Violated	Violated
5	**Violated**	**Violated**	**Violated**	**Violated**	Violated	Violated
6	**Violated**	**Violated**	**Violated**	**Violated**	Violated	Violated
7	**Violated**	**Violated**	**Violated**	**Violated**	**Violated**	Violated
8	**Violated**	**Violated**	**Violated**	**Complies**	**Violated**	**Violated**

Note: * **Incandescent lamps**

Green Seal Standards only applicable for CFLs

Note from Table (3.5) that all the CFLs tested violate each of the harmonic standards. By introducing a diversity load factor, the ratio of harmonic current to the total load current is reduced. Thus, the IEC 555-2 and Green Seal standards, which are focused at the equipment level, are unaffected by introducing a diversity load factor. These standards are concerned with the consumption of harmonic current by the nonlinear device itself The IEEE 519-1992 Standard, which provides a harmonic current limit at the utility system level, is affected by introducing a diversity of load. The compliance with the maximum individual harmonic amplitudes specified by IEEE 519-1992 can be achieved for the CFLs tested with approximately a 10 to 1 ratio of

linear to CFL load (i.e., 7.1% diversity factor of CFL/linear load). Compliance with the current TDD limit can be achieved with approximately a 17 to 1 ratio of linear to CFL load (i.e., 5.2% diversity factor of CFL/linear load).

3.5 Main observations from Tests 8E through 8VIE and 8S through 8VIS

The purpose of this section is to confirm the validity of the PSPICE simulation developed for the LOA electronic ballast CFL. The accuracy of the simulation was determined by comparing simulation results obtained from PSPICE with those obtained experimentally. The comparison of the simulation and experimental results are presented both qualitatively and quantitatively.

A comparison of the voltage, current, and power characteristics of the experimental and simulated LOA electronic ballast CFL. Table (3.6).Figures (3.26) through (3.28) show a comparison of the simulation and experimental tube characteristics, V_{tube}, I_{rms} and P_{rms} respectively. These plots provide an insight of the accuracy of the fluorescent tube modeled as a resistor in PSPICE. Figure (3.29) shows a comparison of the simulation and experimental supply current.

Table 3.6 Comparison of supply voltage, current, and power characteristics of experimental and simulated LOA 30 W Circline electronic ballast CFL

	Experimental	Simulated
V_{rms} (volts)	120.85	120
I_{rms} (amps)	0.47	0.53
P (watts)	28.3	33.25
S (VA)	56.36	63.19
tPF	0.5	0.53
dPF	0.91	0.92
THD_v (%)	4.09	0.01
THD_i (%)	153.04	144.47
CF_i	5.07	3.88

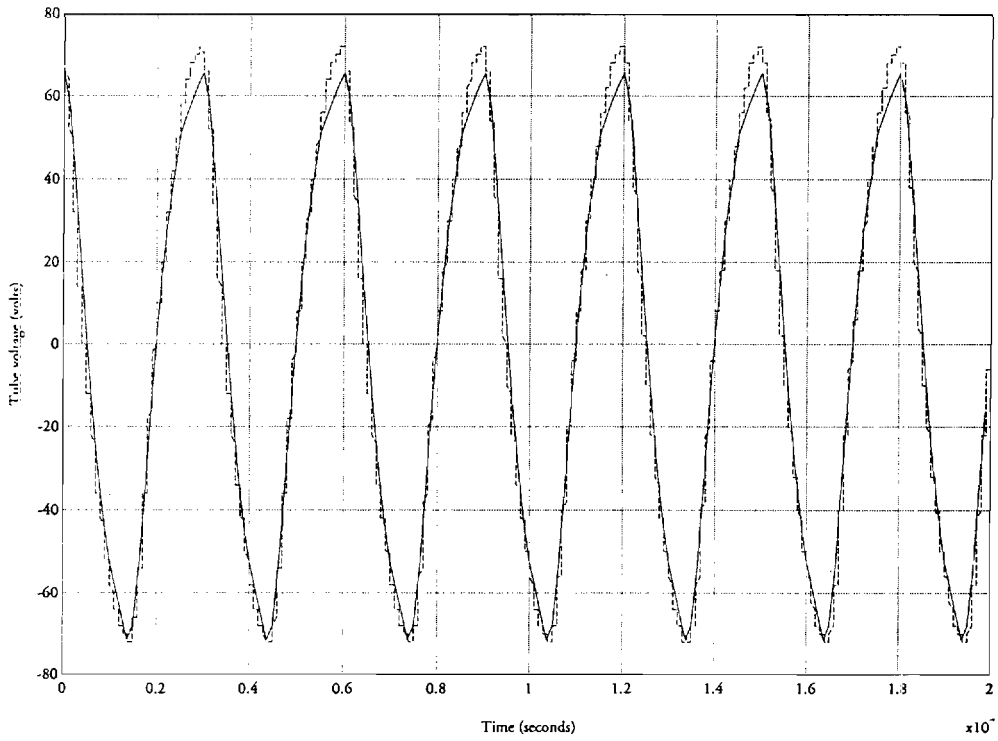

Figure 3.26 Comparison of experimental and simulated tube voltage of LOA 30 W Circline electronic ballast CFL

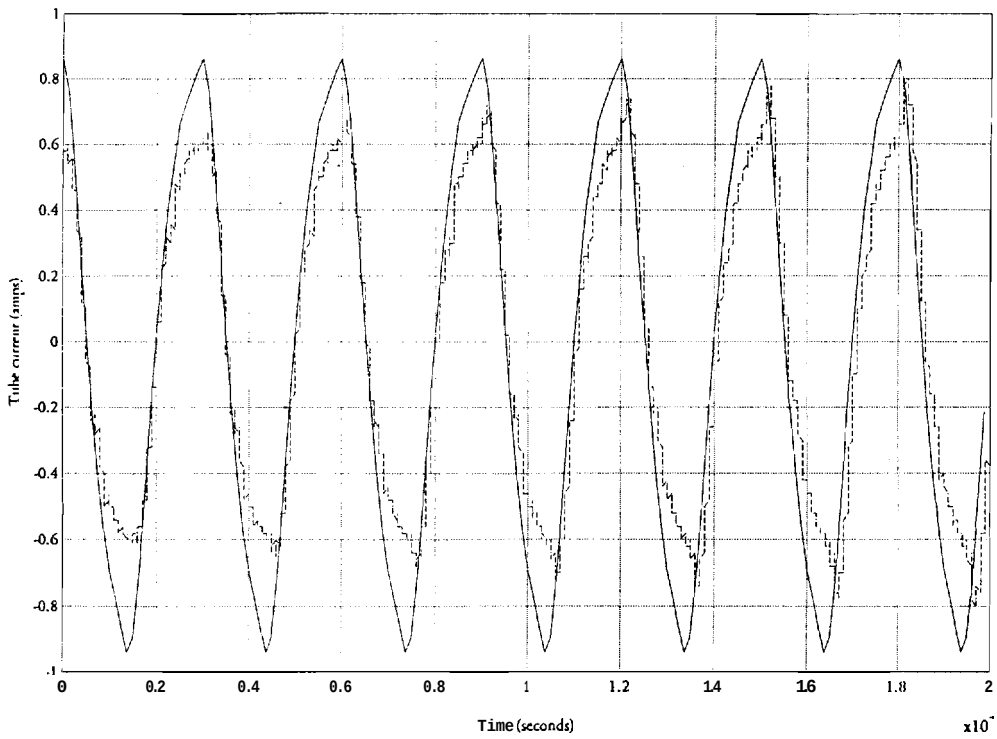

Figure **3.27** Comparison of experimental and simulated tube current of LOA 30 W Circline electronic ballast CFL

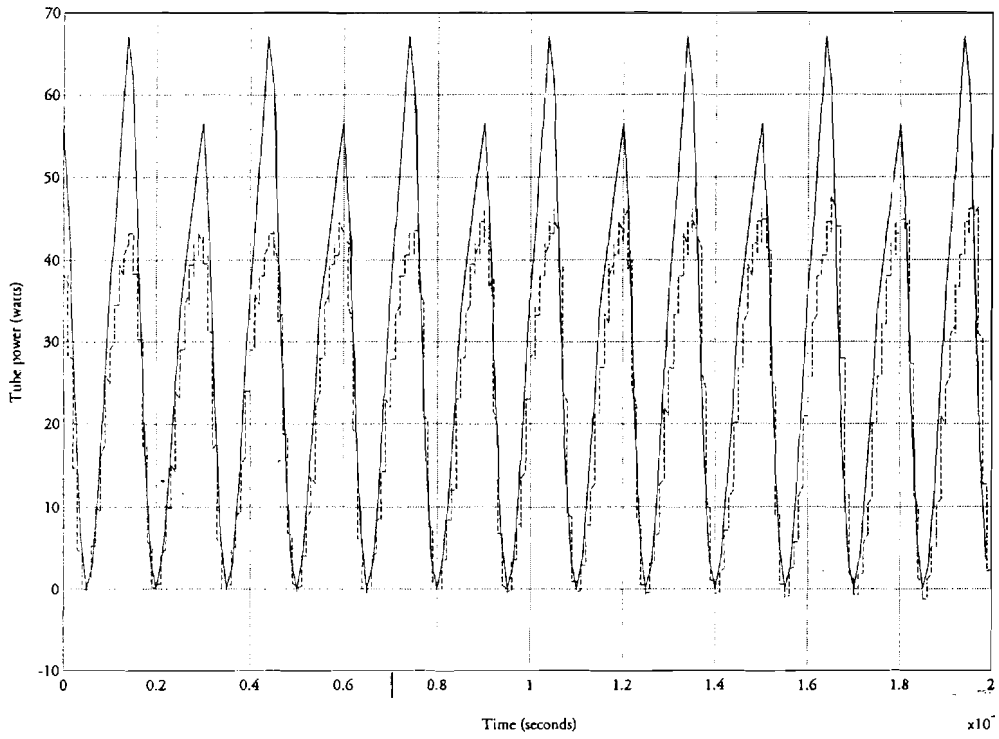

Figure **3.28** Comparison of experimental and simulated tube power of LOA 30 W Circline electronic ballast CFL

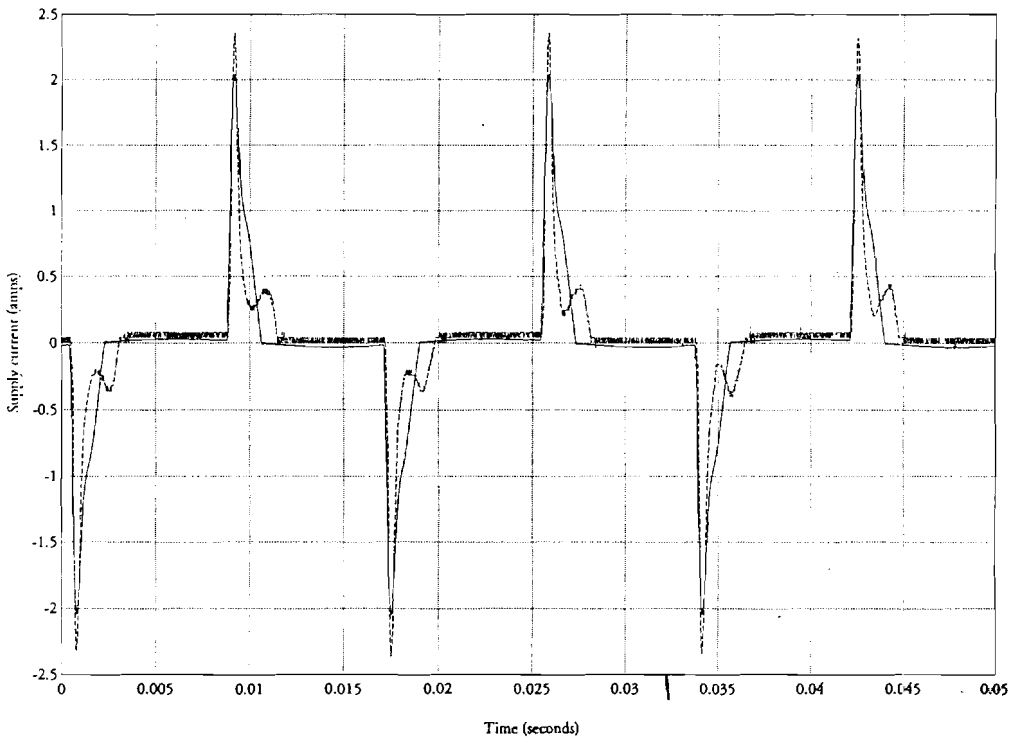

Figure 3.29 Comparison of experimental and simulated supply current of LOA 30 W Circline electronic ballast CFL

CHAPTER 4
SIMULATION APPLICATIONS

4.1 Introduction

In this chapter, various applications of the PSPICE simulation of the LOA electronic ballast CFL developed in Section 3.3 will be presented. Single-phase applications include the quantification of harmonic current throughout the distribution network, compliance with the various harmonic standards (IEEE 519-1992, IEC 555-2, and Green Seal), distribution transformer derating (IEEE C57.110-1982), and harmonic current reduction techniques. Three-phase applications include the quantification of neutral wire current flow and phase wire current capacity derating.

4.2 Single-phase applications

In this section, the electronic ballast CFL simulation developed in Section 3.3 will be applied to a typical single-phase distribution network and further simulated in PSPICE. The circuit used for simulation by PSPICE is shown in Figure (4.1). The applications of the single-phase CFL/distribution network simulation will be described below.

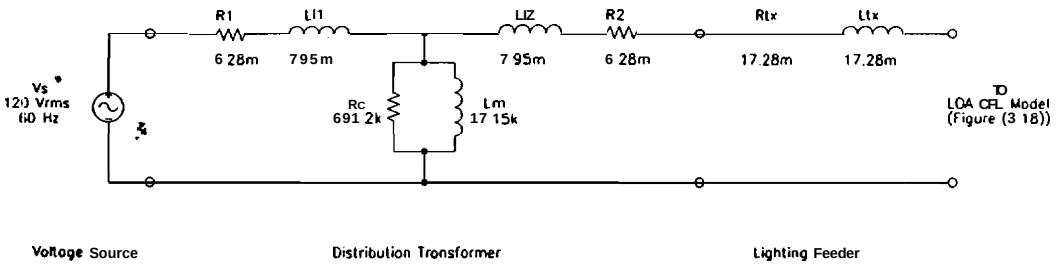

Figure 4.1 PSPICE simulation schematic for single-phase distribution network with LOA 30 W Circline electronic ballast CFL load

• Compliance with harmonic standards. One of the applications of the simulation developed is to determine the effects of harmonic currents produced by CFL loads on typical distribution networks. This application would be particularly effective in determining the effects of electronic ballast CFLs in a single-phase network before their actual implementation.

The compliance of the simulated LOA electronic ballast CFL and single-phase distiibution network with the various harmonic standards is shown in Table (4.1). Depending on the situation, the PCC may either be on the primary or secondary side of the distribution transformer. In most residential settings where a number of households are often served by 'a common feeder and distribution transformer, the PCC is taken at the secondary side of the transformer. In the commercial and residential settings where the customer is often solely served by the feeder and distiibution transformer, the PCC is taken at the primary side of the transformer. Thus, the harmonic compliance is shown for the PCC taken at both the primary and secondary sides of the distribution transformer. Note that it is assumed that the entire electrical load is a CFL load. Also, a short circuit ratio of < 20 is assumed.

Table 4.1 Simulation compliance with IEEE 519-1992, IEC 555-2, and Green Seal standards (100% CFL load)

Point at which PCC is taken	IEEE 519-1992		IEC 555-2		Green Seal Standards	
	Maximum individual harmonic amplitude	Current total demand distortion (TDD)	Masimum harmonic current (Class D)		Power Quality (Class A compliance)	
			Odd	Even	tPF	THD_i
Primary	Violates	Violates	Violates	Violates	N/A	N/A
Secondary	Violates	Violates	Violates	Violates	N/A	N/A

• Distribution transformer derating. The ANSI/IEEE C57.110-1986 standard is applied to the results obtained from the PSPICE simulation of the single phase distribution network loaded with a LOA 30 W Circline electronic: ballast CFL. Further discussion of the ANSI/IEEE C57.110-1986 standard can be found in Section (1.4). The distribution transformer used in this simulation has 7620/240/120 V, 25 kVA, single phase, 1.8% rated values. The fill load loss is assumed to be 3% of the kVA rating, or 750 VA. The core loss is assumed to be 10% of the fill load loss, or 75 VA. The 1^2R loss of the transformer is assumed to be 90 W. Assuming the R^21 loss of the transformer is referred to the 240 V secondary winding, the winding resistance of the secondary is 0.0083 ohms and the winding resistance of the primary is 7.4 ohms. The required load current characteristics obtained from the PSPICE simulation are summarized in Table (4.2). Substituting the transformer and load curreni data into the equation for the derating of a transformer,

$$I_{\max} = \left[\frac{P_{\text{LL-R(pu)}}}{1+\left[\left(\sum_{h=1}^{h_{\max}} f_h^2 h^2 / \sum_{h=1}^{h_{\max}} f_h^2\right) P_{\text{EC-R(pu)}}\right]} \right]^{1/2} = \left[\frac{750/90}{1+\left[\left(\frac{144.25}{3.08}\right)\left(\frac{75}{90}\right)\right]} \right]^{1/2} = 0.4563$$

Note that for the specified transformer loaded 100% with the given magnitude of harmonic component, the transformer is capable of supplying only 45.63% of its fill load rated value. Although the ANSI/IEEE C57.110-1986 standard provides a

conservative derating for transformers, it can be concluded that a transformer with a significant electronic ballast CFL load needs to be oversized to avoid transformer overheating beyond design limits.

Table 4.2 LOA 30 W Circline electronic ballast CFL current harmonic data (obtained from PSPICE simulation) required for ANSI/IEEE C57.110-1986

h	h^2	I_h	I_h^2	$I_h^2 h^2$	f_h	f_h^2	$f_h^2 h^2$
1	1	0.3	0.09	0.09	1	1	1
3	9	0.27	0.07	0.63	0.88	0.78	7.05
5	25	0.22	0.05	1.18	0.73	0.53	13.17
7	49	0.16	0.03	1.27	0.54	0.29	14.11
9	81	0.11	0.01	0.98	0.37	0.13	10.91
11	121	0.08	0.01	0.79	0.27	0.07	8.77
13	169	0.08	0.01	0.95	0.25	0.06	10.58
15	225	0.07	0.01	1.26	0.25	0.06	14.02
17	289	0.07	0	1.36	0.23	0.05	15.14
19	361	0.06	0	1.17	0.19	0.04	13.01
21	441	0.04	0	0.89	0.15	0.02	9.9
23	529	0.04	0	0.71	0.12	0.01	7.93
25	625	0.03	0	0.62	0.11	0.01	6.95
27	729	0.03	0	0.5	0.09	0.01	5.61
29	841	0.02	0	0.34	0.07	0	3.78
31	961	0.01	0	0.21	0.05	0	2.31
					Σ	3.08	144.25

- Harmonic current reduction. Another potential application of the PSPICE simulation is the development of CFLs with reduced harmonic current distortion. As an example of this application, a potential current harmonic reduction technique for

electronic ballasts will be presented. It has been found that the introduction of a dc-dc boost converter into the electronic ballast circuitry significantly reduces the current harmonic distortion produced by electronic ballast CFLs [22]. The boost converter, which is often used as a true power factor correction circuit, serves as an active filter, effectively filtering out harmonics caused by rectifier circuits with capacitive output filters. The schematic for a typical boost converter is shown in Figure (4.2).

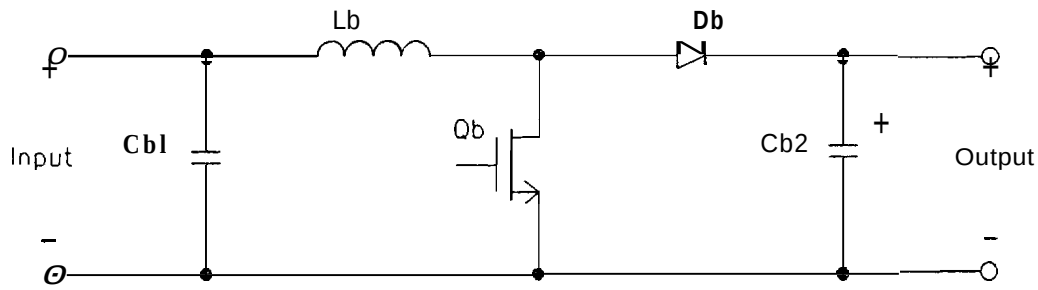

Figure **4.2** Schematic for a typical dc-dc boost converter

To reduce the consumption of harmonic currents by the electronic ballast CFL, the boost converter is incorporated into the electronic ballast between the rectifier/filter capacitor and the high frequency oscillator. The simulated LOA electronic ballast CFL with the boost converter modification is shown in Figure **(4.3).** Because the oscillator contains the MOSFET and diode required by the boost converter, the boost converter can easily be integrated with the oscillator by adding a capacitor, C_b, and inductor, L_b, additionally required by the boost converter [10]. A diode, D_b, is also added in series between the output of the rectifier and the input of the boost converter to prevent the change of direction of current through the inductor.

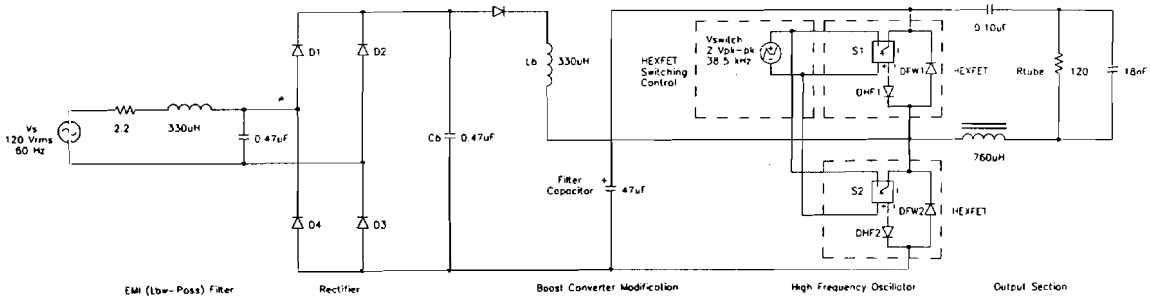

Figure 4.3 PSPICE simulation schematic for LOA 30 W Circline electronic ballast CFL with boost converter modification

Because of the incorporation of the boost converter into the oscillator circuit, the boost converter operates at the same frequency as the oscillator with a duty ratio of 0.5. The high frequency harmonics which are consumed by the ballast are then filtered out by a low pass filter whose breakpoint is chosen as the geometric mean of the fundamental frequency consumed by the ballast (i.e., 60 Hz), f_1, and the switching frequency of the converter/oscillator, f_b. The supply voltage and current plots obtained from the PSPICE simulation of the LOA 30 W Circline electronic ballast CFL with the boost converter modification is shown in Figure (4.4).

Preliminary laboratory results confer that the boost converter modification reduces the supply current THD to approximately 10.48% and increase:; the tPF and dPF to (0.99) and (1.00), respectively. Although the current harmonic distortion is reduced significantly, it is at the expense of an increase in power consumption by the lamp. The rms supply current increased to approximately 1.87 A and the active and apparent power increased to 222.83 W and 224.12 VA, respectively. Further investigation of the boost converter modification in CFLs is required to obtain an optimal reduction in supply current THD and power consumption by the lamp.

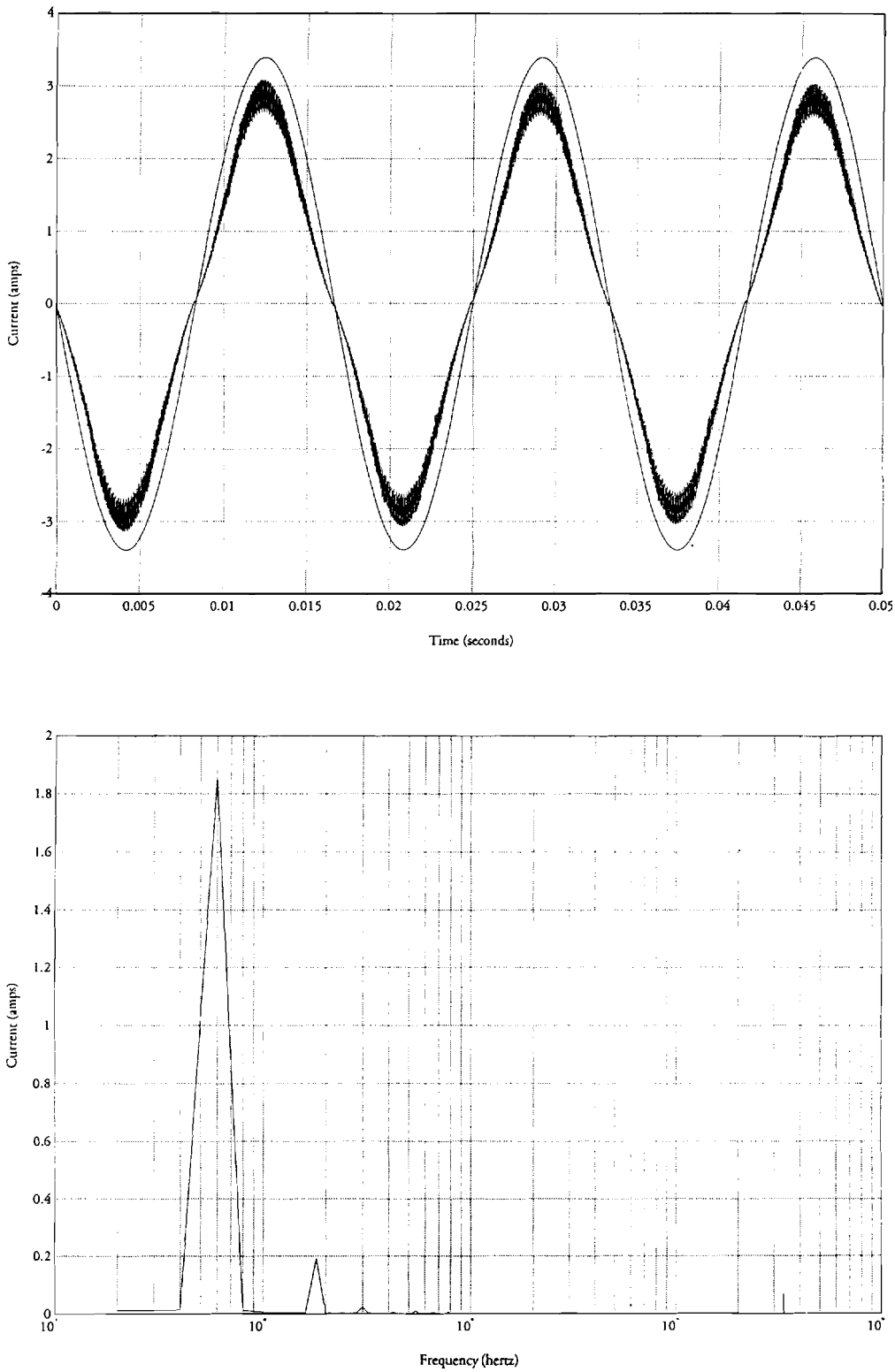

Figure 4.4 Supply voltage and current plots obtained from PSPICE simulation of LOA 30 W Circline electronic ballast CFL with boost converter modification

4.3 Three-phase application

In this section, the electronic ballast CFL simulation developed in Section (3.3) will be applied to a typical three-phase distribution network and further simulated in PSPICE. The circuit used for simulation by PSPICE is shown in Figure (4.5). The application of the three-phase CFL/distribution network simulation will be described below.

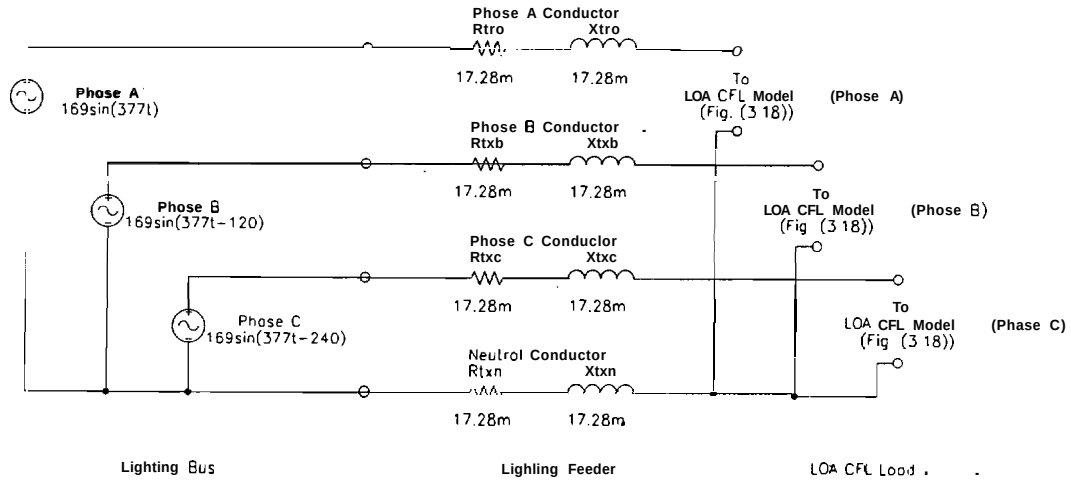

Figure 4.5 PSPICE simulation schematic for three-phase distribution network with LOA 30 W Circline electronic ballast CFL load

♦ Neutral conductor current. The presence of electronic loads which consume large amounts of harmonic current on three-phase four-wire distribution networks have been of increased concern due to their cause of an increased current flow in the neutral conductor. When harmonic current is present in the phase wires of the network, the harmonic "triplens" (e.g., n=3, 6, 9, 12, etc.) sum in the neutral conductor and contribute to the rms neutral conductor current. The plots of the Phase A voltage, neutral conductor current, and FFT of the neutral conductor current obtained experimentally are shown in Figure (4.6). Similar plots obtained from the three-phase simulation are shown in Figure (4.7). Various data for the simulated and experimental three-phase case is shown in Table (4.3).

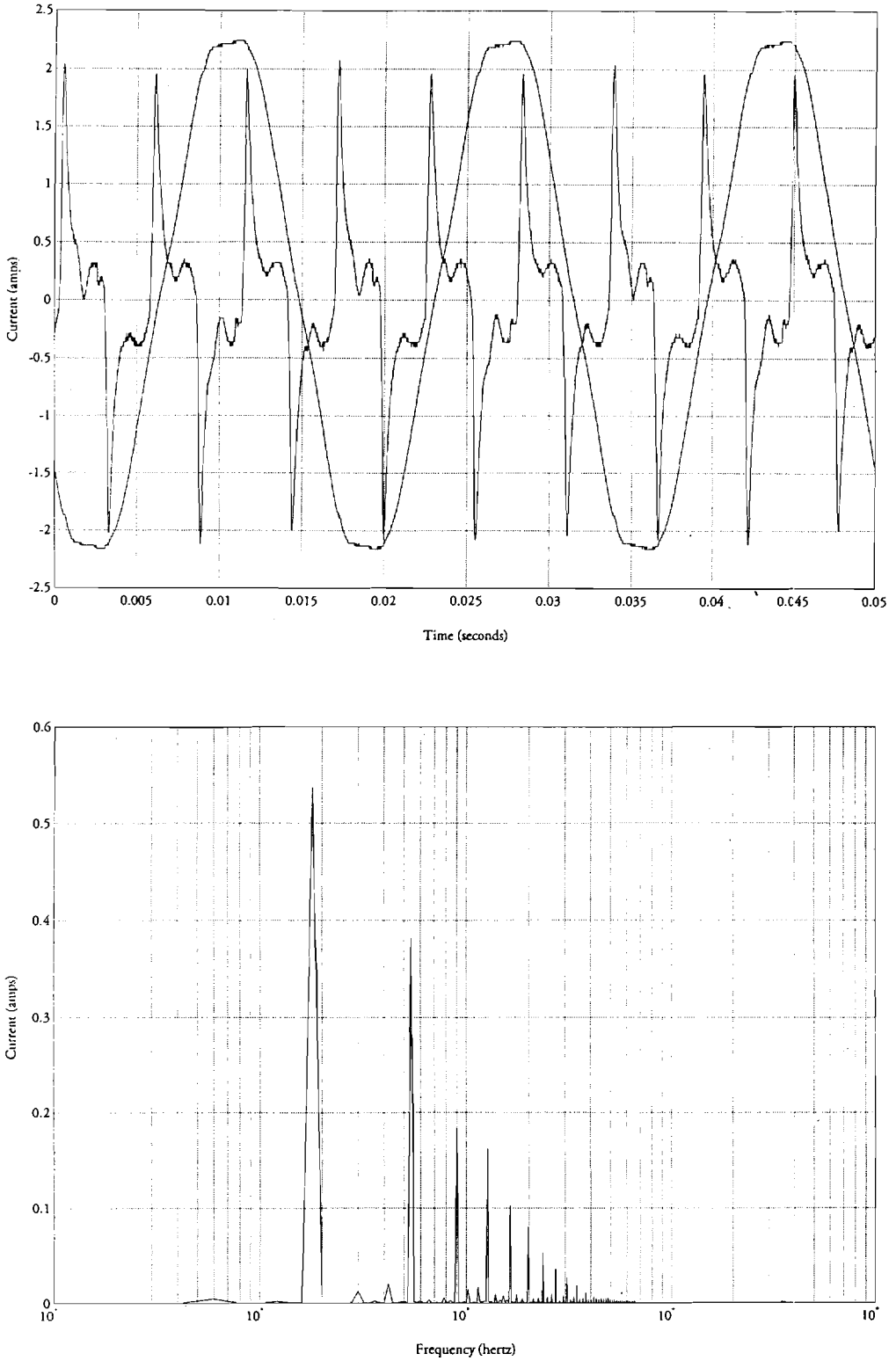

Figure 4.6 Plot of experimental neutral conductor current obtained from three-phase distribution network with LOA 30 W Circline electronic ballast CFL load

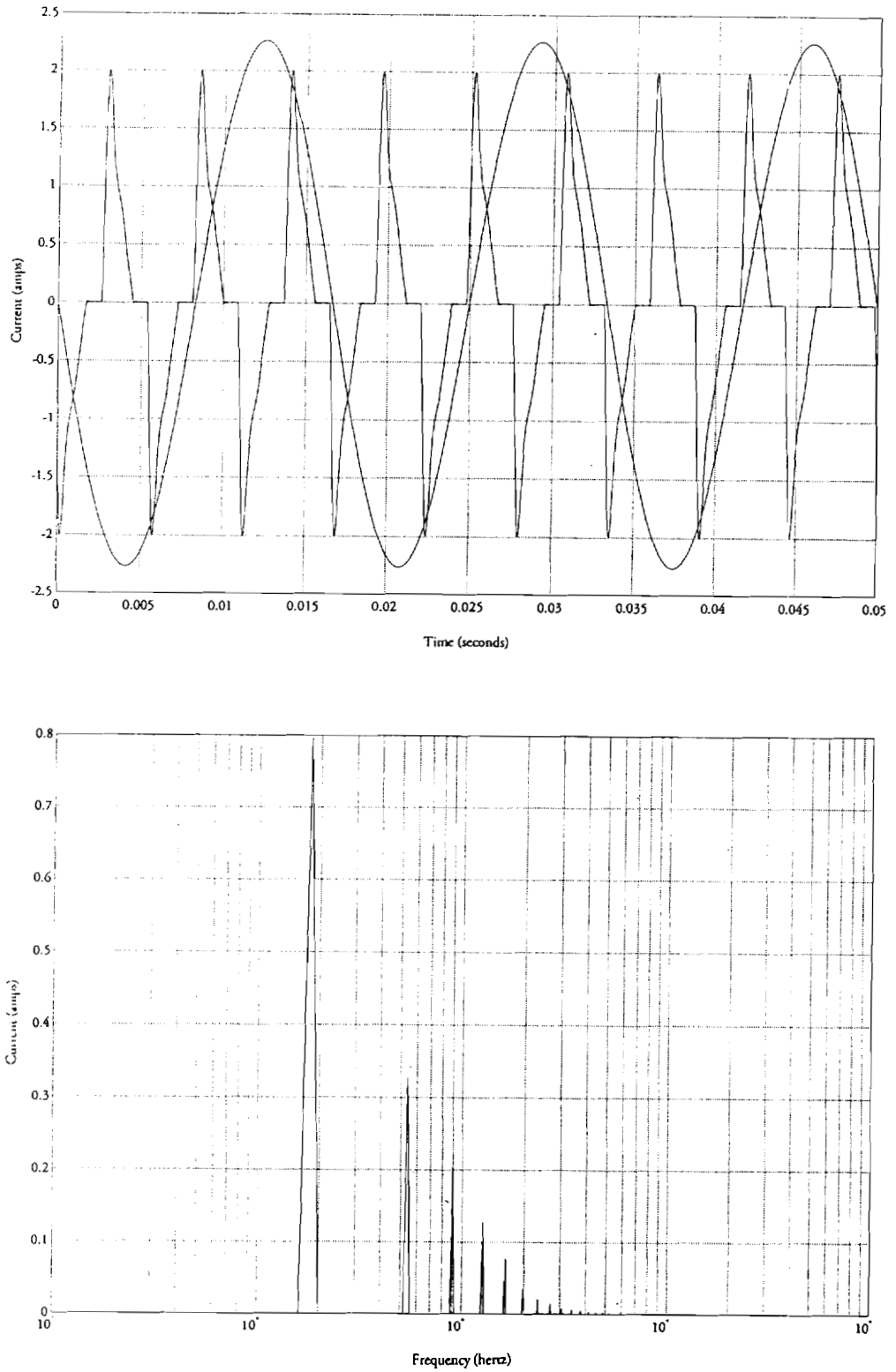

Figure 4.7 Neutral conductor current plot obtained from PSPICE simulation of three-phase distribution network with LOA 30 W Circline electronic ballast CFL load

Table 4.3 Data for simulated and experimental three-phase case

	Simulation	Experimental
V_{Arms} (volts)	120	120.95
I_{Arms} (amperes)	0.53	0.47
I_{Nrms} (amperes)	0.9	0.72
I_{Nrms}/I_{Arms}	1.7	1.53
Circuit derating (%)	58.89	65.28

Note: **Circuit derating** = I_{Arms}/I_{Nrms} x 100

The National Electrical Code (NEC) is the code followed by electrical engineers when designing electrical, illumination, and communication installations [24]. Its purpose is for the practical safeguarding of persons and property from hazards arising from the use of electricity. When designing for a feeder neutral load for a three-phase four-wire installation, the NEC requires a neutral conductor sized for a maximum net computed load between the neutral and any one ungrounded conductor. In most cases, the neutral conductor is sized the same as the phase conductor. When harmonic loads such as electronic ballast CFLs are applied to the phase conductors, the neutral conductor may be undersized to handle the additional harmonic current present. From Table (4.3), it can be seen that a three-phase circuit loaded with one LOA electronic ballast CFL per phase, the rms neutral current is approximately 1.7 times the rms phase current. This corresponds to an approximate derating of the phase conductor current capacity by 72%.

Table (4.4) shows the various sizes of phase and neutral conductors of a typical three-phase lighting feeder loaded with LOA electronic ballast CFLs. This table gives the ampacities for different phase and neutral conductor sizes ranging from 14 to 4 AWG. Note that the phase and neutral conductors are assumed to be sized the same (i.e., a circuit with 10 AWG phase conductors would have a 10 AWG neutral conductor). In addition, all phases are assumed 100% CFL load. This table shows the maximum phase current consumption by the lamps (and hence, the maximum number

of lamps) allowable for a fully loaded neutral conductor. The phase conductor ampacity derating is also shown.

Table (4.5) shows the sizing of the phase and neutral conductors of a typical three-phase lighting feeder loaded with LOA electronic ballast CFLs. This table gives the ampacities for different phase conductor sizes ranging from 14 to 4 AWG. Note that the sizing of the neutral conductor in this table accounts for the additional harmonic neutral current consumed by the lamps. In addition, all phases are assumed 100% CFL load.

Table 4.4 Derated phase conductors of a typical three-phase lighting feeder loaded with LOA electronic ballast CFLs [24]

Phase and neutral conductor size (AWG)	Ampacity* per phase	Maximum no. of lamps per phase	Maximum neutral current @ 0.73 A per 3 lamps, 1 lamp per phase (amperes)	Phase current @ 0.47 A per lamp per phase (amperes)	Phase conductor ampacity derating (%)
14	30	41	29.93	19.27	64.23
12	35	47	34.31	22.09	63.11
10	50	68	49.64	31.96	63.92
8	70	95	69.35	44.65	63.79
6	95	130	94.9	61.1	64.32
4	125	171	124.83	80.37	64.3

Note: * Ampacities of single insulated conductors, rated 0 through 2000 volts, in free air, based on ambient air temperature of 30°C (86°F). Also, ampacities based on conductor temperature rating of 75°C (167°F), corresponding to conductor types FEPW, RH, RHW, THW, THWN, XHHW, and ZW.

Table 4.5 Increased size neutral conductor of a typical three-phase lighting feeder loaded with LOA electronic ballast CFLs [24]

Phase conductor size (AWG)	Ampacity* per phase	Maximum no. of lamps per phase	Maximum phase current @ 0.47 A per lamp per phase (amperes)	Neutral current @ 0.73 A per 3 lamps, 1 lamp per phase (amperes)	Required neutral conductor size (AWG)
14	30	63	29.61	45.99	10
12	35	74	34.78	54.02	8
10	50	106	49.82	77.38	6
8	70	148	69.56	108.04	4
6	95	202	94.94	147.46	2
4	125	265	124.55	193.45	1

Note: * **Ampacities of single insulated conductors, rated 0 through 2000 volts, in free air, based on ambient air temperature of 30°C (86°F). Also, ampacities based on conductor temperature rating of 75°C (167°F), corresponding to conductor types FEPW, RH, RHW, THW, THWN, XHHW, and ZW.**

CHAPTER 5

CONCLUSIONS AND RECOMMENDATIONS

5.1 Conclusions

The electronic ballast compact fluorescent lamp has drawn the attention of utilities and the residential, commercial, and industrial sectors. Although these lamps offer a higher efficacy and longer life as compared to conventional incandescent and fluorescent lamps, they do consume large amounts of harmonic current which cause detrimental effects on the power distribution system. Experimental measurements taken on a number of electronic ballast CFLs show that these lamps produce harmonic current THDs of approximately 150% and have true power factors of approximately (0.50). A simulation based on one of the electronic ballast CFLs tested was developed and used for the investigation of its effects on the power distribution system. These effects include:

- Compliance with harmonic standards
- Distribution transformer derating
- Harmonic current reduction
- Neutral conductor current.

The PSPICE simulation of the electronic ballast CFL proved to be accurate and effective in its use for the applications noted above. For the simulation of a single phase distribution network loaded with the modeled electronic ballast CFL, the large harmonic current distortion produced by the lamp exceeded the limits set forth by the IEEE 519-1992 and Green Seal standards. Applying ANSI/IEEE C57.110-1986, a typical 25 kVA distribution transformer was found to be derated to 45.63% of full

load capacity. When a typical three-phase circuit loaded with electronic ballast CFLs was simulated, the neutral conductor current was found to be in excess of the individual phase current by approximately 140%. Although in all applications it was assumed that the load was 100% CFL, the results obtained provide an insight of the effects of electronic ballast CFLs. These results depend on the CFL used and the given distribution circuit parameters; however, the results are believed to typify actual CFL loads.

5.2 Recommendations

In certain cases, such as a dedicated three-phase lighting feeder retrofitted with electronic ballast CFLs, the applications presented provide results that are fairly accurate. It is recommended for these applications that an analytical investigation be performed before its actual implementation. The initiation of a preliminary investigation, such as those presented, may obviate detrimental effects of harmonic current distortion produced by electronic ballast CFLs on the power distribution system.

To confirm the effects of electronic ballast CFLs in large-scale deployment on the power distribution system, it is recommended that detailed field tests be performed of a system highly loaded with electronic ballast CFLs. One such example would be of a lighting feeder retrofitted with CFLs.

Since the problem of a significant amount of harmonic current distortion stems from the electronic ballast itself, it is recommended that harmonic reduction methods in the design of the electronic ballast be investigated. As discussed in Section (4.2), cost-effective harmonic reduction techniques for electronic ballast CFLs are available. The investigation of these techniques can easily be done with a simulation such the one presented. These techniques should also be applied to electrodeless CFLs, which are the next generation of energy-efficient lighting.

LIST OF REFERENCES

LIST OF REFERENCES

[1] Maremont, M., "1994 Industry Outlook/Services/Utilities/Danger: Competition Dead Ahead," Business Week, No. 3353, 10 January 1994, p. 100.

[2] Ouellette, M., "The Evaluation of Compact Fluorescent Lamps for Energy Conservation," Canadian Electrical Association, Montreal, September 1993.

[3] Public Service Indiana, videotaped advertisement broadcast in central Indiana, 1994.

[4] 'IEEE Recommended Practices and Requirements for Harmonic Control in Electrical Power Systems,' The Institute of Electrical and Electronic Engineers, Inc., 345 East 47th Street, New York, NY, IEEE Std. 519-1992.

[5] Meyer, C., and H. Nienhuis, Discharge Lamps, Philips Technical Library, Deventer, 1988.

[6] "Green Seal Sets Standards for Compact Fluorescents," article obtained from personal correspondence with Southern Indiana Gas & Electric.

[7] Osram Corporation, "Compact Fluorescent Lamps," lighting catalog, 1993.

[8] "Compact Fluorescent Lighting: Energy-Efficient Alternatives to Incandescent Lighting," Electric Power Research Institute, CU-2042% May 1993.

[9] "Advanced Lighting Guidelines: 1993," Electric Power Research Institute, TR-101022-R1, May 1993.

[10] Weiss, P., "Lighting the Way Towards More Efficient Lighting," Home Energy, January/February 1989, pp. 16-23.

1 1 "Retrofit Lighting Technologies: Cost-Effective Lighting for Commercial Applications," Electric Power Research Institute, CU-3040R, July 1991.

[12] Shinomiya, M., K. Kobayashi, M. Higashikawa, S. Ukegawa, J. Matsuura, and K. Tanigawa, "Development of the Electrodeless Fluorescent Lamp," Journal of the Illuminating Engineering Society, Winter 1991, pp. 44-49.

[13] Pileggi, D., T. Gentile, and A. Emanuel, "The Effect of Modern Compact Fluorescent Lights on Voltage Distortion," IEEE Transactions on Power Deliverv, Vol. 8, No. 3, July 1993, pp. 1451-1459.

[14] Knisley, J., "Understanding the Use of New Fluorescent Ballast Designs," Electrical Construction and Maintenance, Vol. 89, No. 3, March 1990, pp. 67-73.

[15] Kassakian, J., M. Schlecht, and G. Verghese, Principles of Power Electronics, Addison-Wesley, Massachusetts, 1991.

[16] de Almeida, A., "Overcoming Problems with Harmonics and Low Power Factors," Energy, Vol. 18, No. 2, 1993, pp. 90-106.

[17] Moncrief, W., "International Harmonic Standards," IEEE 519 Application Panel Session, 1994 IEEEFES Winter Power Conference, New York, January 30-:February 3, 1994.

[18] American National Standards Institute, Inc., 'Recommended Practice for Establishing Transformer Capability when Supplying Nonsinusoidal Load Currents,' The Institute of Electrical and Electronic Engineers, Inc., 345 East 47th Street, New York, NY, ANSI/IEEE C57.110-1986.

[19] Verderber, R., O. Morse, and W. Alling, "Harmonics from Compact Fluorescent Lamps," IEEE/IAS Conference Proceedings, Dearborn, September 28-October 4, 1991.

[20] McBride, K., "Compact Fluorescent Lamps: A Power Quality Analysis of Different Lamps and How the Lamps/Harmonics Can Affect a Transformer," 1993 American Power Conference Proceedinas, Chicago, April 1993.

[21] Schwabe, R., C. Melhorn, "Commercial Building Harmonics-Impact of Electronic Ballasts," obtained from the 1994 IEEE/PES Winter Power Conference, New York, January 30-February 3, 1994.

[22] Najjar, M., "Reduced Harmonic Distortion Content for Electrodeless Compact Fluorescent Lights," obtained from personal correspondence, Cleveland State University, November 1993.

[23] Fitzgerald, A, C. Kingsley, and S. Umans, Electric Machinery, Mc-Graw Hill, New York, 1990.

[24] 1987 National Electrical Code, National Fire Protection Association, Quincy, MA, 1987.

[25] Nielsen, B., "Load-Shape Data for Residential Lighting: Survey Results for Inciindescent and Compact Fluorescent Lamps," Energy, Vol. 18, No. 2, 1993, pp. 211-217.

[26] McGranaghan, M., "Harmonics fiom Residential Customers," obtained from the 1994 IEEE/PES Winter Power Conference, New York, January 30-February 3, 1994.

[27] Emanuel, A., D. Pileggi, and T. Gentile, "Distribution Feeders with Nonlinear in the Northeast U.S.A.: Part I - Voltage Distortion Forecast," 1994 IEEEEES Winter Power Conference Proceedings, New York, January 30-February 3, 1994.

[28] Emanuel, A., D. Pileggi, and T. Gentile, "Distribution Feeders with Nonlinear in the Northeast U.S.A.: Part II - Economic Evaluation of Harmonic Effects," 1994 IEEE/PES Winter Power Conference Proceedings, New York, January 30-February 3, 1994.

[29] Alyasin, S., S. Hoffman, and R. Sasaki, "The Identificatin of the True Energy Savings Realized fiom High-Efficiency Electronic Loads," 1994 IEEEEES Transmission and Distribution Conference Proceedings, Chicago, April 10-15, 1994.

[30] Stevenson, W., Elements of Power System Analysis, Mc-Graw Hill, New York, 1982.

APPENDICES

Appendix A MATLAB function code

```
function expfft(t,v,i)

% EXPFFT(T;V,I)   Single-phase experimental
%                 Plot the Y-point FFT of the current I versus the corresponding
%                 frequency axis for the given sampling frequency Z. Also, plot
%                 the voltage V and current I versus the corresponding time axis
%                 T.

% Clear previous graph

clg;

% Define number of points Y and sampling frequency Z

y = 4000;
z = 80000;

% Calculate the Y-point FFT of the voltage V

temp1 = fft(v,y);
temp2 = temp1/(y/2*sqrt(2));
fftv = temp2(1:(y/2));

% Calculate the Y-point FFT of the current I

temp1 = fft(i,y);
temp2 = temp1/(y/2*sqrt(2));
ffti = temp2(1:(y/2));

% Calculate the frequency axis for the Y-point FFT given the sampling frequency Z

freqaxis = (z*(0:((y/2)-1))/y)';

% Plot the voltage V and current I versus its corresponding time axis T

subplot(211);
plot(t,v/100);
hold on;
plot(t,i);
hold off;
grid;
title('Figure 3.x.x  GE 26W Electronic Ballast CFL');
```

```
xlabel('Time (seconds)');
ylabel('Current (amps)');

% Plot the FFT of the current I versus its correspondingfrequency axis

fftiplot = abs(ffti);
subplot(212);
semilogx(freqaxis,fftiplot);
grid:
xlabel('Frequency (hertz)');
ylabel('Current (amps)');

% Calculate fbndamental current I1rms, fbndamental voltage V1rms,
%       RMS current Irms, RMS voltage Vrms, active power P, apparent power S,
%       true power factor tPF, displacement power factor dPF, total harmonic
%       distortion of current THDi, total harmonic distortion of voltage THDv,
%       and crest factor CF

sumv = 0.0;
sumi = 0.0;
sump = 0.0;

% Fundamental current I1rms and fundamental voltgae V1rms

V1rms = abs(fftv(4,1))
I1rms = abs(ffti(4,1))

% RMS current Irms and RMS voltage Vrms

for n = 4:6:(y/2),
sumv = sumv + (abs(fftv(n,1)))^2;
sumi = sumi + (abs(ffti(n,1)))^2;
sump = sump + real(fftv(n,1)*conj(ffti(n,1)));
end

Vrms = sqrt(sumv)
Irms = sqrt(sumi)

% Active power P

P = sump

% Apparent power S

S = Vrms*Irms
```

```
% True power factor tPF

tPF = P/S

% Displacement power factor dPF

deltav = atan2(imag(fftv(4,1)),real(fftv(4,1)));
deltai = atan2(imag(ffti(4,1)),real(ffti(4,1)));
dPF = cos(deltai-deltav)

% Total harmonic distortion of current THDi and total harmonic distortion of
%       voltage THDv

sumvh = sumv-(abs(fftv(4,1)))^2;
sumiih = sumi-(abs(ffti(4,1)))^2;
THDv = sqrt(sumvh)/abs(fftv(4,1))*100
THDi = sqrt(sumih)/abs(ffti(4,1))*100

% Crest factor CF

CF = max(i)/Irms



function exptube(time,tubev,tubecur,tubec1,tubec2,ptype)

% EXPTUBE(TIME,TUBEV,TUBECUR,TUBEC1,TUBEC2,PTYPE)
%
%       Single-phase experimental - tube voltage and current
%
%       Plot TIME, TUBEV, TUBECUR, TUBEC1, and TUBEC2

% Clear previous graph

clg;

if ptype == 1,

% Plot TUBEC1, TUBEC2, AND TUBECUR versus TIME

axis([0,2e-04,-1,1]);
plot(time,tubec1,'--',time,tubec2,'-.',time,tubecur,'-');
grid;
title('LOA 30W Circline CFL (Experimental - Tube)');
```

```
xlabel('Time (seconds)');
ylabel('Current (amps)');
axis;

elseif ptype == 2,

% Plot TUBEV, TUBECUR, AND TUBEPWR versus TIME

axis([0,2e-04,-100,1001);
plot(time,tubev,'--',time,tubecur*100,'-.',time,tubev.*tubecur,'-');
grid;
title('LOA 30W Circline CFL (Experimental - Tube)');
xlabel('Time (seconds)');
ylabel('Current (amps)');
axis,;

end;



function simfft(file)

% SIMFFT(FILE)
%
%       Single-phase simulation - FFT of supply voltage and current
%
%       Plot the Y-point FFT of the voltage V and the
%       current I versus the corresponding frequency axis
%       for the given sampling frequency Z. Also,
%       plot the voltage V and current I versus the
%       corresponding time axis T (given the input FILE)

% Define total number of points in FILE

pts = 5335;

% Define number of evaluation points Y and sampling frequency Z

y = 4000;
z = 80000;

% Clear previous graph

clg;
```

```
% Extract T, V, and I from input FILE

for n = 1:1:y,
        t(n,1) = (n-1)*1.25e-05;
end

for n = y:-1:1,
        v(n,1) = file((pts-y)+n,2);
        i(n,1) = file((pts-y)+n,3);
end

% Clalculate the Y-point FFT of the voltage V

temp1 = fft(v,y);
temp2 = temp1/(y/2*sqrt(2));
fftv = temp2(1:(y/2));

% C'alculatethe Y-point FFT of the current I

temp1 = fft(i,y);
temp2 = temp1/(y/2*sqrt(2));
ffti = temp2(1:(y/2));

% Calculate the frequency axis for the Y-point FFT given
%       the sampling frequency Z

freqaxis = (z*(0:((y/2)-1))/y)';

% Plot the voltage V and current I versus its corresponding time axis T

subplot(211);
plot(t,v/75);
hold on;
plot(t,i);
hold off;
grid;
title('LOA 30W Circline CFL (PSPICE Simulation  Supply)');
xlabel('Time (seconds)');
ylabel('Current (amps)');

% Plot the FFT of the current I versus its corresponding frequency axis

fftiplot = abs(ffti);

subplot(212)
```

```
semilogx(freqaxis,fftiplot)
grid
xlabel('Frequency (hertz)')
ylabel('Current (amps)')

% Calculate fbndamental current I1rms, fbndamental voltage Vlrms,
%       RMS current Irms, RMS voltage Vrms, active power P, apparent power S,
%       true power factor tPF, displacement power factor dPF, total harmonic
%       distortion of current THDi,    total harmonic distortion of voltage THDv,
%       and crest factor CF

sumv = 0.0;
sumi = 0.0;
sump = 0.0;

% Fundamental current Ilrms and fbndamental voltgae Vlrms

V1nns = abs(fftv(4,1))
I1rms = abs(ffti(4,1))

% RMS current Irms and RMS voltage Vrms

for n = 4:6:(y/2),
        sumv  =  sumv + (abs(fftv(n,1)))^2;
        sumi  =  sumi + (abs(ffti(n,1)))^2;
        sump  =  sump + real(fftv(n,1)*conj(ffti(n,1)));
end

Vrms = sqrt(sumv)
Irms = sqrt(sumi)

% Active power P

P = sump

% Apparent power S

S = Vrms*Irms

% True power factor tPF

tPF = PIS

% Displacement power factor dPF
```

```
deltav = atan2(imag(fftv(4,1)),real(fftv(4,1)));
deltai = atan2(imag(ffti(4,1)),real(ffti(4,1)));

dPF = cos(deltai-deltav)

% Total harmonic distortion of current THDi and total harmonic distortion
%       of voltage THDv

sumvh = sumv-(abs(fftv(4,1)))^2;
sumih = sumi-(abs(ffti(4,1)))^2;

THDv = sqrt(sumvh)/abs(fftv(4,1))*100
THDi = sqrt(sumih)/abs(ffti(4,1))*100

% Crest factor CF

CF = max(i)/Irms


function simtube(file,ptype)

% SIMTUBE(FILE)
%
%       Single-phase simulation - tube voltage and current
%
%       Extract TIME, TUBEV, TUBECUR, TUBEC1, and TUBEC2
%       from input FILE and plot

% Clear previous graph

clg;

% Extract TIME, TUBEV, TUBECUR, TUBEC1, and TUBEC2 from input FILE

extime   = file*[1;0;0;0;0];
extubev  = file*[0;1;0;0;0];
extubecur = file*[0;0;1;0;0];
extubec1  = file*[0;0;0;1;0];
extubec2  = file*[0;0;0;0;1];

% Extract 160 pts (200 usec) starting at point 288 (360 usec)

for n = 1:1:160,
        time(n,1)   = extime(n,1);
        tubev(n,1)  = -extubev(n+277,1);
        tubecur(n,1) = -extubecur(n+277,1);
```

```
        tubec1(n,1) = -extubec1(n+277,1);
        tubec2(n,1) = -extubec2(n+277,1);
end

if ptype == 1,

% Plot TUBEC1, TUBEC2, AND TUBECUR versus TIME

plot(time,tubec1,'--',time,tubec2,'-.',time,tubecur,'-');
grid;
title('LOA 30W Circline CFL (PSPICE Simulation - Tube)');
xlabel('Time (seconds)');
ylabel('Current (amps)');

elseif ptype == 2,

% Plot TUBEV, TUBECUR, AND TUBEPWR versus TIME

plot(time,tubev,'--',time,tubecur*100,'-.',time,tubev.*tubecur,'-');
grid;
title('LOA 30W Circline CFL (PSPICE Simulation - Tube)');
xlabel('Time (seconds)');
ylabel('Current (amps)');

end;



function simfft3p(file1,file2))

% SIMFFT3P(FILE1,FILE2)
%
%       Three-phase simulation - FFT of neutral current
%
%       Plot the Y-point FFT of the voltage V and the
%       current I versus the corresponding frequency axis
%       for the given sampling frequency Z.  Also,
%       plot the voltage V and current I versus the
%       corresponding time axis T (given the input FILEs)

% Define total number of points in FILEs

pts = 5335;

% Define number of evaluation points Y and sampling frequency Z
```

```
y = 4000;
z = 80000;

% Clear previous graph

clg;

% Extract T, V1, I(V1), V2, I(V2), V3, I(V3), and I(NEUT)
% from input FILE

for n = 1:1:y,
        t(n,1) = (n-1)*1.25e-05;
end

for n = y:-1:1,
        v1(n,1) = file1((pts-y)+n,2);
        i1(n,1) = file1((pts-y)+n,3);
        v2(n,1) = file1((pts-y)+n,4);
        i2(n,1) = file1((pts-y)+n,5);
        v3(n,1) = file1((pts-y)+n,6);
        i3(n,1) = file2((pts-y)+n,2);
        ineut(n,1) = file2((pts-y)+n,3);
end

% Calculate the Y-point FFT of the voltage V

temp1 = fft(v1,y);
temp2 = temp1/(y/2*sqrt(2));
fftv = temp2(1:(y/2));

% Calculate the Y-point FFT of the current INEUT

temp1 = fft(ineut,y);
temp2 = temp1/(y/2*sqrt(2));
ffti = temp2(1:(y/2));

% Calculate the frequency axis for the Y-point FFT given
%       the sampling frequency Z

freqaxis = (z*(0:((y/2)-1))/y)';


% Plot the voltage V and current I versus its corresponding time axis T
```

```
subplot(211);
plot(t,v1/75);
hold on;
plot(t,v2/75);
hold on;
plot(t,v3/75);
hold on;
plot(t,ineut);
hold off;
grid;
title('LOA 30W Circline CFL (PSPICE Simulation - 3-phase supply)');
xlabel('Time (seconds)');'
ylabel('Current (amps)');

% Plot the FFT of the current I versus its corresponding frequency axis

fftiplot = abs(ffti);

subplot(212)
semilogx(freqaxis,fftiplot)
grid
xlabel('Frequency (hertz)')
ylabel('Current (amps)')

% Calculate fundamental current I1rms, fundamental voltage V1rms,
%       RMS current Irms, RMS voltage Vrms, active power P, apparent power S,
%       true power factor tPF, displacement power factor dPF, total harmonic
%       distortion of current THDi,    total harmonic distortion of voltage THDv,
%       and crest factor CF

sumv = 0.0;
sumi = 0.0;
sump = 0.0;

% Fundamental current I1rms and fundamental voltgae V1rms

V1rms = abs(fftv(4,1))
I1rms = abs(ffti(4,1))

% RMS current Irms and RMS voltage Vrms

for n = 4:6:(y/2),
        sumv  =  sumv + (abs(fftv(n,1)))^2;
        sumi  =  sumi + (abs(ffti(n,1)))^2;
        sump  =  sump + real(fftv(n,1)*conj(ffti(n,1)));
```

```
end

Vrms = sqrt(sumv)
Irms = sqrt(sumi)

% Active power P

P = sump

% Apparent power S

S = Vrms*Irms

% True power factor tPF

tPF = P/S

% Displacement power factor dPF

deltav = atan2(imag(fftv(4,1)),real(fftv(4,1)));
deltai = atan2(imag(ffti(4,1)),real(ffti(4,1)));

dPF = cos(deltai-deltav)

% Total harmonic distortion of current THDi and total harmonic distortion
%       of voltage THDv

sumvh = sumv-(abs(fftv(4,1)))^2;
sumih = sumi-(abs(ffti(4,1)))^2;

THDv = sqrt(sumvh)/abs(fftv(4,1))*100
THDi = sqrt(sumih)/abs(ffti(4,1))*100

% Crest factor CF

CF = max(i)/Irms
```

Appendix B. PSPICE simulation code

CFL1E.CIR

```
* SINGLE-PHASE SIMULATION
* LOA 2030 CIRCLINE CFL
* BOOST CONVERTER MODIFTCATION

*** BEGIN SCHEMATIC DIAGRAM DEFINITION ***

* Voltage source, VS=169.7sin(wt)
VS    0   1   SIN(0 169.7 60 0 0 0)

* AC-side EMI filter
R12   1   2   2.2
L23   2   3   330uH
C30   3   0   0.47uF

* Rectifier diodes
D1    3   4   DDEFAULT
D2    0   4   DDEFAULT
D3    5   0   DDEFAULT
D4    5   3   DDEFAULT

* RC timing network
*R420  4   20  220K
*R47   4   7   220K
*R421  4   21  22
*C217  21  7   1nF
*D207  20  7   DDEFAULT
*C200  20  5   0.1uF

* Boost converter
D413  4   13  DDEFAULT
L137  13  7   330uH
C145  4   5   0.47uF

* Filter capacitance
C45   4   5   47uF

* HEXFET switching model
DHF1  14  6   DDEFAULT
SHF1  6   7   11  0   SMOD1
```

```
DFW1  7   14  DDEFALJLT
DHF2  7   8   DDEFAULT
SHF2  8   5   11  0   SMOD2
DFW2  5   7   DDEFAULT
VHF   11  0   PULSE(-1.01 1.01 0 lu lu 15.0e-6 30.0e-6)

* Fluorescent tube model
C49   14  9   0.10uF
L710  7   10  760uH
C910  9   10  18nF
RTUBE 9   10  120

*** END SCHEMATIC DIAGRAM DEFINITION ***

* Define part models
.model DDEFALJLT D
.model SMOD1 VSWITCH [RON 0.01 VON 1.0]
.model SMOD2 VSWITCH [RON 0.01 VON -1.0]

* Transient analysis
.tran  12.5u  0.0666667

* Define transient analysis options
.options GMIN = 1.0u ; *ipsp*
.options ITL4 = 10000
.options ITL5 = 0
.options RELTOL = 0.01

* Enable graphic processor
.probe I(VS)

* Print output table
.print tran V(1,0) I(VS)

.END
```

CFL1E.CIR

```
* THREE-PHASE SIMULATION
* LOA 2030 CIRCLINE CFL

*** BEGIN SCHEMATIC DIAGRAM DEFINITION ***
```

```
*** PHASE A ***

* Voltage source, VA=169.7sin(wt)
VA    0     1    SIN(0 169.7 60 0 0 0)

* Neutral leg resistance
RNEUT 0     50    0.1

* AC-side EMI filter
R12   1     2    2.2
L23   2     3    330uH
C350  3     50   0.47uF

* Rectifier diodes
D1A   3     4    DDEFAULT
D2A   50    4    DDEFAULT
D3A   5     50   DDEFAULT
D4A   5     3    DDEFAULT

* DC-side filter capacitance
C45   4     5    47uF

* HEXFET switching model
DHF1A 4     6    DDEFAULT
SHF1A 6     7    11  0   SMOD1
DFW1A 7     4    DDEFAULT
DHF2A 7     8    DDEFAULT
SHF2A 8     5    11  0   SMOD2
DFW2A 5     7    DDEFAULT
VHF   11    0    PULSE(-1.01 1.01 0 lu lu 15.0e-6 30.0e-6)

* Fluorescent tube model
C49   4     9    0.10uF
L710  7     10   760uH
C910  9     10   18nF
RTUBEA 9    10   120

*** PHASE B ***

* Voltage source, VB=169.7sin(wt)
VB    0     21   SIN(0 169.7600 0-120)

* AC-side EMI filter
R2122 21    22   2.2
L2223 22    23   330uH
```

```
C2350 23   50   0.47uF

* Rectifier diodes
D1B   23   24   DDEFAULT
D2B   50   24   DDEFAULT
D3B   25   50   DDEFAULT
D4B   25   23   DDEFAULT

* DC-side filter capacitance
C2425 24   25   47uF

* HEXFET switching model
DHF1B 24   26   DDEFAULT
SHF1B 26   27   11  0   SMOD1
DFW1B 27   24   DDEFAULT
DHF2B 27   28   DDEFAULT
SHF2B 28   25   11  0   SMOD2
DFW2B 25   27   DDEFAULT

* Fluorescent tube model
C2429 24   29   0.10uF
L2730 27   30   760uH
C2930 29   30   18nF
RTUBEB 29  30   120

*** PHASE C ***

* Voltage source, VC=169.7sin(wt)
VC    0    31   SIN(0 169.7 60 0 0 -240)

* AC-side EMI filter
R3132 31   32   2.2
L3233 32   33   330uH
C3350 33   50   0.47uF

* Rectifier diodes
D1C   33   34   DDEFAULT
D2C   50   34   DDEFAULT
D3C   35   50   DDEFAULT
D4C   35   33   DDEFAULT

* DC-side filter capacitance
C3435 34   35   47uF

* HEXFET switching model
```

```
DHF1C 34   36   DDEFAULT
SHF1C 36   37   11  0   SMOD1
DFW1C 37   34   DDEFAULT
DHF2C 37   38   DDEFAULT
SHF2C 38   35   11  0   SMOD2
DFW2C 35   37   DDEFAULT

* Fluorescent tube model
C3439 34   39   0.10uF
L3740 37   40   760uH
C3940 39   40   18nF
RTUBEC 39  40   120

*** END SCHEMATIC DIAGRAM DEFINITION ***

* Enable transient analysis
.tran   12.5u   0.0666667

* Enable graphic processor
.probe I(RNEUT)

* Print output table
.print tran V(1,0) I(VA) V(21,0) I(VB) V(31,0) I(VC) I(RNEUT)

* Define part models
.model DDEFAULT D
.model SMOD1 VSWITCH [RON 0.01 VON 1.O]
.model SMOD2 VSWITCH [RON 0.01 VON -1.O]

* Define transient analysis options
.options GMIN = 1.0u ; *ipsp*
.options ITL4 = 10000
.options ITL5 = 0
.options RELTOL = 0.01

.END
```